PROCESS DEVELOPMENT FOR EFFECTIVE, RECOVERABLE AND REUSABLE MAGNETIC NANOBIOCATALYSTS FOR BIOMASS HYDROLYSIS

A Dissertation
Submitted to the Graduate Faculty
of the
North Dakota State University
of Agriculture and Applied Science

By

Ademola Monsur Hammed

In Partial Fulfillment of the Requirements
for the Degree of
DOCTOR OF PHILOSOPHY

Major Department:
Agricultural and Biosystems Engineering

June 2021

Fargo, North Dakota

North Dakota State University

Graduate School

Title

PROCESS DEVELOPMENT FOR EFFECTIVE, RECOVERABLE AND REUSABLE MAGNETIC NANOBIOCATALYSTS FOR BIOMASS HYDROLYSIS

By

Ademola Monsur Hammed

The Supervisory Committee certifies that this ***disquisition*** complies with North Dakota State University's regulations and meets the accepted standards for the degree of

DOCTOR OF PHILOSOPHY

SUPERVISORY COMMITTEE:

Dr. Scott W. Pryor
Chair

Dr. Andriy Voronov

Dr. Shafiqur Rahman

Dr. Achintya Bezbaruah

Approved:

11/12/2021
Date

Kenneth Hellevang
Department Chair

ABSTRACT

Recovery and reuse of enzymes can reduce the high enzyme costs that are challenging for cellulosic biorefineries. Attaching enzymes to magnetic nanoparticles to make magnetic nanobiocatalysts (MNBCs) can facilitate enzyme recovery and reuse. One approach for MNBC synthesis is by attaching enzymes to flexible polymer molecules to form polymer-enzyme conjugates (PECs) which in turn can be attached to superparamagnetic iron-oxide nanoparticles (SPIONs). However, this approach can be complex and unscalable. The research objective is to develop a scalable process to produce effective, recoverable and reusable cellulolytic MNBCs

PECs were produced and tested before incorporation into MNBCs in order to test efficacy and reusability. The effects of different biomass pretreatment methods, temperature, pH and solid loading on PEC efficacy were determined. Hydrolysis conditions affect PEC and free enzyme (FE) efficacy equally suggesting that attachment to the polymer did not interfere with substrate-enzyme interaction. PEC has higher efficacy than FE at higher substrate loading offering potential for processing more substrate per batch. The recovered PECs were effective for subsequent hydrolysis and reduced enzyme requirement to 40% of free enzyme needed in the first stage.

A tubular electrochemical system (TES), an electrochemical reactor containing electrolytes flowing through a cathode tube with an inner anode rod, was developed to overcome scalability and sustainability challenges of SPION synthesis. The effects of current density, electrolyte concentration, electrolyte feeding strategy, and flow rate on TES productivity and SPION characteristics were determined. TES productivity and SPION characteristics were both affected by the reaction conditions. Increasing electrolyte flow rate caused a decrease in average

SPION size and size-distribution. The flow rate can be used to control SPION size distribution and shape. Gradual addition of more electrolyte resulted in 75% increase in SPION yield.

Silica coating of SPIONs improves SPION longevity and adsorption capacity. A single-step process for silica-coated SPION (Si-SPION) synthesis using TES was developed. The coating agent (Na_2SiO_3) concentration did not affect Si-SPION morphology, but increasing Na_2SiO_3 concentration reduces SPION productivity. The Si-SPIONs did not dissolve in an acidic environment for 48 h and were suitable support for MNBC synthesis. The MNBCs were recovered and reused four times.

ACKNOWLEDGMENTS

I would like to express my unwavering appreciation to my major advisor Dr. Scott W. Pryor for his guidance and support throughout my research. I am equally thankful to my committee members, Dr. Andriy Voronov, Dr. Shafiqur Rahman, and Dr. Achintya Bezbaruah for their time and contribution. I acknowledge University of North Dakota for the support to use one of its laboratories.

My appreciation also goes to my beloved ones including Tawakalit Asiyanbi, Aisha Stanley and Mr. and Mrs. Hammed for their love and care. Thanks to my family members for their constant encouragement. Special thank goes to my kids, Hikmah, Ikhlas, Hudhayfah, and Humaid for their emotional support.

DEDICATION

To Almighty Allah, for His mercy.

TABLE OF CONTENTS

LIST OF TABLES

LIST OF FIGURES

1. GENERAL INTRODUCTION

Decades of human practices have threatened the environment in many ways including climate change, ozone layer depletion, water pollution, and resource depletion. These environmental concerns have been a driving force behind the emergence and pursuit of alternative industrial practices including biomass-based manufacturing, green technology, and bioprocessing (Gross & Kalra, 2002). Also, liquid fuels from biomass are the only near-term liquid alternatives to fossil-based fuels. Meanwhile, the fact that economic development is tightly related to manufacturing and energy means that the future economy will likely depend on biomass (Banerjee et al., 2010). However, there are some technological challenges that often make biomass-based products and bioenergy costlier than their petroleum-based counterparts (Banerjee et al., 2010). Therefore, our preparation for the green-economy age requires thorough investigation and development of cost-effective biomass conversion technologies.

Biomass technologies generally rely on the availability of low cost and abundant biomass feedstocks. A suitable biomass resource should also contribute less environmental stressors and be rich in the required polysaccharides for biofuel production. Out of all the different sources of biomass, lignocellulosic biomass (LB) – stems or leaves of grasses and woody plants – have been identified as an abundant and promising resource (Gross & Kalra, 2002). For instance, ethanol production from LB has the potential to reduce life cycle greenhouse gas emissions by 60% compared to ethanol production from corn grain. LB resources are very high in polysaccharides (i.e. cellulose and hemicellulose) that may be hydrolyzed to fermentable sugars. LB potential in North Dakota is primarily in the form of perennial grasses and agricultural residues (Lee, 2007). Switchgrass is a common example of a perennial grass which gives high yield, requires low fertilizer, reduces erosion, and has a deep root system which promotes carbon

sequestration and makes the crop more drought tolerant. The cellulose and hemicellulose in plant cell walls are tightly intertwined and cemented together by lignin, a complex aromatic polymer, resulting in a rigid structure that leads to challenges during processing (Lee, 2007).

An essential step during biomass processing for biofuel production is hydrolysis – the release of monomers from the polymers. LB hydrolysis can be achieved through chemical or biological processing. Biological hydrolysis involves the use of enzymes and has been recognized to be the more economically and environmentally friendly option. Other reasons for using enzymes include high reaction specificity and less formation of inhibiting by-products (Dutta & Wu, 2014). However, the high price of enzymes still contributes significantly to LB-hydrolysis cost (Nguyenhuynh, Nithyanandam, Hwa Chong, & Krishnaiah, 2017; Stickel, Adhikari, Sievers, & Pellegrino, 2018). Many research efforts on enzymatic biomass hydrolysis have focused on areas including process optimization, biomass pretreatment, and enzyme recovery and reuse.

Prior to enzymatic hydrolysis, LB is first pretreated to reduce recalcitrance. The most common methods for LB pretreatment use acidic or alkaline conditions at elevated temperatures. The mechanisms of these types of pretreatment methods are different as are the properties of the resulting pretreated material (Wyman et al., 2005). Briefly, acid-pretreated LB tends to retain a high lignin content with low hemicellulose content, but may contain enzyme inhibitors (Wyman et al., 2005). Alkali-pretreated LB will have low lignin content while retaining more hemicellulose. Therefore, both the structure and composition of the pretreated biomass will vary based on pretreatment method (Hsu, 1996). The biomass-enzyme interaction and enzyme hydrolytic efficiency are similarly affected by the pretreatment method. Since acidic and alkaline

pretreatment methods are leading technologies industrially, development of new enzymatic hydrolysis methods should be tested with both types of biomass pretreatment.

One strategy to improve and reduce costs of LB hydrolysis is enzyme immobilization. Enzyme immobilization involves the attachment of enzymes on physical supports to enhance recovery and reuse (Kudina et al., 2014). The cost of bioprocessing could be reduced if the active enzymes in the spent biomass and the effluent were recovered and reused. Researchers have developed many enzyme immobilization methods using different supports and physical or chemical attachment modes (Zdarta, Pinelo, Jesionowski, & Meyer, 2018). The enzyme hydrolytic efficiency and the ease of recovery depend on the type of immobilization method. Most immobilization methods usually lead to lower hydrolytic activity and often require extra recovery step(s). Hence, development of improved enzyme immobilization methods is still ongoing. Recent approaches involve the development of enzyme immobilization methods that mimic natural systems.

Living systems have evolved efficient approaches to carry out biochemical processes including enzymatic hydrolysis of biomass. Biochemical studies on living systems have revealed that cellulolytic enzymes are often organized into clusters. Some microbes secrete cellulase clusters called cellulosomes (Artzi, Bayer, & Moraïs, 2017). Structurally, cellulosomes contain many cellulase enzymes that are covalently immobilized on a threadlike protein-scaffold. Efficient biomass hydrolysis is achieved through collaborative actions of the immobilized cellulases (Artzi et al., 2017; Fontes & Gilbert, 2010). Unlike many conventional immobilization methods, cellulosome enzymes have a high degree of movement due to the flexibility of the supports (threadlike protein-scaffold) (Hyeon, Jeon, Whang, & Han, 2011). Biotechnological

routes of producing cellulosomes are complex to synthesize. Some research efforts focus on the development of artificial biomimetic cellulosomes that could be easily produced.

Artificial biomimetic cellulosomes are a type of nano-biocatalyst (NBC) containing cellulase enzymes that have been immobilized on flexible polymers. The polymer epoxy groups can be activated to covalently link to an enzymes lysine thereby serving as an immobilization support. The polymer thus functions similarly to the protein-scaffold in natural cellulosomes. The polymer properties (e.g. molecular weight, conformation, amphiphilicity, viscosity, etc.) could affect enzymes efficacy. Since one goal of immobilization is to facilitate enzyme recovery and reuse, work on artificial cellulosomes (NBCs) has also included enzyme recovery.

Membrane filtration is among the enzyme recovery strategies that selectively partitions substances based on molecular size. Membrane technology operates at mild temperatures suitable to maintain enzyme efficacy. Many researchers have reported that membrane filtration could be used to recover enzymes that remain in solution after hydrolysis. One of the major challenges of using membrane filtration is fouling – blockage of the membrane pores by larger soluble molecules and other non-soluble residual material. Fouling leads to costly membrane cleaning operations and replacement. To the best of our knowledge, membrane recovery of NBCs has not been reported. Since NBCs may contain many individual enzyme molecules that are anchored on the polymer, they are larger than free enzymes. The increased size of NBCs could ease separation of artificial cellulosome NBCs from hydrolysates using membranes with a larger (> 40kD) pore size.

Another approach to ease NBC recovery is the development of magnetic NBCs which enable separation via magnetic attraction. A magnetic NBC is a nano-scaled structure that is comprised of immobilized enzyme clusters attached to a superparamagnetic metallic core.

Researchers have developed many types of magnetic NBCs with varying architectural designs, modes of immobilization (physical or chemical), and enzymes (including cellulases) (Tabañag & Shen-Long, 2017). For LB hydrolysis, research has shown that the architectural design and reaction conditions affect the hydrolytic efficiency of the immobilized cellulases (Khoshnevisan et al., 2017). Although cellulolytic magnetic NBCs may exhibit lower hydrolytic rates than those of free enzymes, their overall hydrolytic yield can improve when recovered and reused. However, current production methods for magnetic NBCs are not scalable at an industrial level.

Among several superparamagnetic nanoparticles that have been synthesized, those formed from iron-oxides have received most attention. Superparamagnetic iron-oxide nanoparticles (SPIONs) are generally considered non-toxic and environmentally friendly. Early studies on SPIONs used them for biomedical applications for site-directed applications of active-medicinal compounds (Ramimoghadam, Bagheri, & Hamid, 2014). Recently, SPIONs have been used for the development of cellulolytic magnetic NBCs (Khoshnevisan et al., 2017). Synthesis of SPIONs is the first step during the development of cellulolytic magnetic NBCs. One of the main challenges during SPION synthesis is size control. Production of SPIONs with a monodispersed or narrow size-distribution is desired for proper understanding of their physical properties (Robertson et al., 2016). Among several methods, electrochemical synthesis which involves the use of electrical current on iron-contained solution is the most promising to produce size-controlled SPIONs on a large scale (Ramimoghadam et al., 2014).

This research is among the ongoing efforts to overcome some of the aforementioned challenges facing enzymatic hydrolysis via the development membrane separation of NBCs, electro-synthesis of SPIONs and recovery of magnetic NBCs during LB hydrolysis.

1.1. References

Artzi, L., Bayer, E. A., & Moraïs, S. (2017). Cellulosomes: Bacterial nanomachines for dismantling plant polysaccharides. *Nature Reviews Microbiology*, *15*(2), 83.

Banerjee, S., Mudliar, S., Sen, R., Giri, B., Satpute, D., Chakrabarti, T., & Pandey, R. A. (2010). Commercializing lignocellulosic bioethanol: Technology bottlenecks and possible remedies. *Biofuels, Bioproducts and Biorefining: Innovation for a Sustainable Economy*, *4*(1), 77–93.

Dutta, S., & Wu, K. C.-W. (2014). Enzymatic breakdown of biomass: Enzyme active sites, immobilization, and biofuel production. *Green Chemistry*, *16*(11), 4615–4626.

Fontes, C. M., & Gilbert, H. J. (2010). Cellulosomes: Highly efficient nanomachines designed to deconstruct plant cell wall complex carbohydrates. *Annual Review of Biochemistry*, *79*, 655–681.

Gross, R. A., & Kalra, B. (2002). Biodegradable polymers for the environment. *Science*, *297*(5582), 803–807.

Hsu, T.-A. (1996). Pretreatment of biomass. Handbook on bioethanol: Production and utilization. *Wyman, CE Pp179-212. Ed. Taylor & Francis, Washington DC, USA*.

Hyeon, J. E., Jeon, W. J., Whang, S. Y., & Han, S. O. (2011). Production of minicellulosomes for the enhanced hydrolysis of cellulosic substrates by recombinant Corynebacterium glutamicum. *Enzyme and Microbial Technology*, *48*(4–5), 371–377.

Khoshnevisan, K., Vakhshiteh, F., Barkhi, M., Baharifar, H., Poor-Akbar, E., Zari, N., … Bordbar, A.-K. (2017). Immobilization of cellulase enzyme onto magnetic nanoparticles: Applications and recent advances. *Molecular Catalysis*, *442*, 66–73. https://doi.org/10.1016/j.mcat.2017.09.006

Kudina, O., Zakharchenko, A., Trotsenko, O., Tokarev, A., Ionov, L., Stoychev, G., … Minko, S. (2014). Highly Efficient Phase Boundary Biocatalysis with Enzymogel Nanoparticles. *Angewandte Chemie International Edition*, *53*(2), 483–487. https://doi.org/10.1002/anie.201306831

Lee, D. (2007). *Composition of herbaceous biomass feedstocks*. North Central Sun Grant Center, South Dakota State University.

Nguyenhuynh, T., Nithyanandam, R., Hwa Chong, C., & Krishnaiah, D. (2017). A review on using membrane reactors in enzymatic hydrolysis of cellulose. *J. Eng. Sci. Technol*, *12*(4), 1129–1152.

Ramimoghadam, D., Bagheri, S., & Hamid, S. B. A. (2014). Progress in electrochemical synthesis of magnetic iron oxide nanoparticles. *Journal of Magnetism and Magnetic Materials*, *368*, 207–229. https://doi.org/10.1016/j.jmmm.2014.05.015

Stickel, J. J., Adhikari, B., Sievers, D. A., & Pellegrino, J. (2018). Continuous enzymatic hydrolysis of lignocellulosic biomass in a membrane-reactor system. *Journal of Chemical Technology & Biotechnology*, *93*(8), 2181–2190.

Tabañag, I. D. F., & Shen-Long T. (2017). Biological Strategies in Nanobiocatalyst Assembly. In Biocatalysis and Nanotechnology. Jenny Stanford Publishing, pp. 151-241..

Wyman, C. E., Dale, B. E., Elander, R. T., Holtzapple, M., Ladisch, M. R., & Lee, Y. Y. (2005). Coordinated development of leading biomass pretreatment technologies. *Bioresource Technology*, *96*(18), 1959–1966.

Zdarta, J., Pinelo, M., Jesionowski, T., & Meyer, A. S. (2018). Upgrading of Biomass Monosaccharides by Immobilized Glucose Dehydrogenase and Xylose Dehydrogenase. *ChemCatChem*, *10*(22), 5164–5173. https://doi.org/10.1002/cctc.201801335

2. LITERATURE REVIEW

2.1. Biomass-Based Fuels and Products

2.1.1. Emerging need of biomass-based fuels and products

Our world is energy-driven and the aspired growth in population, economy, health, and mobility are largely dependent on energy from fossil fuels and nuclear sources (Dresselhaus & Thomas, 2001). All fossil fuel sources produce CO_2, a greenhouse gas that contributes to climate change. Although nuclear power plants do not directly emit CO_2, they produce radioactive wastes with equally problematic disposal challenges (Gin et al., 2013). Also, large petroleum importation has economic disadvantages for countries like USA (D. Lee, 2007). Apart from energy, synthetic materials like plastics and fabrics also make use of petroleum as starting materials. This production pathway is challenged with the dwindling supply and volatile cost of petroleum (Tuck, Pérez, Horváth, Sheldon, & Poliakoff, 2012). Most petroleum-based products are not biodegradable and are a nuisance in the environment (Gross & Kalra, 2002). The aforementioned challenges have prompted research in biomass-based fuels and products.

2.1.2. Biomass: a viable alternative source of fuels and products

Biomass is defined as plant and plant-derived materials comprised largely of structural carbohydrates and other molecules derived from photosynthesis. Biomass also include livestock manure. Most biomass resources are often underutilized or considered waste; therefore, biomass can be a less expensive raw-material for industrial processes. Biomass conversion has been identified as an alternative way to produce fuels and products. The biomass-to-fuel concept is most preferred among other alternative energy sources because it is the only near-term source of renewable liquid fuels that can be used in most of our current transportation systems. Biomass-based products are biodegradable and can be disposed of more easily (Gross & Kalra, 2002). The

use of plant biomass as feedstock for industrial processes will equally help encourage cultivation of plants and thus help in sequestering atmospheric CO_2.

Since most countries have biomass resources, production of fuels and products using biomass can reduce reliance on petroleum importation across the globe (D. Lee, 2007). According to USDOE and USDA report (D. Lee, 2007), the projected capacity of biomass production in U.S (1.3 billion dry tons) is more than the required amount (1 billion dry tons) to meet the target of 30% renewable energy production by the year 2030. According to Figure 1, about three times as much biomass is projected to be available from agricultural lands compared to forestlands. The distribution of biomass from agricultural lands are mostly from annual crop residue and perennial crops. Biomass from grains has lower potential while biomass from other sources such as animal manure, aquatic plants and process residue make up the remainder (Perlack et al., 2005).

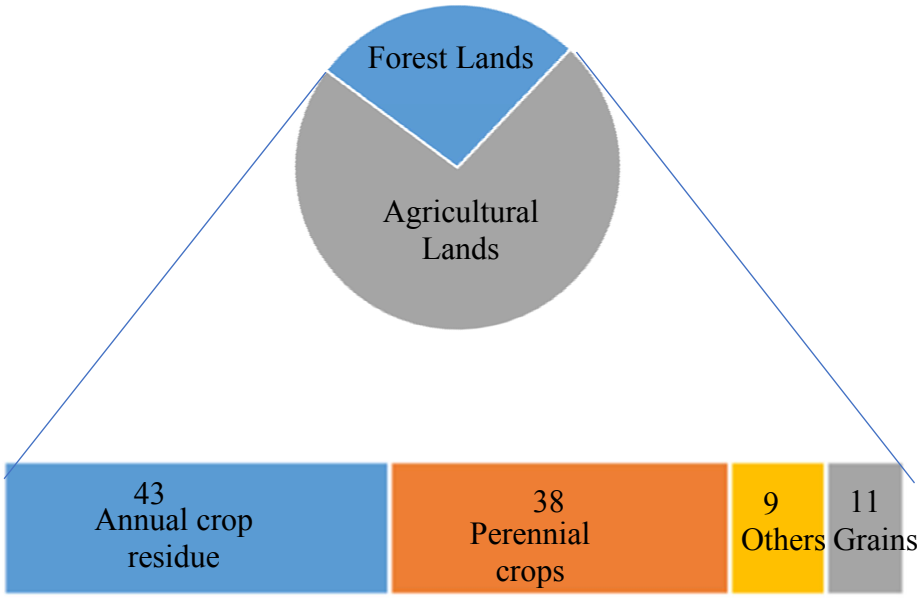

Figure 1. Quantity and types of biomass sources in US, adapted from Perlack et al. (2005) and D. Lee (2007)

2.1.3. Biomass-based products and production pathways

Numerous efforts have shown the possibility of converting biomass to fuels and products through a number of production pathways. During biochemical processing, biomass structural carbohydrates are usually converted to monomeric sugars, which can then be converted to ethanol or other fuels. Also, the sugar can be converted to a wide variety of other compounds like sorbitol, furfural, xylitol and 5-hydroxymethyl fufural — bioplatform intermediate products – that are then converted to other products (Figure 2) (Luterbacher, Alonso, & Dumesic, 2014). Therefore, production of fermentable sugars from biomass is central during biochemical processing of biomass.

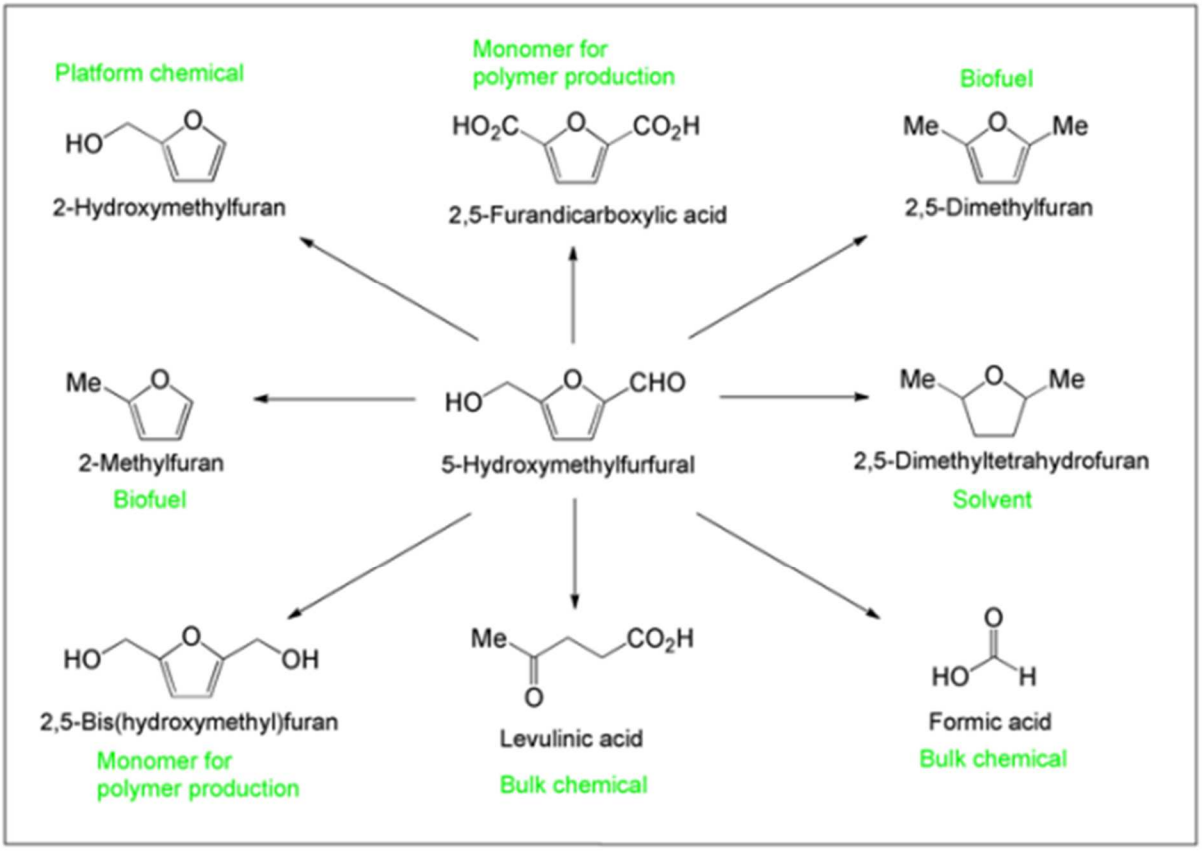

Figure 2. Possible products using 5-hydroxymethylfurfural as a biobased platform chemical (Barros, 2016)

In order to make biomass-based products more economically competitive with petroleum products, improvement efforts must be intensified. Some researchers have adopted biotechnological methods to increase biomass production (Juknys et al., 2011; Pereira-Flores et al., 2016) and to modify biomass so it can be more easily processed (Fu et al., 2011; B. Xu et al., 2011). Others have focused on how to improve process efficiency and to reduce the cost of processing in order to achieve attractive investor returns (Wyman et al., 2005). However, plant biomass contains sugars in polymeric form (cellulose and hemicellulose) that are resistant to degradation in native form and therefore pose processing challenges. Processing of plant biomass to fermentable sugars typically involves thermochemical pretreatment prior to enzymatic hydrolysis. Since this research work focuses on hydrolysis improvement for pretreated

lignocellulosic plant biomass, the subsequent sections of this document will outline the chemical composition of lignocellulosic of plant biomass, pretreatment of plant biomass, and hydrolysis of plant biomass using free and immobilized enzymes.

2.2. Compositional Chemistry of Lignocellulosic Biomass

2.2.1. Composition of lignocellulosic biomass

Plants rely on their rigid cell wall to provide structural and protective functions against biotic and abiotic stress. Plant cell walls are made up of carbohydrate and non-carbohydrate polymers (including cellulose, hemicellulose and lignin). These polymers are intertwined to provide structural support for plant cells (Figure 3). The microfibrils of cellulose have high tensile strength which confers the strength in cell walls (O'sullivan, 1997). Lignin and hemicellulose also contribute to the cell wall strength by binding cellulose (Moreira & Filho, 2008). Table 1 shows the typical composition of lignocellulosic biomass of different plants. Due to their high cellulose and hemicellulose content, some of these plants have been identified as energy crops to be used as feedstocks for fuel and bioproduct production.

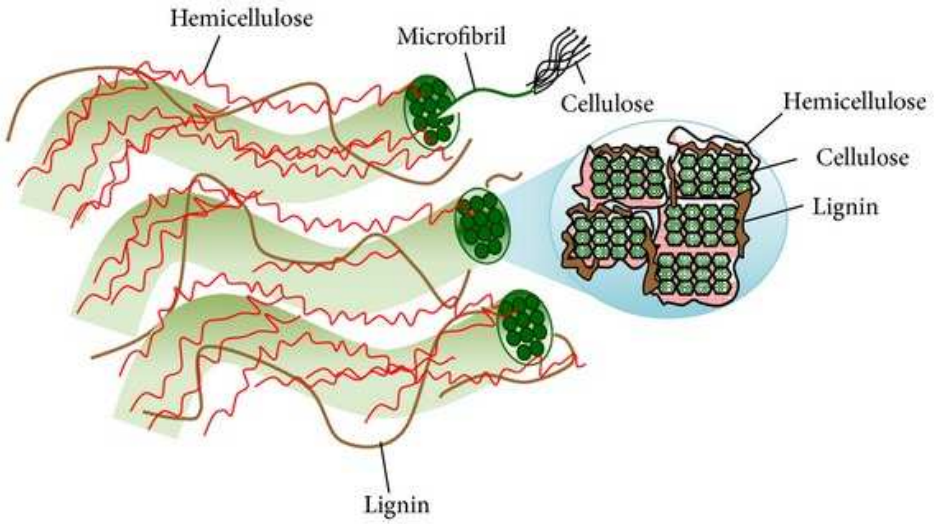

Figure 3. Schematic diagram of lignocellulosic biomass of plant (Moreira & Filho, 2008)

Table 1. Composition of some agricultural lignocellulosic biomass (Saha, 2003)

Plants	Composition (%, dry basis)		
	Cellulose	Hemicellulose	Lignin
Corn fiber	15	35	8
Corn cob	45	35	15
Corn stover	40	25	17
Rice straw	35	25	12
Wheat straw	30	50	20
Sugarcane bagasse	40	24	25
Switchgrass	45	30	12
Coastal bermuda grass	25	35	6

2.2.2. Structural properties of the cellulose and hemicellulose of plant biomass

2.2.2.1. Cellulose

This is the most abundant naturally occurring organic substance with annual production of about 1.5×10^{12} tons. Cellulose is an unbranched polymer and has molecular formula of $(C_6H_{10}O_5)_n$ with 49.39, 44.4 and 6.17 % of carbon, oxygen and hydrogen, respectively. The repeating unit of cellulose is cellobiose – (1→4)-β-D-glucan (O'sullivan, 1997). Due to the presence of multiple hydroxyl groups, intra- and inter- hydrogen bonds are also present in cellulose fibrils (Figure 4). The intra-hydrogen bond occur within the same chain of cellulose while the inter-hydrogen bond occur between neighboring chains of cellulose (C. Zhou & Wu, 2012). Several polymer chains of cellulose are bound together to form microfibrils that appear to be 4 – 10 nm wide. The cellulose microfibrils have both amorphous and crystalline regions. The amorphous regions are weakly bonded and relatively hydrophilic while the crystalline regions are strongly bonded with intra- and inter-molecular bonds and are more hydrophobic (C. Zhou &

Wu, 2012). Cellulose is expected to be the primary source of fermentable sugar for second generation biorefineries.

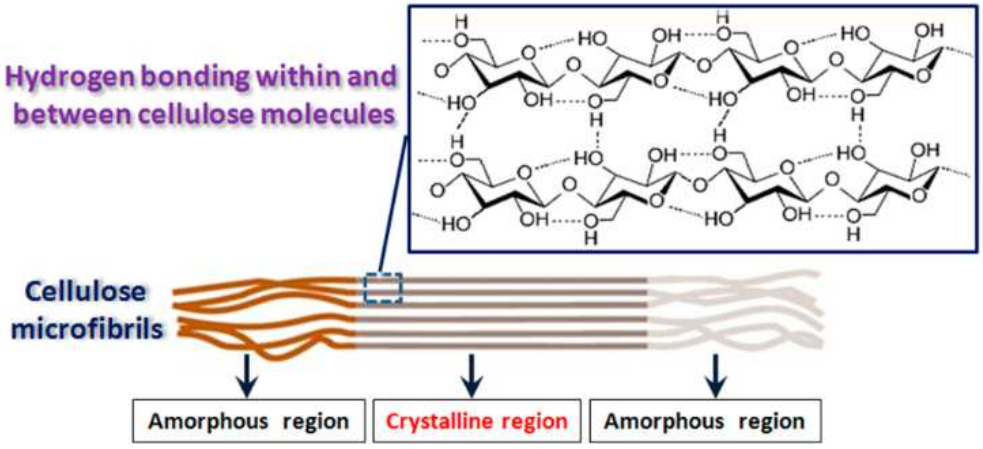

Figure 4. Schematic of cellulose crystalline and amorphous regions (Yuan & Cheng, 2015; C. Zhou & Wu, 2012)

2.2.2.2. Hemicellulose

After cellulose, hemicellulose is the second most common plant-based polysaccharide in lignocellulosic biomass. Hemicellulose is a chemical heterogeneous polymer of pentoses (e.g. xylose and arabinose), hexoses (e.g. mannose, glucose, and galactose), 4-O methyl glucuronic acid, and galacturonic acid residues. They have lower molecular weight than cellulose, and hemicellulose typically has a more branched structure (Moreira & Filho, 2008). The backbone of hemicellulose includes xylans, mannans, mixed linkage β-glucans, and cyloglucans (Mamman et al., 2008).

Xylan is the most abundant component of hemicellulose in most plants. Xylan is a polymer of xylose with a linear backbone of β-D-(1-4) linked xylosepyranose units (Saha, 2003). Xylan can be categorized as homoxylan, arabinoglucorononxylan, glucuronoxylan and glucuronoarabinoxylan depending on other components of the polymer (Figure 5). The exact structural composition of xylan and hemicellulose depends on the specie of origin (Saha, 2003).

Mannan is a linear or branched polymer consisting of D-mannose, D-galactose and D-glucose. The backbone of mannans comprises of β-D-(1→4)-linked mannose and might be combined with glucose or substituted with α-(1→6)-linked galactose residues. Mannan can be classified as linear mannan, glucomannan, galactomannan and galactoglucomannan (Figure 6) (Moreira & Filho, 2008). Degradation of hemicellulose eases enzymatic hydrolysis of cellulose but less fermentable sugars compared to glucose. In fact, fermentability is especially poor in mixtures with glucose present.

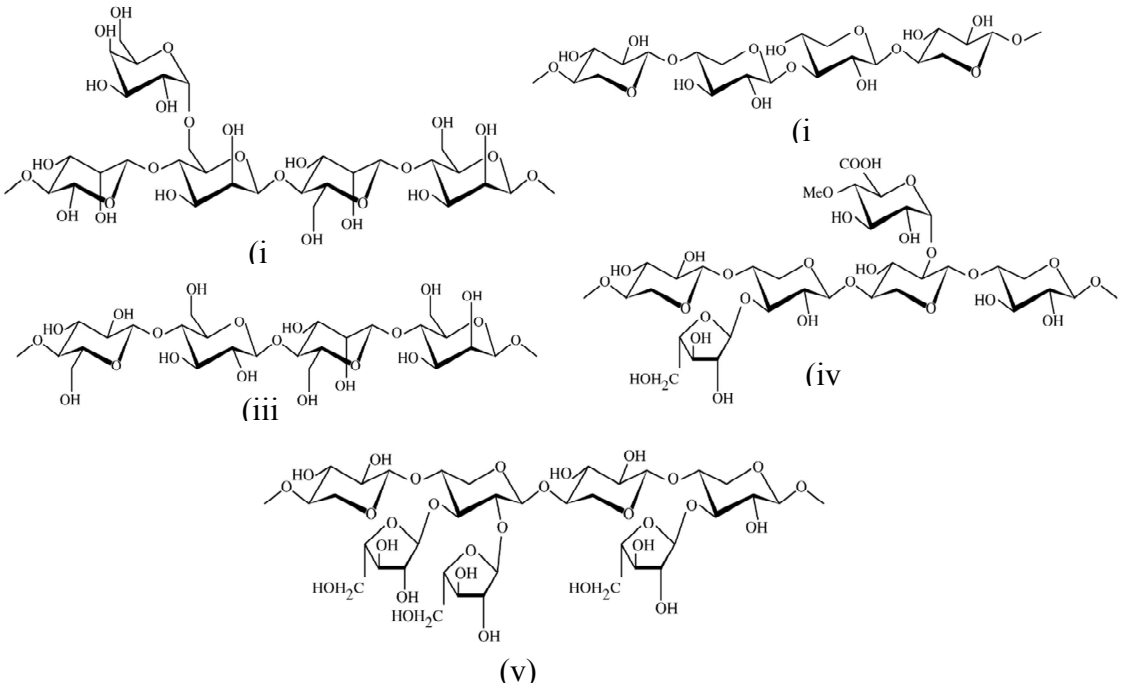

Figure 5. Structures of different forms of xylans (i) homoxylan, (ii) galactomannan, (iii) glucomannan, (iv) (arabino)glucuronoxylan and (v) arabinoxylan (Saha, 2003)

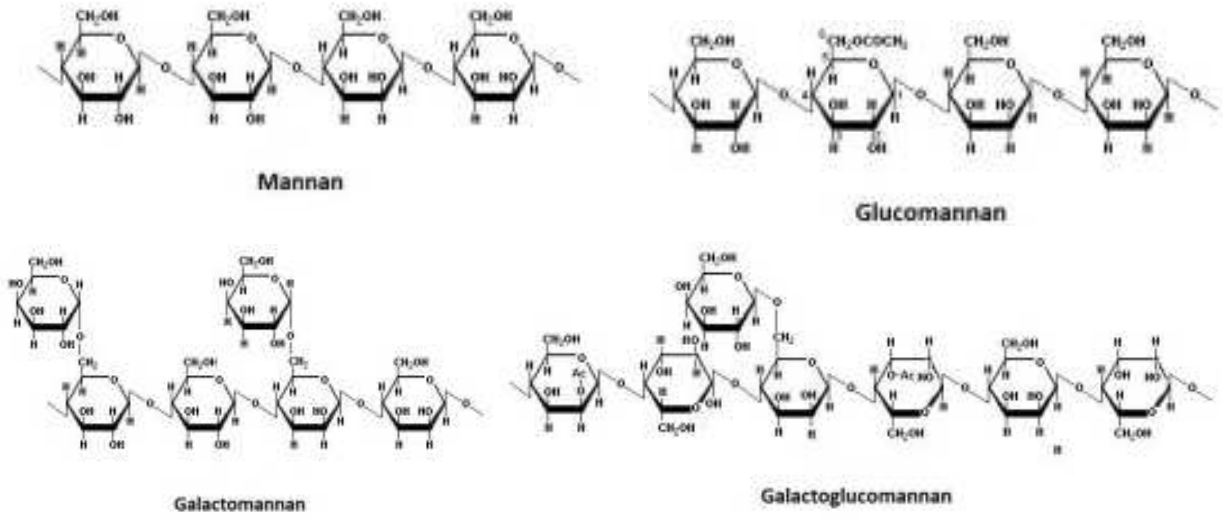

Figure 6. Structures of different forms of mannans (Moreira & Filho, 2008)

2.2.2.3. Lignin

Lignin is a complex and irregular aromatic biopolymer. It consists of a series of phenylpropane units with a variety of linkages (β-O-4, β-5, β-β, etc.) (Brunow, 2008). The three major phenylpropanes that are the building blocks of lignin are guaiacylpropane, syringylpropane and hydroxyphenylpropane. The complexity of lignin structure is due to randomness of linkage generation and the high number of possible isomers (Ralph et al., 2004). Although, it is difficult to qualitatively study the structure of lignin because of its complexity, the important structural features of lignins are shown in Figure 7. The presence of additional functional groups including carboxylates and sulfonates is also possible (Vanholme, Demedts, Morreel, Ralph, & Boerjan, 2010). Although lignin is not a valued as a fermentation feedstock, it can be used for electricity generation.

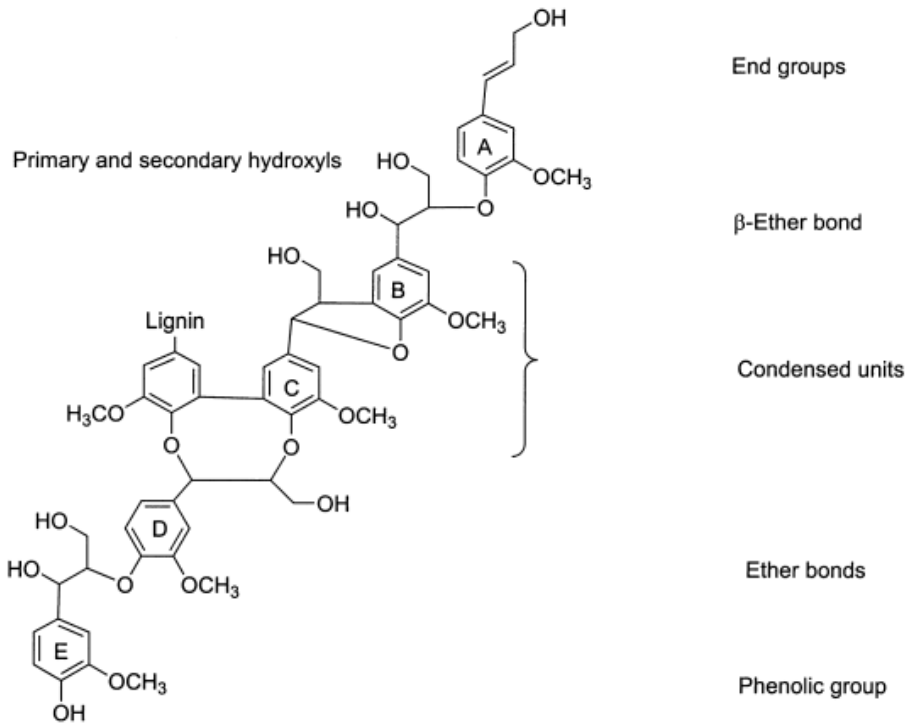

Figure 7. Important structural features of lignins (Brunow, 2008)

2.3. Pretreatment of Lignocellulosic Biomass

Pretreatment is defined as any initial processing step done to reduce lignocellulosic material's recalcitrance to enzymatic hydrolysis. Pretreatment has been recognized as an essential step for biological processing of lignocellulosic biomass. Efficient pretreatment of lignocellulosic materials will also reduce the quantity and cost of enzymes required for hydrolysis (Wyman et al., 2005). Pretreatment removes structural barriers and alters the composition of lignocellulosic biomass (Figure 8). Plant cell wall structural barriers are removed through breaking chemical bonds. The disruption of plant cell wall results to reduction in mechanical properties, cellulose crystallinity and lignin (Wyman et al., 2005). Composition alteration occurs through hydrolysis or solubilisation of individual components.

According to J.-W. Lee and Jeffries (2011), pretreatment should achieve the following:

i. Yield substrate with a high concentration of cellulose for enzyme degradation

ii. Produce little or no fermentation inhibitors such as carboxylic acids, and sugar degradation products (e.g. phenolics, furfural, or 5-hydroxymethylfurfural - HMF) (see Table 2).

iii. Allow high recovery of valuable hemicellulose-derived products

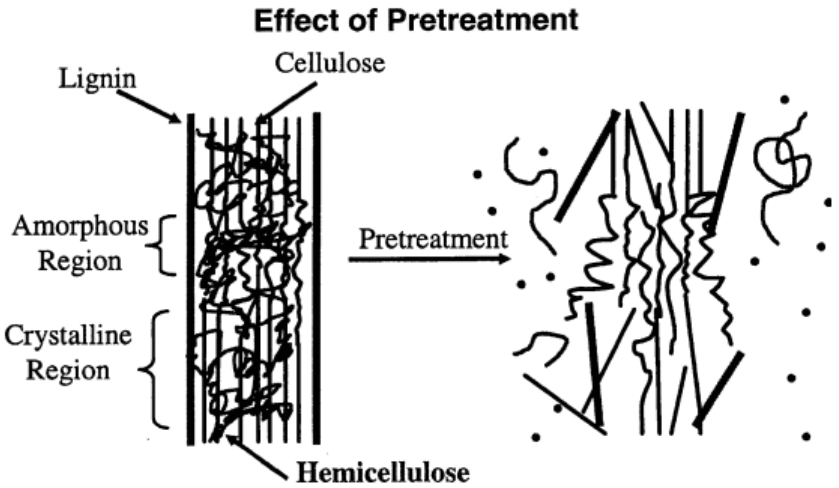

Figure 8. Schematic diagram showing the mechanism of lignocellulosic material pretreatment (Mosier et al., 2005)

Table 2. Inhibitory role of some compounds on enzymatic hydrolysis or microbial fermentation (Pienkos & Zhang, 2009)

Compounds	Inhibitory role
Furfural and HMF *	Interfere with dehydrogenase activity and thus reduce growth rates and cell yield
Phenolics	Damage membranes and lead to loss of membrane integrity, alter cell growth and sugar transport across the membrane
Aldehyde	Exhibit hydrophobicity of cell surrounding thus alter osmotic-balance of cell.
Acids	Interrupt energy production of cell through the collapse of pH gradients.
Alcohol	Exhibit hydrophobicity and breakdown of cell membrane

*HMF: 5-hydroxymethylfurfural

There are numerous types of pretreatment technologies that have been developed. Pretreatment methods can be broadly classified as biological, physical, and chemical. Chemical methods (acid and base pretreatment) are the most promising in terms of removal of hemicellulose and lignin. The use of dilute sulfuric acid, ammonia, and lime are currently being considered for pH control due to economic reason (Wyman et al., 2005).

2.3.1. Alkaline pretreatment

2.3.1.1. Lime approaches

Lime pretreatment involves the use of alkali (0.05 – 0.15 g $Ca(OH)_2$/g biomass) at a temperature of 25 – 130 ^oC, and pressure of 1 – 6 atm. Low temperatures and pressures require days or weeks while increasing temperature can reduce time to hours. Lime pretreatment removes mostly lignin, and disrupts acetyl groups and uronic acid substitution on hemicellulose (Mosier et al., 2005). This approach has been recognized as a low cost means for lignin removal (Wyman et al., 2005). However, the lime is difficult to recycle as the salt that are formed are irrecoverable (Mosier et al., 2005). This also prevents further use of lignin.

2.3.1.2. Ammonia fiber expansion (AFEX)

Biomass is subjected to 10 – 15 wt. % of anhydrous ammonia, temperatures of 70 – 90 ^oC, and pressures of 9 – 17 atm for less than 5 minutes. The explosion (rapid pressure release) of ammonia causes expansion and increase in biomass surface area. AFEX possibly depolymerizes hemicellulose and alters lignin structure thus enhancing enzymatic hydrolysis of cellulose (Wyman et al., 2005). Although, AFEX has little impact on removal of lignin and hemicellulose, it decrystalizes cellulose and deacetylates acetyl linkages. This technology has the following advantages:

i. The ammonia can be recycled.

ii. It required less expensive reaction vessels compared to that of dilute acid pre-treatment.

iii. The hydrolysate is amiable to microbes without the need for further conditioning.

iv. The residual ammonia enhances fermentation.

2.3.1.3. Soaking in aqueous ammonia (SAA)

SAA involves batch treatment whereby biomass is soaked in 12 – 18 % aqueous ammonia at a temperature between 25 – 60 ^{o}C under atmospheric pressure. Similar to AFEX, most of the cellulose and hemicellulose are not degraded. SAA alters lignin-hemicellulose bonds (Hsu, 2018). Since most of the hemicellulose is retained in the solid, recovery of cellulose or hemicellulose from effluent is unnecessary.

2.3.2. Acid pretreatment

2.3.2.1. Dilute acid

During dilute acid pretreatment, biomass is heated in 0.5 – 3.0 % sulfuric acid or hydrochloric acid at a temperature of 130 – 200 ^{o}C and a pressure of 3 – 15 atm for 2 – 30 minutes. This pretreatment technology solubilizes hemicellulose but not lignin. The lignin structure is still disrupted, thereby allowing cellulose to be accessible to enzyme during hydrolysis. Apart from being inexpensive, the use of sulfuric acid for biomass pretreatment results in high yield (~90 %) of glucose (Wyman et al., 2005). However, this process has the following disadvantages:

i. Requires costly reactor materials of construction to prevent corrosion from acid

ii. Safety concerns due to high operational pressure

iii. Neutralization and conditioning of solution requires large volumes of base

iv. Results in some non-productive binding of enzyme with lignin

v. Enzyme inhibitors reduces hydrolysis of cellulose

2.3.2.2. Controlled pH

This method involves maintaining the pH of the reactor system between 4 and7 under high pressures (6 – 14 atm), at temperatures of 190 – 200 ^{o}C for 10 – 30 minutes. The high pressure causes water to enter the cell structure, hydrating cellulose and disrupting hemicellulose and lignin. The controlled pH method results in breaking hemiacetal linkages and ether linkages. This leads to the formation of oligosaccharides and less monosaccharides compared to dilute acid method (Wyman et al., 2005). Formation of less monosaccharide lowers the synthesis of enzyme inhibitors from degraded monosaccharide.

2.4. Enzymatic Biomass Hydrolysis

2.4.1. Biomass degrading enzymes

Pretreated biomass is rich in cellulose but also contain hemicellulose and lignin. Deconstruction of plant biomass requires enzymes to facilitate hydrolysis and redox reactions. Unlike chemical and physical methods, biological processing makes use of enzymes. Enzyme processing has some advantages including mild reaction conditions, high specificity, lower energy requirement and less formation of inhibiting by-products. Since the 1990s, the enzymatic hydrolysis has been found useful to produce biomass hydrolysis (Dutta & Wu, 2014). However, release of glucose from cellulose in biomass is hindered by complex structure and presence of hemicellulose and lignin.

Biomass degrading enzymes (BDE) can be grouped into three broad categories: cellulases, hemicellulases and lignocellulose oxidoreductases. Hemicellulases and lignocellulose oxidoreductases are often referred to as accessory enzymes. As shown in Figure 9, degradation of cellulose, hemicellulose and lignin require multiple enzymes. Naturally, microbes produce

enzyme mixtures for biomass degradation (Dutta & Wu, 2014). There are more types of hemicelullases than cellulases because hemicellulose are structurally diverse than cellulose. However, most of the hemicellulases are usually produced in smaller amounts by microbes.

Table 3 shows the list and description of various BDEs. Enzymes that help in final release of glucose – the main target of biomass degradation – are most essential. The BDEs are diverse in terms of the substrate, catalytic family, shape of active sites and presence or absence of carbohydrate binding modules (CBMs). CBMs binds to cellulose thus ensures enzymes stay close to the substrate. Only the cellobiohydrolase (exoglucanases), endoglucanase, feruloyl esterase, mannanase and endo-xylanases contain CBMs (Dutta & Wu, 2014).

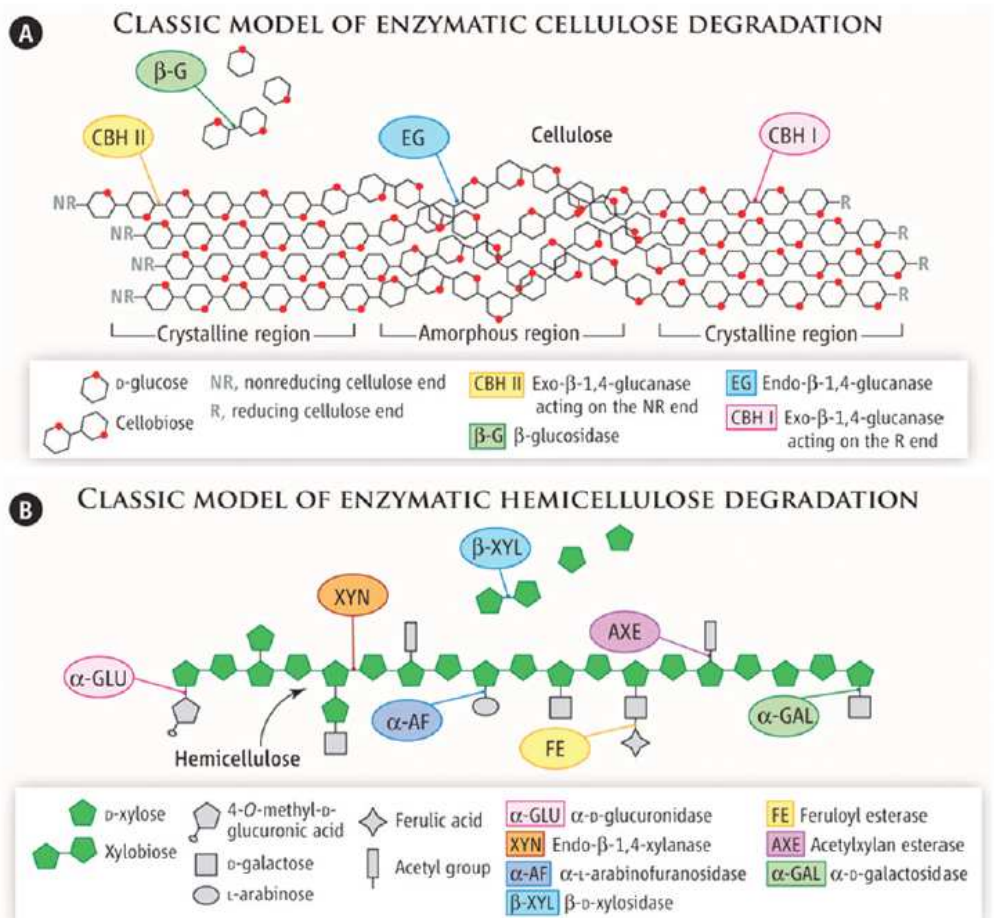

Figure 9. Classic model for enzymatic cellulose and hemicellulos degradation (Dutta & Wu, 2014)

2.4.2. Mechanisms of biomass hydrolysis

Almost all cellulases and hemicellulases are hydrolases while ligninases are classified as oxidoreductases. The carbohydrate hydrolases adopt two reaction mechanisms namely 'retaining' and 'inverting' (Figure 10). The 'retaining' mechanism is a 'double-displacement' hydrolysis of glycosidic bond the produce products of the same anomeric configuration. The 'inverting' mechanism is a 'single nucleophilic-displacement' hydrolysis of glycosidic bond that yields products of opposite anomeric configuration. Both 'retaining' and 'inverting' mechanisms involve two acidic amino acid residues (Glu or Asp) as a proton donor or general acid and as a nucleophile or base (Sweeney & Xu, 2012).

Table 3. Description of biomass degrading enzymes adapted from (Dutta & Wu, 2014)

Enzymes	Description
Cellobiohydrolase (CBHs) or Exo-β-1-4-glucosidases [c]	• Degrade crystalline cellulose and has tunnel-like actives sites • Found in GH6 (CBH-II)^{NRE}, 7 (CBH-I)^{RE} and 48 families • Many has CBMs that also support processive reactions.
Endo-1,4-β-Glucanase[C]	• Degrade amorphous cellulose and has cleft- or groove-shaped active site • Hydrolyse internal glycosidic bonds in random manner (i.e none-processive) • Very few act processively on crystalline cellulose • Belong to GH5, 7, 9, 12, 45 • and 49 families and contain CBMs
β-Glucosidases[C]	• Degrade soluble cellobioses and cellodextrins • Belong to GH1, 3 and 9 families • Active sites are pocket shaped • Act on noon-reducing end of glucose unit of cellobioses or cellodextrin • Not modular (absence of distinct CBMs)
Endo-β-Xylanases[H]	• Degrade (glucurono)(arabino)xylan • Belong to GH10, 11, 30 and 43 families • May contain CBMs or other domains
Endo-β-Xylosidase[H]	• Degrade xylobiose or other xylooligosaccharides • Belong to GH3, 30, 39, 43, 52 and 54 families. • Most exhibits α-L-arabinofuranosidase activity
Acetyl Xylan Esterase[H]	• Degrade acetyl groups at O2 and O3 sites of backbone glycosyl units of xylan or other hemicelluloses • Belong to CE1, 2, 3, 4, 5, 6, 7 and 12 families
Feruloyl Esterase[H]	• Degrade feruloyl (or other hydroxycinnamoyls) at α-L-Ara (O2 or O5 site), β-D-galactosyl (Gal, O6 site), or α-D-Xyl side chains of arabinan/arabinoxylan, rhamnogalacturonan, or xyloglucan • Belong to CE1 family • Has CBMs

Table 3. Description of biomass degrading enzymes adapted from (Dutta & Wu, 2014) (continued)

Enzymes	Description
Glycuronoyl Esterase[H]	• Demethylates demethylates O6-methyl glucuronoyl (GlcU) α(1→2) linked to backbone Xyl in glucuronoarabinoxylan • Belong to CE15 family • Has the canonical Ser-His-Asp catalytic triad
α-L-Arabinofuranosidase[H]	• Remove Ara substituents esterifying either O2, 3, or 5 site from hemicellulose • Catalytic cores belong to GH3, 43, 51, 54 and 62 families
α-Galactosidase[H]	• Remove α-glycosidic linked Gal substituents on hemicellulose • Belong to GH4, 27, 36, 57 and 110 families
α-Glucuronidase[H]	• Remove α(1→2) linked glycuronoyl or its methyl ester in xylan • Catalytic cores belong to GH67 and 15 families
Glucanase[H]	• Degrade β(1→3), (1→4), or (1→6) glucan • Belong to GH3, 5, 12, 16, 17, 55, 64, and 81 families
Mannanase[H]	• Degradd (galacto)(gluco)mannans, β(1→4)-D-mannosyl or manno/glucopyranosyl polymers with variable α(1→6) D-Gal side chain as well as O2 and/or O3 acetylation • Belong to GH5, 26, and 113 families • Possess CBMs for mannan or cellulose or other domains

Enzymes	Description
Xyloglucan Hydrolase[H]	• Hydrolyze xyloglucan, β(1→4) glucan with α(1→6) linked Xyl substituted by either α(1→2) L-Ara or β(1→2) D-Gal units (partially acetylated or substituted by α(1→2) L-fucopyranosyl (Fuc)) • Catalytic core belong to GH5, 12, 16, 44, and 74 families
Pectinase[H]	• Hydrolyze α(1→4) poly-α-(rhamno)galacturonic acids with variable backbone methylation/acetylation and Ara and Gal side chains branching • Polygalacturonases with GH28, pectin methyl esterase belong to CE8 and pectin/pectate lyases belong to PL1, 2, 3, 9, and 10 families.
Lignin peroxidase[LO] Mn peroxidase[LO] and Versatile peroxidase[LO]	• Oxidative degradation of lignin • Belong to LO2 family • Produce highly reactive Fe(V) or Fe(IV)-oxo species
Laccase[LO]	• Oxidative degradation of lignin • Belong to LO1 family • Multi-copper oxidase
Aryl-alcohol oxidase[LO] Glyoxal oxidase[LO] and various carbohydrate oxidases	• Oxidize aromatic alcohol, glyoxal, or reducing carbohydrate • Generate H_2O_2 that enhance lignin-degrading peroxidases or Fenten-type lignin degradation • Belong to LDA 1 – 6 family
Cellobiose dehydrogenase[LO]	• Dehydrogenate or oxidize cellobiose or cellodextrines to aldonolactones as well as quinone reduction to phenol or O_2 to H_2O_2 • Belong to LO3 family

[C]: Cellulase, [H]: Hemicellulase, [LO]: Lignocellulose oxidoreductases, [NRE]: non-reducing end, [RE]: reducing end, [CBMs]: carbohydrate binding modules.

The oxidoreductases in ligninases are further categorized as peroxidases, oxidases, dehydrogenases, and laccases (Guillén, Martínez, Gutiérrez, & Del Rio, 2005). The active site of some of these enzymes have high valence metals that allows electron-transfer for lignin radicalization, bond scission, or derivatization. The first ligninase to be investigated was laccase which has four copper ions as: (i) electron acceptor from substituted phenols or amines, (ii) electrons donor to reduce dioxygen to water or (iii) electron transfer intermediary involving cysteine and histidine protein residues (Guillén et al., 2005).

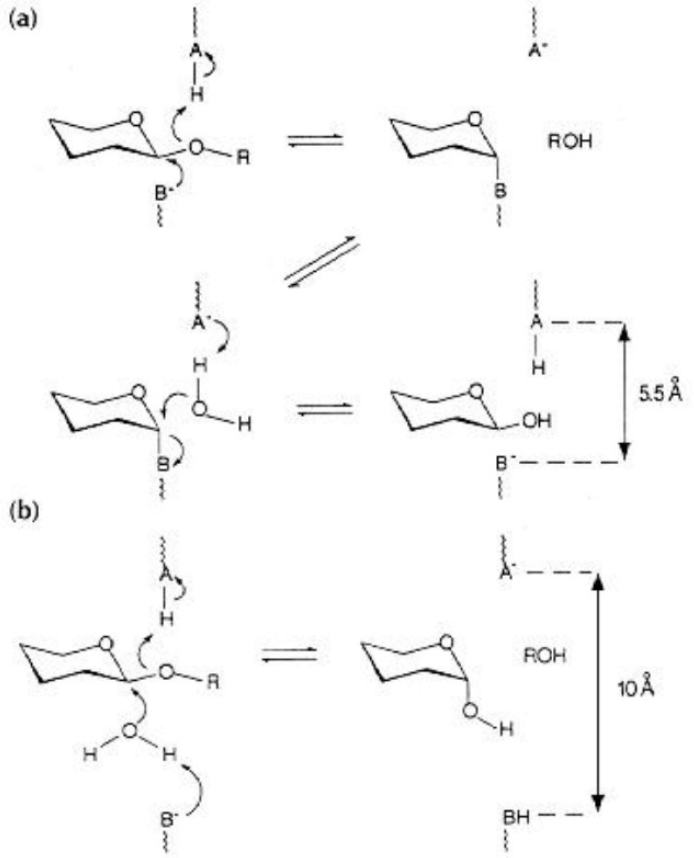

Figure 10. The two mechanism of enzymatic glycosidic bond hydrolysis (a) the retaining mechanism (b) the inverting mechanism. acid catalyst (AH), base B−, (Davies & Henrissat, 1995)

Enzyme topology (Figure 11) also relates to their substrate specificity and mode of action. The pocket or crater topology in β-glucosidases is fit for recognition of a saccharide non-

reducing extremity but not suitable for fibrous substrate like native cellulose. The cleft or groove topology in endo-1,4-β-glucanase enables a random binding of several sugar units in amorphous cellulose. The tunnel topology of cellobiohydrolases (Exo-β-1-4-glucosidases) support threading of polysaccharide chain in cellulose microcrystal. The catalytic site is engulfed in a loop that keeps the enzyme bound on the polysaccharide after cellobiose is released. This enables processive pattern of cellulose hydrolysis especially at the microcrystal region. It is possible that the loop opens occasionally to allow substrate penetration or the substrate penetrate directly from either of the opening ends of the tunnel (Davies & Henrissat, 1995).

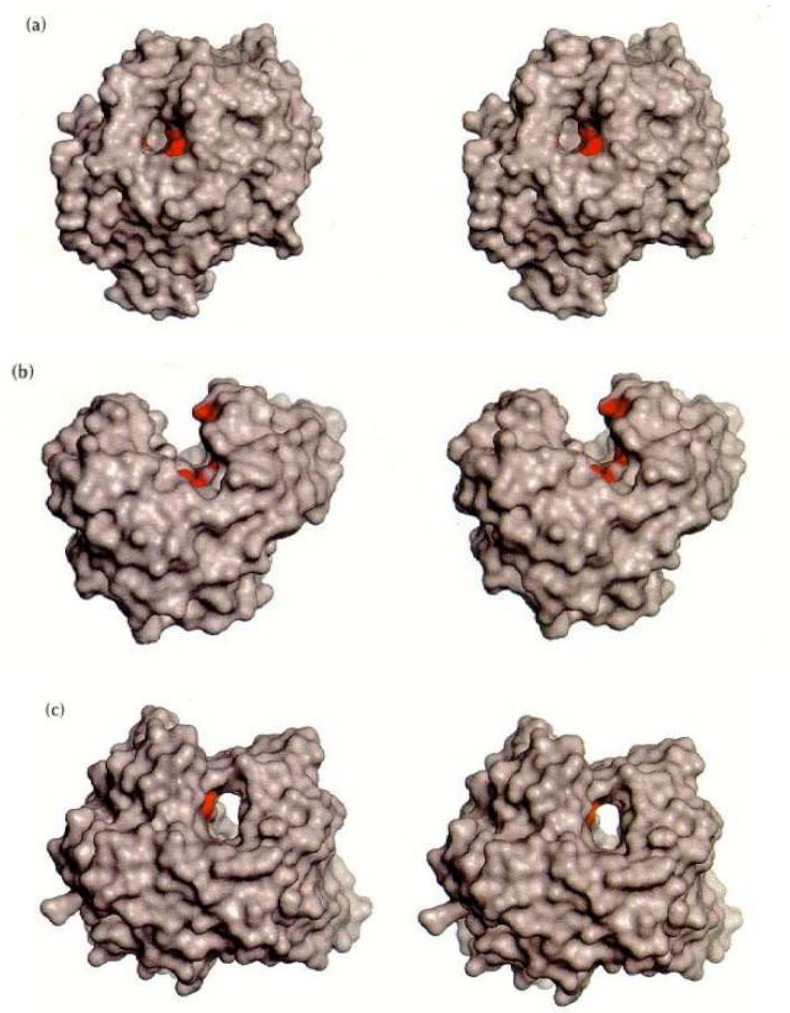

Figure 11. The topology of active site of glycosyl hydrolases (a) the pocket topology (b) the cleft topology (c) the tunnel topology. The active sites of the enzyme are shown in red color (Davies & Henrissat, 1995)

BDEs are structurally modular and have a distinct non-catalytic core but functionally important domains including CBMs, fibronectin-3 like modules, immunoglobulin-like domains, dockerins and other modules (Sweeney & Xu, 2012). These domains equip BDEs with certain functionalities. The following are examples of effects of modularity in BDEs:

i. CBMs direct and anchor BDEs to individual polysaccharide chains or single carbohydrate molecules (Sweeney & Xu, 2012).

ii. Dockerins anchor BDEs onto cellulosome scaffolding (Sweeney & Xu, 2012).

iii. Fibronectin-3 like modules modify the cellulose fiber surface to promote hydrolysis (Kataeva et al., 2002).

iv. Immunoglobulin-like domains help to stabilize the catalytic domain of enzyme (Liu et al., 2010).

v. Multiple CBMs increase the susceptibility of enzymes to non-productive lignin-binding (Sweeney & Xu, 2012). (Jenni L. Rahikainen et al., 2013). The interaction of CBMs to lignin is perhaps related to hydrophobicity and could be pH-dependent (Jenni Liisa Rahikainen et al., 2013).

2.4.3. Challenges of enzymatic biomass hydrolysis

Although, enzymatic hydrolysis of biomass is a promising option for biomass hydrolysis, the following challenges have been identified:

i. High enzyme cost

One of the major challenges of enzyme-based processes is the high enzyme cost. Enzyme cost alone is expected to contributes to about 50% hydrolysis cost and about 20% of the total cost of cellulosic bioethanol processing (Nguyenhuynh et al., 2017).

ii. Loss of activity

As proteins, enzymes are susceptible to processing stresses from mixing, temperature, pH and organic solvents. Enzymes lose their activity with time or repeated use possibly due to denaturation of enzymes or deformation of active site. In addition, enzymes lose activity due to the presence of inhibitors formed during biomass pretreatment.

iii. Product inhibition

Product inhibition has been identified as one of the major challenges of biomass hydrolysis. Product inhibition occurs when the products (glucose or cellobiose) occupy the enzyme active sites thereby reducing enzyme activity. The increase in products concentration as biochemical processes progress contributes to enzyme product inhibition (Stickel et al., 2018). Product inhibition is more predominant at high substrate loadings (Nguyenhuynh et al., 2017).

iv. Non-productive binding

Non-productive binding arises when enzyme are absorbed onto biomass components other than the targeted substrate. Non-productive binding of BDEs is predominantly associated with the presence of lignin.

2.4.4. Biomass hydrolysis at industrial scale

Biomass hydrolysis can be operated in batch or continuous modes. According to Brethauer and Wyman (2010) the basic advantages of continuous over batch processing are:

i. Reduction in reactor downtime needed for cleaning and filling
ii. Reduction in reactor size
iii. Less volumetric productivity
iv. Ease of control at steady state

Apart from the above advantages, researchers have minimized product inhibition through continuous glucose removal of during biomass hydrolysis in membrane reactors. However, most of the researchers use pure cellulose as model feedstocks. Fouling is a known problem with membrane reactors, especially when real biomass is used. Even large-pore membranes are prone to greater internal fouling and pore blockage (Stickel et al., 2018).

Another important shortcoming of membrane reactors is the loss of active enzyme. The use of microfiltration membranes results in removal of free enzyme along with glucose. Although, the use of ultrafiltration membranes allow for enzyme retention, it is achieved at the expense of membrane permeance and enzyme absorbed on biomass were unrecovered. Recent efforts to conduct continuous enzymatic hydrolysis of biomass in membrane bioreactor enabled with lignin purge resulted in loss of 50 % of enzyme (Stickel et al., 2018).

Future research efforts should explore the possibilities of higher cellulose conversion, reduction in product inhibition, higher substrate loading, and enzyme recovery. One way to achieve this is development of CSTRs capable of enzyme recovery. The third objective of our ongoing research will focus on development of CSTR with continuous enzyme recovery and reuse.

2.5. Enzyme Immobilization: An Overview of Current Trends

2.5.1. Overview of enzyme immobilization methods

Enzyme immobilization can be defined as a process of attaching enzymes to a non-enzymatic insoluble solid carrier or support. Enzymes are immobilized in order to overcome some enzymatic process challenges such as lack of stability, enzyme cost, and loss of active enzyme. In order to achieve successful enzyme immobilization, researchers use their knowledge of protein properties, carrier properties and the conjugation processing conditions. One of the reasons for enzyme immobilization is to potentially reduce enzyme process cost (Zdarta et al., 2018). Enzyme immobilization that allows easy recovery for reuse could lower enzyme cost per unit product. Also, recovery of immobilized enzymes will prevent protein contamination in reaction products (Stickel et al., 2018). Another advantage of enzyme immobilization is modulation/partitioning of the catalytic activities. For instance, enhancement of catalytic

activities achieved through synergism from close proximity of multiple enzymes. Researchers have adopted different techniques to immobilize enzymes (Figure 12).

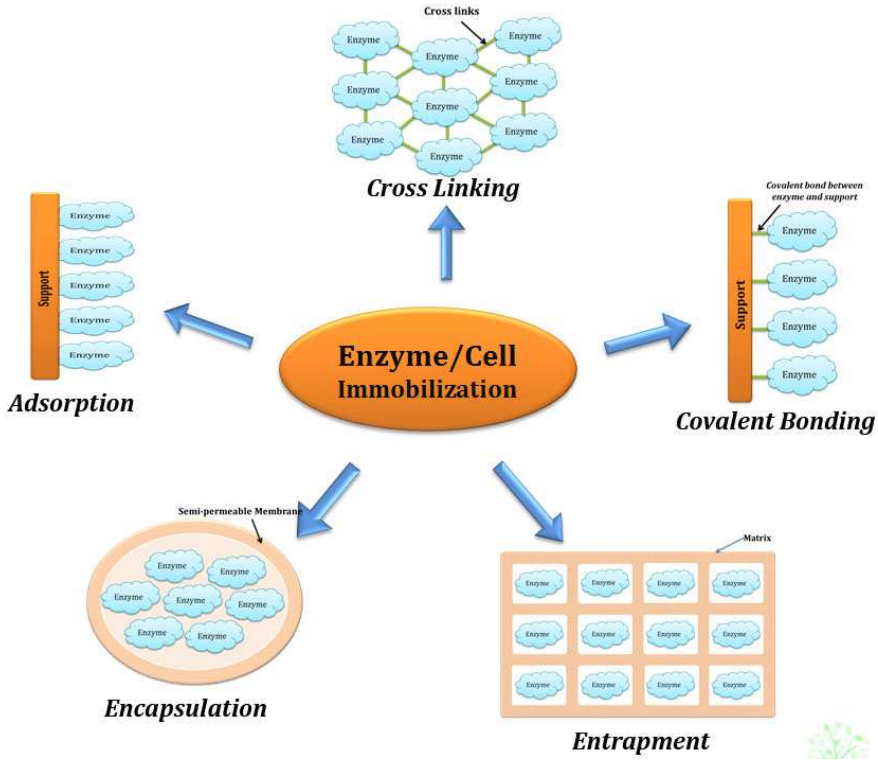

Figure 12. Types of enzyme immobilization (Sirisha, Jain, & Jain, 2016)

2.5.2. Cellulosomes

2.5.2.1. Description of Cellulosome

Cellulosomes are examples of natural immobilized enzyme systems and now referred to as natural nanomachines for dismantling plant polysaccharides (Artzi et al., 2016). Initially, cellulosomes were erroneously defined as simply cellulase aggregates. Later investigations revealed that cellulosomes are discrete multi-enzyme complexes used for the degradation of the lignocellulose in plant cell walls (Edward A. Bayer, Morag, & Lamed, 1994). Cellulosomes are produced by some anaerobic and ruminal microorganisms (e.g. *Clostridium thermocellum, C.*

cellulovorans, Ruminococcus flavefaciens, Acetivibrio cellulolyticus) (E. A. Bayer, Lamed, & Himmel, 2007).

Our understanding of cellulosome structure has increased with advances in biotechnology tools. Structurally, cellulosomes are made up of two types of building blocks (Figure 13) including (i) the dockerin-containing enzymes and (ii) the scaffoldin (Artzi et al., 2016). The scaffoldin is a linear protein structure that contains cohesin modules, dockerin modules and carbohydrate binding modules (CBMs) held together by linker protein. Cohesins and dockerins are complementary modules that bind strongly to one another.

The bindings of scaffoldin-cohesins and enzyme-dockerins (Type I interaction) help to fuse the two building blocks of cellulosome together. The bindings between the scaffoldin-dockerins and cell-surface-cohesins (Type II interaction) anchor some cellulosomes to the microbial cell surface (Arora, Behera, Sharma, & Kumar, 2015). The CBMs ensure prolonged and close association of biocatalyst with appropriate sites of cellulosic biomass substrate (Artzi et al., 2016). This association increases the hydrolysis of recalcitrant polysaccharides.

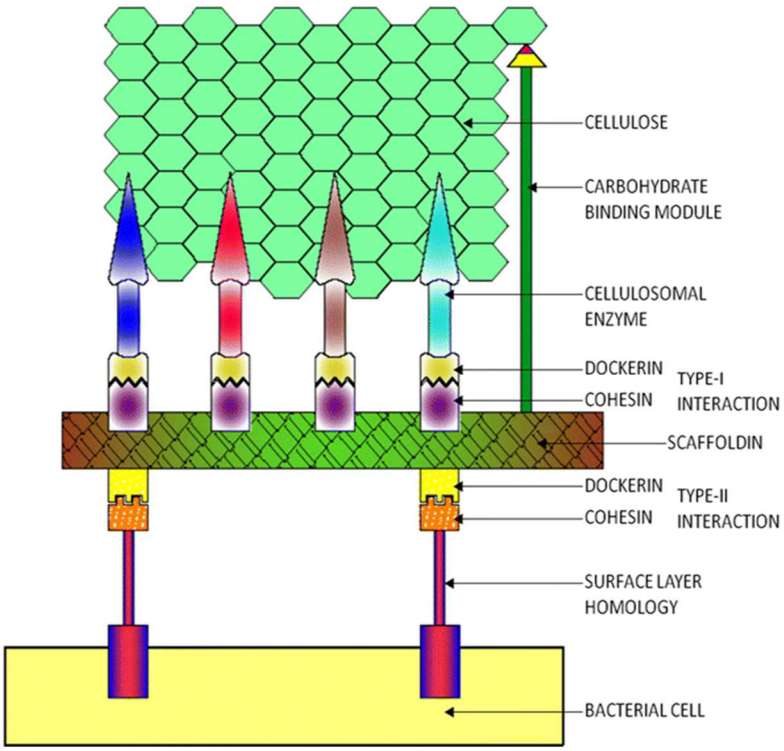

Figure 13. Schematic diagram of cellulosome attached to bacterial cell (Arora et al., 2015)

Microbes produce cellulosomes in order to achieve efficient plant biomass degradation. The advantages of cellulosomes for effective hydrolysis are as follows:

i. Enhancement of enzyme synergy and processivity by ensuring close proximity among complementary enzymes and between enzyme and substrate.
ii. Reduction of non-productive adsorption on non-targeted biomass components.
iii. Reduction of competitiveness in binding to targeted substrate.
iv. Binding and disrupting of hard to reach cellulose crystals.

There have been numerous efforts to improve enzyme functionalities by adopting cellulosome architecture. Some researchers have adopted different biotechnological strategies to engineer cellulosomes for improved and novel functionalities (Fan et al., 2016; Garvey, Klose, Fischer, Lambertz, & Commandeur, 2013; Hyeon et al., 2011; Liang, Si, Ang, & Zhao, 2014). Others have developed surface-anchored polymer brushes that mimic cellulosome design

(Cullen, Mandel, & Gopalan, 2008; Kudina et al., 2014; Landarani-Isfahani et al., 2015; Samaratunga et al., 2015; Zoppe et al., 2017). This second approach is adopted in this research work and will be reviewed in the next section.

2.5.2.2. Cellulosome inspired nano-biocatalysts

Bioprocessing and other technologies are sometimes inspired by natural phenomena. In a quest to improve biocatalysis performance, researchers have developed cellulosome-like NBCs using non-biological methods. Non-biological methods involve the use of solid polyelectrolyte composites (SPCs). An SPC is a polyelectrolyte chain grafted on solid nanoparticles. Similar to cellulosome-protein scaffolding, SPC polyelectrolyte chains provide functional groups for immobilization of multiple enzymes. The polyelectrolyte chains are brush-like and tethered similar to the appearance of cellulosomes on cell surface.

2.5.3. Cellulolytic magnetic NBCs

2.5.3.1. Description of cellulosic magnetic NBCs

The term nanobiocatalyst (NBC) refers to a nano-scale enzyme cluster with active catalytic domains. Unlike higher-scale immobilization techniques, NBCs exhibit pseudo-homogenous behavior with higher substrate accessibility simply because of their high surface to volume ratio (Roth, Schwaminger, Peng, & Berensmeier, 2016). NBCs can be homogenous or heterogeneous in terms of enzyme activity. The homogenous NBCs contain enzymes with the same catalytic activity, while the heterogeneous NBCs contain enzymes with different, but related, catalytic activities.

Magnetic NBCs contain a nano-magnetic core that exhibits superparamagnetic behavior. This behavior describes random flipping, parallel aligning of the magnetic core to the direction of external magnetic field. Without an external magnetic field, the nano-magnetic core lacks

magnetization. Hence, magnetic NBCs will not stick to reactor walls during processing in the absence of external magnetic field (Sodipo & Aziz, 2016).

Potential applications of magnetic NBCs include:

- Biosensors for analytes like glucose, hydrogen peroxide, phenol, catechol, pesticide, uric acid, cholesterol etc. (Shi et al., 2014).
- Molecular analysis using ligase for RNA-polymerase reaction (Herdt, Kim, & Taton, 2007).
- Biomedical field such as site-targeted disinfection of bacteria using β-lactamase (Tsang, Yu, Gao, & Tam, 2006).
- Biodegradation of penicillin and cephalosporins using Penicillin G acylase (Luo & Zhang, 2010).
- Bio-transesterification of oil using lipase for biodiesel production (Zhou, Chen, & Yan, 2014).
- Biomass degradation using cellulolytic enzymes for bioethanol and other biochemical production (Husain, 2017).

The use of magnetic NBCs is promising because of the easy separation procedure that allows for high enzyme recovery (Khoshnevisan et al., 2017).

2.5.3.2. Architecture and composition of cellulolytic magnetic NBCs

According to Figure 14, magnetic NBCs can be categorized into three groups: uncoated, coated and coated-grafted. The uncoated magnetic NBCs contain the metallic core and immobilized enzymes. The coated magnetic NBCs contain a coating layer on the metallic core and the enzyme, while the coated-grafted NBCs have polyelectrolyte chains on the coated metallic NBCs.

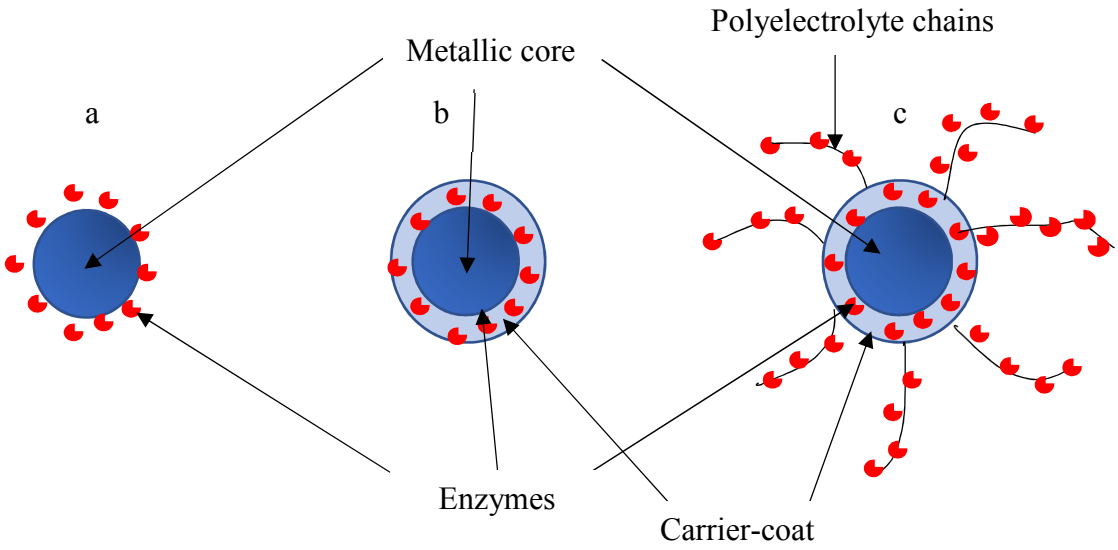

Figure 14. Schematic diagram of different architectural structure of magnetic NBCs a: uncoated, b: coated and c: coated-grafted

According to Shi et al. (2014), oxides of iron, zinc and titanium are the most used metallic oxide for production of magnetic nanoparticles. Among the three metallic oxides, iron oxide nanoparticles (FeO_4 and γ-Fe_2O_3) are the most promising because of ease of production and lack of toxicity (Shi et al., 2014). Due to high surface to volume ratio, Van der Waals forces of attraction and dipole-to-dipole interactions, bare magnetic nanoparticles possess high surface energy and therefore aggregate easily (Sodipo & Aziz, 2016). In addition, the surface chemistry of magnetic nanoparticles is incompatible with most biomolecules and lacks affinity for biological surfaces. This calls for the need to modify the surface chemistry of magnetic nanoparticles using coatings.

Coatings can cover and alter the functional groups of the magnetic nanoparticle surface; thereby, the carrier-coat serves as a functionalization agent. Apart from enabling enzyme immobilization, a suitable functionalization agent will create sufficient repulsive interaction between nanoparticles to prevent aggregation and thus stabilize the colloidal solution. In addition, coatings prevent oxidation of magnetic nanoparticles by air (Wu, He, & Jiang, 2008).

Hence, the coating is an essential component of magnetic NBCs. Magnetic NBCs have been functionalized with silica, graphene, chitosan, and amino-silanes (Khoshnevisan et al., 2017). Other notable functionalizing agents are polymers like poly(ethyleneglycol), poly(vinyl alcohol) poly(lactide acid), alginate, polymethylmethacylate, and polyacrylic acid (Wu et al., 2008).

The polyelectrolyte chains that appear tethered and brush-like, create the soft gel for enzyme immobilization. Polyelectrolytes properties can be controlled by changing pH or temperature. The polyelectrolyte soft gel compartmentalizes the enzyme environment and supports enzyme-proximity (Kudina et al., 2014). The immobilized enzymes are more dispersed in aqueous medium thus minimizing stearic hindrance of substrate mass transfer common with other immobilization technologies. The cores of SPCs are solid or magnetic materials that facilitate enzyme recovery and reuse.

Enzymes can be immobilized on magnetic nanoparticles via nonspecific physical adsorption or covalent bonding. Mechanisms for physical adsorption of enzymes on magnetic nanoparticles includes electrostatic, van der Walls and hydrophobic interactions. However, noncovalent enzyme immobilization is a challenge because of protein leakage. This problem could be overcome with covalent bonding of enzymes to magnetic nanoparticles (Khoshnevisan et al., 2017). Based on the intended application, different enzymes have been immobilized on magnetic nanoparticles. The subsequent sections will focus on the cellulolytic magnetic NBCs for lignocellulosic biomass hydrolysis.

In order to improve biocatalytic processing of lignocellulosic resources, several enzyme-aided technologies have been investigated. Among the enzyme-aided technologies, the most promising is immobilization of cellulolytic enzymes on magnetic nanoparticles. Figure 15, shows the different methods researchers have used to develop cellulolytic magnetic NBCs with

varying enhanced features. The cellulolytic magnetic NBCs vary based on the type of production method, nano-supports, cellulolytic enzymes, and immobilization modes. Cellulolytic magnetic NBCs can contain a single class of enzyme (cellulase or β-glucosidase) or a combination of cellulolytic and accessory enzymes. The immobilization mode can be covalent, adsorption, entrapment or combined (Husain, 2017).

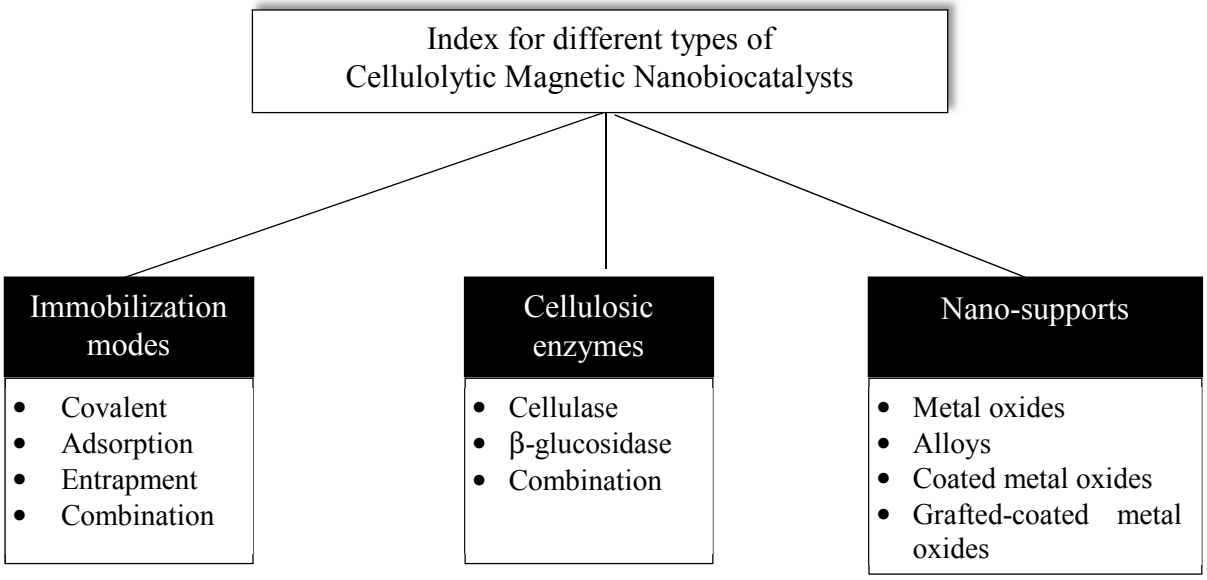

Figure 15. Index for differences in cellulolytic magnetic nanobiocatalysts

2.6. Synthesis of Cellulolytic Magnetic NBCs

2.6.1. General approach for synthesis of cellulolytic magnetic NBCs

Different approaches have been developed and used for synthesis of cellulolytic magnetic NBCs. Figure 16 shows a schematic flow chart for production of cellulolytic magnetic NBCs.

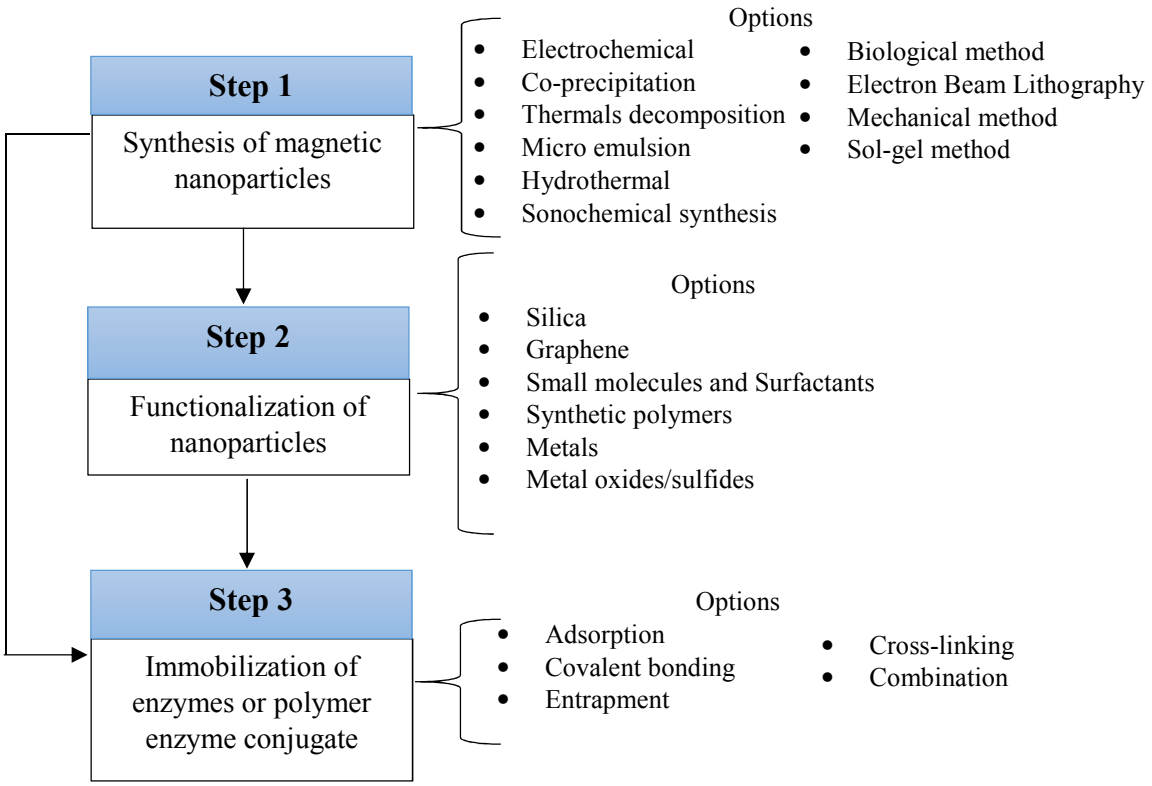

Figure 16. General production stages cellulolytic magnetic NBCs and their various options

There are a number of reaction options for each step of cellulolytic magnetic NBC synthesis. Among the various approaches for enzyme immobilization (Step 3 of Figure 17), covalent immobilization is most preferred because the strong bonds prevent enzyme leaching. The characteristics of resulting cellulolytic magnetic NBCs depend on the methods and the reaction conditions. Although it is difficult to compare the options because of differences in reaction conditions, choice of methods is based on the following criteria:

i. Dispersion of the NPs

ii. Enzyme loading

iii. Ease of the method

iv. Yield

v. Processing cost

vi. Operating temperature

vii. Scalability

According to Gupta and Gupta (2005), desirable nanoparticles should have a high magnetization value, be very small (< 100 nm), and fall in a narrow range of particle size distribution. In addition, the nanoparticles should have uniform and predictable physical and chemical properties. Industrial application of nanoparticles is viable if the processing is inexpensive, easy, and scalable.

In order to improve the methods for cellulolytic magnetic NBC synthesis and to minimize processing steps and cost, researchers have investigated the possibility of combining the processing steps. One- or two-step approaches involve combining nanoparticle synthesis with functionalization or combining all three steps into a single process. One way to reduce production steps and cost of cellulolytic magnetic NBCs is electrochemical synthesis of magnetic nanoparticles.

2.6.2. Electrosynthesis of superparamagnetic iron oxide nanoparticles

As mentioned earlier, iron oxides nanoparticles have attracted researchers' attention due to their nontoxicity to living systems. Iron oxides nanoparticles also exhibit superparamagnetic behavior and therefore referred to superparamagnetic iron oxide nanoparticles (SPIONs). Many studies have used electrochemical process to synthesize SPIONs (Ramimoghadam et al., 2014).

2.6.2.1. Mechanism of electrosynthesis of SPIONs

As shown in Figure 17, electrochemical systems consist of two electrodes (anode and cathode), electrolyte and electricity source. During the electrochemical process, electric current flows through the electrodes into the electrolytes where it triggers chemical reactions.

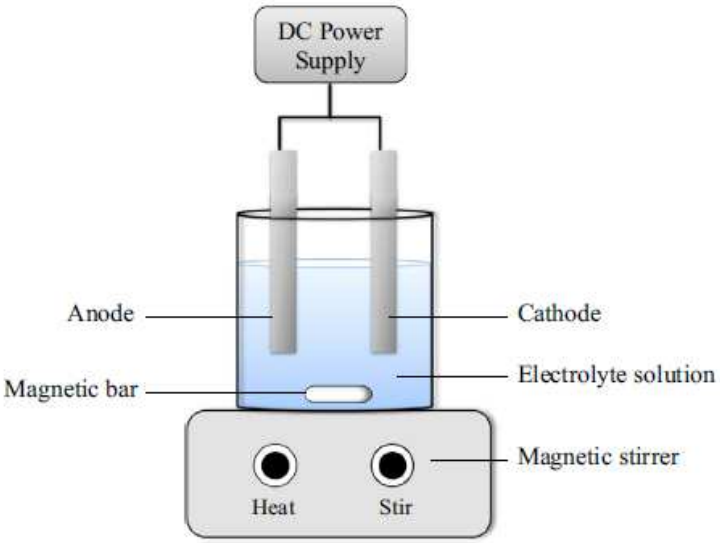

Figure 17. A typical electrochemical cell

As shown in Table 4, 12 reactions have been identified during electrosynthesis of magnetite (Fe_3O_4) and γ-maghemite (Fe_2O_3) nanoparticles. These 12 reactions are used to build Figure 18 as possible routes/pathways to depict the mechanism of electrosynthesis of SPIONs. Generation of OH^- ions is very crucial because of two reasons; the ions are a reactant for the formation of $Fe(OH)_3$, and they increase the electrolyte pH to 8-9 so it is suitable for conversion of $Fe(OH)_3$ to the superparamagnetic nanoparticles. The presence of nitrate often contributes to the increase in OH^-, suggesting the increase in the use of iron nitrate as a reactant during SPION electrosynthesis. In addition, presence of ethanol limits the amount of water, which usually hinders SPION production. The direct reaction of Fe^{3+} with O_2 was reported to be very low during electrochemical process. Presence of trace amounts of a contaminant – goethite (α-FeOOH) – has equally been reportedly (Karimzadeh et al., 2016).

Table 4. The list of reaction mechanisms for SPION electrosynthesis

No.	Reaction mechanism	Point of occurrence
1	$Fe \leftrightarrow Fe^{2+} + 2e^-$	Anode
2	$Fe^{2+} \leftrightarrow Fe^{3+} + 1e^-$	Anode
3	$H_2O \leftrightarrow 2H^+ + 2e^- + ½\ O_2$	Anode
4	$2H_2O + 2e^- \rightarrow H_2 + 2OH^-$	Cathode
5	$Fe^{3+} + 3OH^- \leftrightarrow Fe(OH)_{3(s)}$	Cathode
6	$NO_3^- + H_2O + 2e^- \rightarrow NO_2^- + 2OH^-$	Cathode
7	$3Fe(OH)_{3(s)} + H^+ + e^- \leftrightarrow Fe_3O_{4(s)} + 5\ H_2O$	Cathode
8	$3Fe(OH)_{3(s)} + e^- \leftrightarrow Fe_3O_{4(s)} + 4H_2O + OH^-$	Cathode
9	$2Fe(OH)_{3(s)} \leftrightarrow Fe_2O_{3(s)} + 3H_2O$	Cathode
10	$4Fe^{3+} + 3O_2 + 12\ e^- \rightarrow Fe_2O_{3(s)}$	Cathode
11	$CH_2CH_2OH + ½\ O_2 \rightarrow 2H^+ + 2e^- + CH_3COOH$	Anode
12	$2Fe^{2+} + 4OH^- + ½\ O_2 \rightarrow 2\alpha\text{-}FeOOH + H_2O$	Solution

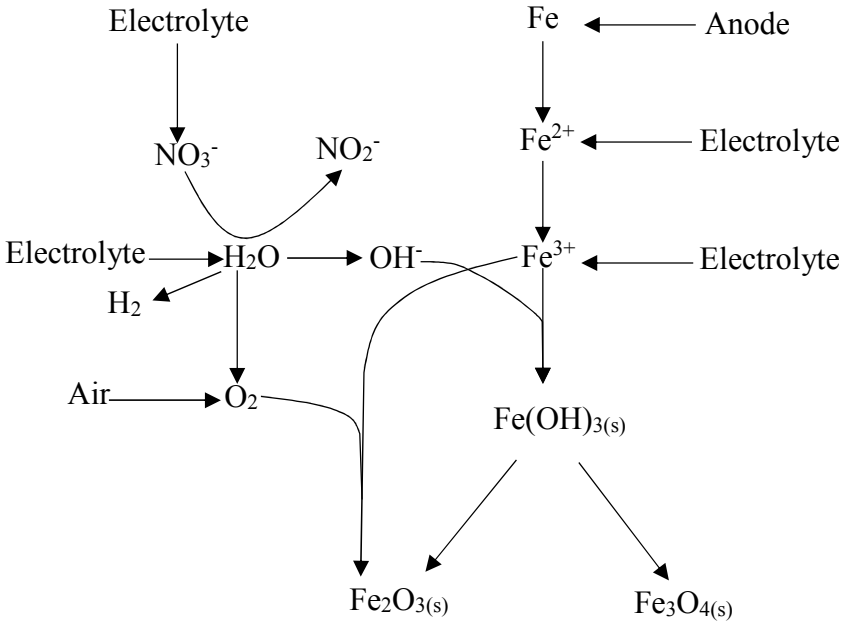

Figure 18. Reaction pathways for the formation of superparamagnetic iron nanoparticles

2.6.2.2. Advantages of electrochemical process

According to Hosik et al. (2008), electrochemical synthesis of nanoparticles has the following advantages compared to other methods:

i. Easy control

ii. Low temperature

iii. Scalable

iv. Fast

The two approaches to produce magnetic nanoparticles through electrochemical process are cathodic and anodic. Both approaches involve precipitation/deposition of the nanoparticles from the electrolytes onto the electrodes or in the electrolytes if agitated. The cathodic process involves reduction of water to produce OH^- responsible for deposition of nanoparticles at the cathode. The anodic process involves oxidation of water at the anode to produce H^+ that causes the deposition. However, anodic SPION electrosynthesis requires more expensive reagents and a high current, and produces an impure product (Karimzadeh et al., 2016).

2.6.2.3. Factors affecting SPION electrosynthesis

The factors that affect the yield and characteristic of SPIONs can be categorized as:

i. Type of electrode: inert or reactive electrodes.

ii. Reaction conditions: temperature, pH, current density, reaction time, distance between the electrodes, electrolyte concentration and type.

iii. Process mode: batch or continuous.

Most work on SPION electrosynthesis has focused on the effect of reaction conditions in a batch process using inert electrodes (Ali et al., 2016; Fajaroh, Setyawan, Widiyastuti, & Winardi, 2012; Park et al., 2008; Ramimoghadam et al., 2014; Salazar-Alvarez, Muhammed, & Zagorodni, 2006; Wu et al., 2008; C. Xu & Teja, 2008). The conclusions from those studies are:

i. Increase in voltage causes a decrease in nanoparticles size.

ii. Reaction time of 30 minutes is adequate for nanoparticle synthesis.

iii. Distance between electrodes should be less than 5 cm.

iv. Alkaline pH is necessary for nanoparticle synthesis.

2.6.3. Continuous synthesis of SPIONs

Compared to batch methods, continuous chemical SPION synthesis using a flow injection system for alkaline precipitation was reported to be more beneficial (Salazar-Alvarez et al., 2006). It was reported that this approach could be used to control the morphology of the resulting nanoparticles. Other advantages of this method are increased product reproducibility and lack of contamination (Salazar-Alvarez et al., 2006). This method, which ensures continuous separation of products from the reaction zone, prevents further reaction of products. Other approaches for continuous SPION synthesis involve the use of supercritical fluids at high pressure of 30 MPa, and temperatures of 400^{o}C (Pascu, Marre, Aymonier, & Roig, 2013; Veriansyah, Kim, Min, & Kim, 2010). Another study used hydrothermal synthesis for continuous SPION production (C. Xu & Teja, 2008). These approaches seem costly and not industrially feasible.

We are not aware of any continuous production of SPIONs in electrochemical systems that allow for continuous separation of product from the reaction zone. Continuous production in a tubular electrochemical system could allow for separation of SPIONs as they are formed. Immediate separation of growing SPIONs can eliminate continuous growth of particles thereby allowing for control of particle size. Future studies on the effect of reaction conditions in a continuous system is worthwhile.

2.7. References

Ali, A., Hira Zafar, M. Z., ul Haq, I., Phull, A. R., Ali, J. S., & Hussain, A. (2016). Synthesis, characterization, applications, and challenges of iron oxide nanoparticles. *Nanotechnology, science and applications, 9*, 49.

Arora, R., Behera, S., Sharma, N. K., & Kumar, S. (2015). Bioprospecting thermostable cellulosomes for efficient biofuel production from lignocellulosic biomass. *Bioresources and Bioprocessing, 2*(1), 38. doi: 10.1186/s40643-015-0066-4

Artzi, L., Bayer, E. A., & Moraïs, S. (2016). Cellulosomes: bacterial nanomachines for dismantling plant polysaccharides. *Nature Reviews Microbiology*.

Banerjee, S., Mudliar, S., Sen, R., Giri, B., Satpute, D., Chakrabarti, T., & Pandey, R. (2010). Commercializing lignocellulosic bioethanol: technology bottlenecks and possible remedies. *Biofuels, Bioproducts and Biorefining: Innovation for a sustainable economy, 4*(1), 77-93.

Barros, J. (2016). Greener Solvents for Making Chemicals from Biomass *Cutting-Edge Chemistry.* Retrieved 30th of June, 2017, from https://www.acs.org/content/acs/en/pressroom/cutting-edge-chemistry/greener-solvents-for-making-chemicals-from-biomass.html

Bayer, E. A., Lamed, R., & Himmel, M. E. (2007). The potential of cellulases and cellulosomes for cellulosic waste management. *Curr Opin Biotechnol, 18*.

Bayer, E. A., Morag, E., & Lamed, R. (1994). The cellulosome — A treasure-trove for biotechnology. *Trends in Biotechnology, 12*(9), 379-386. doi: http://dx.doi.org/10.1016/0167-7799(94)90039-6

Brethauer, S., & Wyman, C. E. (2010). Review: Continuous hydrolysis and fermentation for cellulosic ethanol production. *Bioresource Technology, 101*(13), 4862-4874. doi: https://doi.org/10.1016/j.biortech.2009.11.009

Brunow, G. (2008). Lignin Chemistry and its Role in Biomass Conversion *Biorefineries-Industrial Processes and Products* (pp. 151-163): Wiley-VCH Verlag GmbH.

Cheng, X.-Y., Li, Q., & Liu, C.-Z. (2012). Coproduction of hydrogen and methane via anaerobic fermentation of cornstalk waste in continuous stirred tank reactor integrated with up-flow anaerobic sludge bed. *Bioresource technology, 114*, 327-333.

Cullen, S. P., Mandel, I. C., & Gopalan, P. (2008). Surface-Anchored Poly(2-vinyl-4,4-dimethyl azlactone) Brushes as Templates for Enzyme Immobilization. *Langmuir, 24*(23), 13701-13709. doi: 10.1021/la8024952

Davies, G., & Henrissat, B. (1995). Structures and mechanisms of glycosyl hydrolases. *Structure, 3*(9), 853-859.

Dresselhaus, M. S., & Thomas, I. L. (2001). Alternative energy technologies. *Nature, 414*(6861), 332-337.

Dutta, S., & Wu, K. C.-W. (2014). Enzymatic breakdown of biomass: enzyme active sites, immobilization, and biofuel production. *Green Chemistry, 16*(11), 4615-4626.

Fajaroh, F., Setyawan, H., Widiyastuti, W., & Winardi, S. (2012). Synthesis of magnetite nanoparticles by surfactant-free electrochemical method in an aqueous system. *Advanced Powder Technology, 23*(3), 328-333. doi: https://doi.org/10.1016/j.apt.2011.04.007

Fan, L.-H., Zhang, Z.-J., Mei, S., Lu, Y.-Y., Li, M., Wang, Z.-Y., . . . Tan, T.-W. (2016). Engineering yeast with bifunctional minicellulosome and cellodextrin pathway for co-utilization of cellulose-mixed sugars. *Biotechnology for biofuels, 9*(1), 137.

Fontes, C., & Gilbert, H. J. (2010). Cellulosomes: highly efficient nanomachines designed to deconstruct plant cell wall complex carbohydrates. *Annu Rev Biochem, 79*.

Fu, C., Xiao, X., Xi, Y., Ge, Y., Chen, F., Bouton, J., . . . Wang, Z.-Y. (2011). Downregulation of cinnamyl alcohol dehydrogenase (CAD) leads to improved saccharification efficiency in switchgrass. *BioEnergy Research, 4*(3), 153-164.

Garvey, M., Klose, H., Fischer, R., Lambertz, C., & Commandeur, U. (2013). Cellulases for biomass degradation: comparing recombinant cellulase expression platforms. *Trends in Biotechnology, 31*(10), 581-593.

Gin, S., Abdelouas, A., Criscenti, L. J., Ebert, W. L., Ferrand, K., Geisler, T., . . . Vienna, J. D. (2013). An international initiative on long-term behavior of high-level nuclear waste glass. *Materials Today, 16*(6), 243-248. doi: https://doi.org/10.1016/j.mattod.2013.06.008

Gross, R. A., & Kalra, B. (2002). Biodegradable Polymers for the Environment. *science, 297*(5582), 803-807. doi: 10.1126/science.297.5582.803

Guillén, F., Martínez, M. J., Gutiérrez, A., & Del Rio, J. (2005). Biodegradation of lignocellulosics: microbial, chemical, and enzymatic aspects of the fungal attack of lignin. *International Microbiology, 8*, 195-204.

Gupta, A. K., & Gupta, M. (2005). Synthesis and surface engineering of iron oxide nanoparticles for biomedical applications. *Biomaterials, 26*(18), 3995-4021. doi: https://doi.org/10.1016/j.biomaterials.2004.10.012

Herdt, A. R., Kim, B.-S., & Taton, T. A. (2007). Encapsulated magnetic nanoparticles as supports for proteins and recyclable biocatalysts. *Bioconjugate chemistry, 18*(1), 183-189.

Hsu, T.-A. (2018). Pretreatment of biomass *Handbook on bioethanol* (pp. 179-212): Routledge.

Husain, Q. (2017). Nanomaterials Immobilized Cellulolytic Enzymes and their Industrial Applications: A. *Biol, 4*(3), 1029.

Hyeon, J. E., Jeon, W. J., Whang, S. Y., & Han, S. O. (2011). Production of minicellulosomes for the enhanced hydrolysis of cellulosic substrates by recombinant Corynebacterium glutamicum. *Enzyme and Microbial Technology, 48*(4), 371-377.

Juknys, R., Duchovskis, P., Sliesaravičius, A., Šlepetys, J., Januškaitienė, I., Brazaitytė, A., . . . Sakalauskaitė, J. (2011). Response of different agricultural plants to elevated CO2 and air temperature. *Žemdirbystė (Agriculture), 98*(3), 259-266.

Karimzadeh, I., Aghazadeh, M., Ganjali, M. R., Norouzi, P., Shirvani-Arani, S., Doroudi, T., . . . Gharailou, D. (2016). A novel method for preparation of bare and poly(vinylpyrrolidone) coated superparamagnetic iron oxide nanoparticles for biomedical applications. *Materials Letters, 179*, 5-8. doi: https://doi.org/10.1016/j.matlet.2016.05.048

Karthikeyan, O. P., Selvam, A., & Wong, J. W. (2016). Hydrolysis–acidogenesis of food waste in solid–liquid-separating continuous stirred tank reactor (SLS-CSTR) for volatile organic acid production. *Bioresource technology, 200*, 366-373.

Kataeva, I. A., Seidel, R. D., Shah, A., West, L. T., Li, X.-L., & Ljungdahl, L. G. (2002). The fibronectin type 3-like repeat from the Clostridium thermocellum cellobiohydrolase CbhA promotes hydrolysis of cellulose by modifying its surface. *Applied and environmental microbiology, 68*(9), 4292-4300.

Khoshnevisan, K., Vakhshiteh, F., Barkhi, M., Baharifar, H., Poor-Akbar, E., Zari, N., . . . Bordbar, A.-K. (2017). Immobilization of cellulase enzyme onto magnetic nanoparticles: Applications and recent advances. *Molecular Catalysis, 442*, 66-73.

Kudina, O., Zakharchenko, A., Trotsenko, O., Tokarev, A., Ionov, L., Stoychev, G., . . . Minko, S. (2014). Highly efficient phase boundary biocatalysis with enzymogel nanoparticles. *Angewandte Chemie International Edition, 53*(2), 483-487.

Landarani-Isfahani, A., Taheri-Kafrani, A., Amini, M., Mirkhani, V., Moghadam, M., Soozanipour, A., & Razmjou, A. (2015). Xylanase immobilized on novel multifunctional

hyperbranched polyglycerol-grafted magnetic nanoparticles: an efficient and robust biocatalyst. *Langmuir, 31*(33), 9219-9227.

Lee, D. (2007). *Composition of herbaceous biomass feedstocks*: North Central Sun Grant Center, South Dakota State University.

Lee, J.-W., & Jeffries, T. W. (2011). Efficiencies of acid catalysts in the hydrolysis of lignocellulosic biomass over a range of combined severity factors. *Bioresource Technology, 102*(10), 5884-5890.

Liang, Y., Si, T., Ang, E. L., & Zhao, H. (2014). Engineered pentafunctional minicellulosome for simultaneous saccharification and ethanol fermentation in Saccharomyces cerevisiae. *Applied and environmental microbiology, 80*(21), 6677-6684.

Liu, H., Pereira, J. H., Adams, P. D., Sapra, R., Simmons, B. A., & Sale, K. L. (2010). Molecular simulations provide new insights into the role of the accessory immunoglobulin-like domain of Cel9A. *FEBS letters, 584*(15), 3431-3435.

Luo, X., & Zhang, L. (2010). Immobilization of penicillin G acylase in epoxy-activated magnetic cellulose microspheres for improvement of biocatalytic stability and activities. *Biomacromolecules, 11*(11), 2896-2903.

Luterbacher, J., Alonso, D. M., & Dumesic, J. (2014). Targeted chemical upgrading of lignocellulosic biomass to platform molecules. *Green Chemistry, 16*(12), 4816-4838.

Mamman, A. S., Lee, J. M., Kim, Y. C., Hwang, I. T., Park, N. J., Hwang, Y. K., . . . Hwang, J. S. (2008). Furfural: Hemicellulose/xylosederived biochemical. *Biofuels, Bioproducts and Biorefining, 2*(5), 438-454.

Moreira, L. R., & Filho, E. X. (2008). An overview of mannan structure and mannan-degrading enzyme systems. *Applied Microbiology and Biotechnology, 79*(2), 165-178.

Mosier, N., Wyman, C., Dale, B., Elander, R., Lee, Y. Y., Holtzapple, M., & Ladisch, M. (2005). Features of promising technologies for pretreatment of lignocellulosic biomass. *Bioresource Technology, 96*(6), 673-686. doi: http://dx.doi.org/10.1016/j.biortech.2004.06.025

Nguyenhuynh, T., Nithyanandam, R., Chong, C. H., & Krishnaiah, D. (2017). A review on using membrane reactors in enzymatic hydrolysis of cellulose. *Journal of Engineering Science and Technology, 12*(4), 1129-1152.

O'sullivan, A. C. (1997). Cellulose: the structure slowly unravels. *Cellulose, 4*(3), 173-207.

Park, H., Ayala, P., Deshusses, M. A., Mulchandani, A., Choi, H., & Myung, N. V. (2008). Electrodeposition of maghemite (γ-Fe2O3) nanoparticles. *Chemical Engineering Journal, 139*(1), 208-212. doi: https://doi.org/10.1016/j.cej.2007.10.025

Pascu, O., Marre, S., Aymonier, C., & Roig, A. (2013). Ultrafast and continuous synthesis of crystalline ferrite nanoparticles in supercritical ethanol. *Nanoscale, 5*(5), 2126-2132.

Pereira-Flores, M. E., Justino, F., Ruiz-Vera, U. M., Stordal, F., Melo, A. A. M., & de Ávila Rodrigues, R. (2016). Response of soybean yield components and allocation of dry matter to increased temperature and CO2 concentration. *Australian Journal of Crop Science, 10*(6), 808.

Perlack, R. D., Wright, L. L., Turhollow, A. F., Graham, R. L., Stokes, B. J., & Erbach, D. C. (2005). Biomass as feedstock for a bioenergy and bioproducts industry: the technical feasibility of a billion-ton annual supply: DTIC Document.

Pienkos, P. T., & Zhang, M. (2009). Role of pretreatment and conditioning processes on toxicity of lignocellulosic biomass hydrolysates. *Cellulose, 16*(4), 743-762. doi: 10.1007/s10570-009-9309-x

Rahikainen, J. L., Evans, J. D., Mikander, S., Kalliola, A., Puranen, T., Tamminen, T., . . . Kruus, K. (2013). Cellulase–lignin interactions—The role of carbohydrate-binding module and pH in non-productive binding. *Enzyme and Microbial Technology, 53*(5), 315-321. doi: http://dx.doi.org/10.1016/j.enzmictec.2013.07.003

Rahikainen, J. L., Martin-Sampedro, R., Heikkinen, H., Rovio, S., Marjamaa, K., Tamminen, T., . . . Kruus, K. (2013). Inhibitory effect of lignin during cellulose bioconversion: The effect of lignin chemistry on non-productive enzyme adsorption. *Bioresource Technology, 133*, 270-278. doi: http://dx.doi.org/10.1016/j.biortech.2013.01.075

Ralph, J., Lundquist, K., Brunow, G., Lu, F., Kim, H., Schatz, P. F., . . . Boerjan, W. (2004). Lignins: Natural polymers from oxidative coupling of 4-hydroxyphenyl- propanoids. *Phytochemistry Reviews, 3*(1), 29-60. doi: 10.1023/B:PHYT.0000047809.65444.a4

Ramimoghadam, D., Bagheri, S., & Hamid, S. B. A. (2014). Progress in electrochemical synthesis of magnetic iron oxide nanoparticles. *Journal of Magnetism and Magnetic Materials, 368*, 207-229.

Robertson, J. D., Rizzello, L., Avila-Olias, M., Gaitzsch, J., Contini, C., Magoń, M. S., . . . Battaglia, G. (2016). Purification of Nanoparticles by Size and Shape. *Scientific Reports, 6*, 27494. doi: 10.1038/srep27494.

Roth, H. C., Schwaminger, S. P., Peng, F., & Berensmeier, S. (2016). Immobilization of cellulase on magnetic nanocarriers. *ChemistryOpen, 5*(3), 183-187.

Saha, B. C. (2003). Hemicellulose bioconversion. *Journal of industrial microbiology & biotechnology, 30*(5), 279-291.

Salazar-Alvarez, G., Muhammed, M., & Zagorodni, A. A. (2006). Novel flow injection synthesis of iron oxide nanoparticles with narrow size distribution. *Chemical Engineering Science, 61*(14), 4625-4633. doi: https://doi.org/10.1016/j.ces.2006.02.032

Samaratunga, A., Kudina, O., Nahar, N., Zakharchenko, A., Minko, S., Voronov, A., & Pryor, S. W. (2015). Modeling the Effect of pH and Temperature for Cellulases Immobilized on Enzymogel Nanoparticles. *Applied biochemistry and biotechnology, 176*(4), 1114-1130.

Shi, X., Gu, W., Li, B., Chen, N., Zhao, K., & Xian, Y. (2014). Enzymatic biosensors based on the use of metal oxide nanoparticles. *Microchimica Acta, 181*(1), 1-22. doi: 10.1007/s00604-013-1069-5

Sirisha, V. L., Jain, A., & Jain, A. (2016). Enzyme Immobilization. *Advances in Food and Nutrition Research, 79*, 179-211. doi: http://dx.doi.org/10.1016/bs.afnr.2016.07.004

Sluiter, A., Hames, B., Hyman, D., Payne, C., Ruiz, R., Scarlata, C., . . . Wolfe, J. (2008). Determination of total solids in biomass and total dissolved solids in liquid process samples. *National Renewable Energy Laboratory, Golden, CO, NREL Technical Report No. NREL/TP-510-42621*, 1-6.

Sodipo, B. K., & Aziz, A. A. (2016). Recent advances in synthesis and surface modification of superparamagnetic iron oxide nanoparticles with silica. *Journal of Magnetism and Magnetic Materials, 416*, 275-291.

Stickel, J. J., Adhikari, B., Sievers, D. A., & Pellegrino, J. (2018). Continuous enzymatic hydrolysis of lignocellulosic biomass in a membrane-reactor system. *Journal of Chemical Technology & Biotechnology*.

Sweeney, M. D., & Xu, F. (2012). Biomass converting enzymes as industrial biocatalysts for fuels and chemicals: recent developments. *Catalysts, 2*(2), 244-263.

Tsang, S. C., Yu, C. H., Gao, X., & Tam, K. (2006). Silica-encapsulated nanomagnetic particle as a new recoverable biocatalyst carrier. *The Journal of Physical Chemistry B, 110*(34), 16914-16922.

Tuck, C. O., Pérez, E., Horváth, I. T., Sheldon, R. A., & Poliakoff, M. (2012). Valorization of Biomass: Deriving More Value from Waste. *science, 337*(6095), 695-699. doi: 10.1126/science.1218930

Vanholme, R., Demedts, B., Morreel, K., Ralph, J., & Boerjan, W. (2010). Lignin biosynthesis and structure. *Plant Physiology, 153*(3), 895-905.

Veriansyah, B., Kim, J.-D., Min, B. K., & Kim, J. (2010). Continuous synthesis of magnetite nanoparticles in supercritical methanol. *Materials Letters, 64*(20), 2197-2200. doi: https://doi.org/10.1016/j.matlet.2010.07.018

Wu, W., He, Q., & Jiang, C. (2008). Magnetic Iron Oxide Nanoparticles: Synthesis and Surface Functionalization Strategies. *Nanoscale Research Letters, 3*(11), 397-415. doi: 10.1007/s11671-008-9174-9

Wyman, C. E., Dale, B. E., Elander, R. T., Holtzapple, M., Ladisch, M. R., & Lee, Y. Y. (2005). Coordinated development of leading biomass pretreatment technologies. *Bioresource Technology, 96*(18), 1959-1966. doi: http://dx.doi.org/10.1016/j.biortech.2005.01.010

Xu, B., Escamilla-Treviño, L. L., Sathitsuksanoh, N., Shen, Z., Shen, H., Percival Zhang, Y. H., . . . Zhao, B. (2011). Silencing of 4-coumarate: coenzyme A ligase in switchgrass leads to reduced lignin content and improved fermentable sugar yields for biofuel production. *New phytologist, 192*(3), 611-625.

Xu, C., & Teja, A. S. (2008). Continuous hydrothermal synthesis of iron oxide and PVA-protected iron oxide nanoparticles. *The Journal of Supercritical Fluids, 44*(1), 85-91. doi: https://doi.org/10.1016/j.supflu.2007.09.033

Yuan, X., & Cheng, G. (2015). From cellulose fibrils to single chains: understanding cellulose dissolution in ionic liquids. *Physical Chemistry Chemical Physics, 17*(47), 31592-31607.

Zdarta, J., Meyer, A., Jesionowski, T., & Pinelo, M. (2018). A general overview of support materials for enzyme immobilization: Characteristics, properties, practical utility. *Catalysts, 8*(2), 92.

Zhou, C., & Wu, Q. (2012). Recent development in applications of cellulose nanocrystals for advanced polymer-based nanocomposites by novel fabrication strategies *Nanocrystals-synthesis, characterization and applications*: Intech.

Zhou, G.-x., Chen, G.-y., & Yan, B.-b. (2014). Biodiesel production in a magnetically-stabilized, fluidized bed reactor with an immobilized lipase in magnetic chitosan microspheres. *Biotechnology Letters, 36*(1), 63-68. doi: 10.1007/s10529-013-1336-x

Zoppe, J. O., Ataman, N. C., Mocny, P., Wang, J., Moraes, J., & Klok, H.-A. (2017). Surface-Initiated Controlled Radical Polymerization: State-of-the-Art, Opportunities, and Challenges in Surface and Interface Engineering with Polymer Brushes. *Chemical Reviews, 117*(3), 1105-1318. doi: 10.1021/acs.chemrev.6b00314.

3. PROBLEM STATEMENT AND OBJECTIVES

3.1. Problem Statement

Although the economics of biomass hydrolysis could be improved through cellulase recovery for reuse, most recovery methods only capture a fraction of enzymes from spent biomass or hydrolysates. Also, the enzyme recovery methods usually require additional costly steps. Recent studies have shown that cellulolytic magnetic NBCs (magnetic nanoparticles containing immobilized cellulases) could support easier and less expensive recovery and reuse. However, industrial application is questionable because the current production routes of cellulolytic magnetic NBCs are cumbersome and challenging.

Enzymes are sensitive to their immediate environment. The immediate environment of MNBC enzymes includes polymer ligands and SPIONs. The presence of polymer ligands during enzymatic hydrolysis of biomass could adversely affect enzyme efficacy in a number of ways. The polymers could act as a physical barrier between enzyme and substrate restricting enzyme-substrate interaction. Since polymers are susceptible to hydrolysis temperature and pH, their conformation can change and alter the attached enzymes proximity. The polymer chemical properties, most especially amphiphilicity, has equally been reported to alter biomass surface activity which eventually affects enzyme-substrate binding.

Magnetic NBCs may require magnetic particles like SPIONs in order to become magnetic. Research evidence has shown that production methods affect SPION properties such as size distribution and morphology. Conventional chemical precipitation methods are simple but difficult to control and the resulting nanoparticles have a broad size range and irregular morphology (Park et al., 2008). Although, thermal methods produce monodispersed nanoparticles, they involve the use of high temperatures (100 – 300^{o}C), require toxic and

expensive reagents, and lack the ability to control nanoparticle morphology including shape and size distribution (Park et al., 2008). Monodispersed nanoparticles can be produced by a variety of techniques but some require expensive alkoxide reactants, high temperature and long reaction times (Fajaroh, Setyawan, Widiyastuti, & Winardi, 2012). Alternatively, anodic electrochemical methods have also been identified as promising for nanoparticle synthesis, but are complicated because they require high voltages, and the presence of chemicals (surfactant). Cathodic electrochemical methods could possibly overcome the drawbacks of anodic electrochemical method, but the synthesized nanoparticles often contain impurities such as FeOOH (Karimzadeh et al., 2016). Many studies have reported that SPIONs adhere on the electrodes surface during electrosynthesis. The covering caused reduction in electrode electrical conductivity and irregular current distribution, respectively, reducing the system productivity and widening particle size distribution of SPION.

Furthermore, surface dissolution and aggregation are known problem of SPIONs and will impact MNBCs. Aggregation of SPIONs will reduce available surface for enzyme immobilization, thus reducing the amount of enzyme that could have been attached. Also aggregated SPIONs are not well dispersed during the reaction and will reduce MNBC interaction with the substrate. SPION surfaces also contain OH^- functional groups that are reactive in acid solutions. These functional groups react easily with surrounding oxygen molecules that eventually result in surface corrosion. Since SPIONs are responsible for the magnetic property of MNBCs, their dissolution mean MNBCs may no longer be magnetically recoverable.

3.2. Research Objectives

3.2.1. Goal

The goal of this research is to develop and characterize cellulolytic magnetic NBCs for hydrolysis of pretreated lignocellulosic biomass.

3.2.2. Hypotheses and specific objectives

In order to achieve the main goal, the following three hypotheses and objectives have been set.

1	Hypothesis	Cellulase efficacy and membrane recovery during biomass hydrolysis could be affected by covalently grafting to polymer.
	Objective	To quantify the effect of polymer enzyme conjugation on enzyme efficacy and membrane recovery during biomass hydrolysis using acid- and alkaline-pretreated biomass.
2	Hypothesis	The yield, purity, and particle size distribution of SPIONs are dependent on the flow rate, electrolyte concentration, pH and current density during tubular electrosynthesis.
	Objective	To develop a continuous tubular electrochemical SPION production synthesis method with improved yield, controlled particle distribution, and reduced electrolyte use.
3	Hypothesis	The concentration Na-silicate could affect productivity and morphology of silica-coated SPIONs (Si-SPIONs) via TES and PEC adsorption on Si-SPION could affect cellulolytic magnetic NBC efficacy and reuse.
	Objective	To synthesize cellulolytic magnetic NBCs from Si-SPIONs for biomass hydrolysis.

3.3. References

Fajaroh, F., Setyawan, H., Widiyastuti, W., & Winardi, S. (2012). Synthesis of magnetite nanoparticles by surfactant-free electrochemical method in an aqueous system. *Advanced Powder Technology*, *23*(3), 328–333. https://doi.org/10.1016/j.apt.2011.04.007

Karimzadeh, I., Aghazadeh, M., Ganjali, M. R., Norouzi, P., Shirvani-Arani, S., Doroudi, T., … Gharailou, D. (2016). A novel method for preparation of bare and poly(vinylpyrrolidone) coated superparamagnetic iron oxide nanoparticles for biomedical applications. *Materials Letters*, *179*, 5–8. https://doi.org/10.1016/j.matlet.2016.05.048

Park, H., Ayala, P., Deshusses, M. A., Mulchandani, A., Choi, H., & Myung, N. V. (2008). Electrodeposition of maghemite (γ-Fe2O3) nanoparticles. *Chemical Engineering Journal*, *139*(1), 208–212. https://doi.org/10.1016/j.cej.2007.10.025

4. GLUCAN CONVERSION AND MEMBRANE RECOVERY OF BIOMIMETIC CELLULOSOMES DURING LIGNOCELLULOSIC BIOMASS HYDROLYSIS[1]

4.1. Abstract

Enzyme immobilization has been identified as one way to recycle enzymes for reducing high processing costs during enzymatic hydrolysis of lignocellulosic materials. However, most immobilization methods have not been attractive to lignocellulosic processing plants. In this study, cellulase enzymes were attached to a copolymer of glycidyl methacrylate (GMA) and poly(ethylene glycol) methyl ether methacrylate (PEGMA) to make polymer-enzyme conjugates (PECs) and facilitate recovery using a 50-kDa molecular weight cutoff membrane. Glucan conversion during biomass hydrolysis was investigated using PECs and PECs recovered after an initial hydrolysis step. Enzyme immobilization on PECs did not reduce effectiveness during the initial hydrolysis stage. Temperature and pH have similar effects on free enzymes and PECs. PECs facilitated higher conversion rates than free enzymes at high biomass loadings. Recovered PECs could achieve about 100% glucan conversion in a subsequent hydrolysis step when supplemented with 40% of the free enzyme used in the first stage. The combination of PECs and membrane recovery has the potential to reduce hydrolysis cost during cellulosic bioprocessing.

4.2. Keywords

Membrane recovery; Enzyme immobilization; Lignocellulose hydrolysis; Biomimetic cellulosomes.

[1] This paper is published in Applied Biochemistry Biotechnology journal. Cited as: Hammed, A., Polunin, Y., Voronov, A. et al. Glucan Conversion and Membrane Recovery of Biomimetic Cellulosomes During Lignocellulosic Biomass Hydrolysis. Applied Biochemistry Biotechnology (2021). https://doi.org/10.1007/s12010-021-03569-x. Ademola Hammed had primary responsibility of conducting, collecting, and analyzing laboratory data under direct supervision of Polunin Yehor helped with material synthesis, Dr. Scott W. Pryor. and Dr. Voronov helped in proofreading.

4.3. Introduction

Environmental concerns stemming from decades of fossil fuel use have become a driving force in the pursuit of biomass-based manufacturing (Gross & Kalra, 2002). Among various forms of biomass, lignocellulosic biomass (LB) – stems or leaves of grasses and woody plants – are the most abundant resource (Gross & Kalra, 2002). However, LB cellulose and hemicellulose are tightly intertwined with lignin resulting in a rigid structure resistant to enzymatic hydrolysis, thereby making hydrolysis challenging and expensive (D. Lee, Owens, Boe, & Jeranyama, 2007). The lack of inexpensive processing of LB cellulose is a possible reason why most cellulosic ethanol plants have been either been put on hold or idled (Padella, O'Connell, & Prussi, 2019).

LB hydrolysis can be achieved through either chemical or biological processing. Biological hydrolysis involves the use of enzymes and has been recognized to be more economical and environmentally-friendly than chemical processing (F.-Y. Wang, Li, Liu, & Liu, 2015). Other advantages of using enzymes include high reaction specificity and less formation of fermentation-inhibiting by-products (Dutta & Wu, 2014). However, the high price of enzymes still contributes significantly to LB hydrolysis costs (Nguyenhuynh, Nithyanandam, Hwa Chong, & Krishnaiah, 2017; Stickel, Adhikari, Sievers, & Pellegrino, 2018). Many research efforts on enzymatic biomass hydrolysis have focused on process optimization, biomass pretreatment, and enzyme recycling (Cassales, de Souza-Cruz, Rech, & Záchia Ayub, 2011; Jiang et al., 2017; Torabi, Satari, & Hassan-Beygi, 2020; Xiong et al., 2020). Enzyme immobilization and recycling via membrane separation are promising technologies to recycle enzymes and thereby reduce overall bioprocessing costs.

Cellulosomes are natural structures made of flexible protein scaffolds with attached cellulases and other supplementary enzymes, and have been shown to be efficient in LB hydrolysis. Cellulase enzymes can be immobilized on polymer chains to make polymer-enzyme conjugates (PECs) that function as artificial cellulosomes. Other artificial cellulosome systems have increased hydrolysis rates or yields by improving enzyme processivity, synergy, or enzyme-substrate interactions (Ying Wang et al., 2019). Although natural cellulosomes contain a combination of enzymes that enables synergistic interactions, a primary motivation for artificial cellulosomes can be to facilitate recovery and reuse of these biological catalysts. However, most studies on artificial cellulosomes have used enzymes at concentrations that were too low for industrial applications (Budinova, Mori, Tanaka, & Kamiya, 2018; C. C. Lee, Kibblewhite, Paavola, Orts, & Wagschal, 2017; Lu et al., 2019; Mori et al., 2013; Sun & Chen, 2016). Similar to other immobilization methods, PEC synthesis includes additional costs due to immobilization supports and reaction processes. PEC recovery and reuse could potentially offset these production costs to reduce overall processing costs.

In order to improve cost efficiency of biomass enzymatic hydrolysis, several studies have used membrane filtration to recover enzymes from the solution. Membrane filtration systems are attractive because they can be used under mild conditions that do not affect enzyme activity (Saltik, Özkan, Jacobs, & van der Padt, 2016). Enzyme recovery typically requires small membranes with pore sizes ranging between 1 and 10 kDa (Winarni et al., 2013). An overview of these enzyme recovery studies shows that about 55 - 60% of enzymes typically remain in solution after separation following hydrolysis (Knutsen & Davis, 2004). However, fouling is a major challenge in industrial applications of membrane technology. Membrane recovery of PECs could potentially reduce protein deposition, adsorption, and accumulation because PECs are

larger than free enzymes, and can therefore be more easily recovered using larger-pore membranes (Harrison, Todd, Rudge, & Petrides, 2015).

The aim of this study was to quantify the effect of polymer enzyme conjugation on enzyme efficacy during biomass hydrolysis using acid- and alkaline-pretreated biomass. Testing included hydrolysis under different conditions including temperature, pH, and biomass loading. Membrane recovery was used to separate PECs after hydrolysis, and effectiveness of the recovered PECs were determined in subsequent hydrolysis experiments. We determined the amount of enzyme reduction enabled by reusing recovered PECs during subsequent biomass hydrolysis.

4.4. Methods

4.4.1. Polymer synthesis and characterization

The polymer ligand (Poly(GMA-*co*-PEGMA)) for enzyme immobilization was a copolymer of glycidyl methacrylate (GMA), and poly(ethylene glycol) methyl ether methacrylate ($PEGMA_{300}$ –average molecular weight 300 g/mol). Poly(GMA-*co*-PEGMA) was synthesized by free radical polymerization in solution using 0.3:0.7 ratio of GMA to PEGMA (Yadavalli et al., 2017). Prior to synthesis, GMA and PEGMA were purified using prepacked column and filtered through a 0.2-µm syringe filter. Monomer mixture and 2,2′-Azobis (2-methylpropionitrile) initiator was dissolved in methyl ethyl ketone (MEK) at 0.5 M and 0.01M, respectively. After purging with nitrogen for 45 min, the polymerization was initiated by placing the reaction mixture in a 50^{o}C water bath for 20 h under continuous stirring. The reaction was quenched by opening the flask and allowed reaction mixture to cool at room temperature. Resultant poly(GMA-*co*-PEGMA) was purified by multiple precipitation using diethyl ether. To determine copolymer composition using ^{1}H NMR spectroscopy, polymer sample was dissolved

in deuterated water. ^{1}H NMR spectra of sample were recorded with an AVANCE III HDTM 400 MHz high-performance digital NMR spectrometer at 22.5°C. The weight and number average molecular weight of the poly(GMA-*co*-PEGMA) was determined by gel permeation chromatography (Mn and PDI values of 22,800 g/mol and 2.17, respectively).

4.4.2. Synthesis and characterization of polymer-enzyme conjugates (PECs)

Conjugation of cellulase enzymes (Cellic CTec, from Novozymes A/S, Demark) was conducted by mixing 200-µg equivalents of cellulase enzymes and 50 ml of phosphate buffer (pH 7.4, 10 mM) and stirred for 10 min. Then 12 ml of the 25% (w/w) polymer aqueous solution was added dropwise to the enzyme-phosphate buffer pre-mixture under vigorous stirring for 4.5 h at room temperature. Citrate buffer (pH 4.6, 100 mM) was added to bring to 100 ml of total volume and stirred for an additional 15 min. 1 M citric acid was used to adjust to a pH of 4.6. The resultant PECs were stored at 4ºC.

PEC conjugation efficiency was determined using the Bradford assay to quantify enzyme concentration before and after dialysis. A PEC stock solution (0.1 ml) was diluted in 5.9 ml of citrate buffer (pH 4.6) to a final enzyme concentration of 50 µg/ml. The conjugates were transferred into membrane tubes with a 50-kDa cut-off and dialyzed for 24 h to allow free enzymes to pass through while retaining PECs. Enzyme concentrations before and after dialysis were determined by the Bradford protein assay. A 0.1 ml of conjugate solution was mixed with 1 ml of the Bradford reagent and incubated at room temperature for 5 min. UV-Vis absorbance was measured against a blank solution at 595 nm. The enzyme concentration was calculated using a calibration plot obtained for the Bovine serum albumin (BSA) standard. The conjugation efficiency was calculated from the difference in the concentration of enzymes before and after dialysis.

The conversion of glucan during hydrolysis of carboxymethyl cellulose (CMC) – a soluble substrate – was determined using commercial bicinchonicnic acid (BCA) assay kit. A fresh BCA solution was prepared for each experiment. Reagents A (ligand and salts) and B (cupric sulfate solution) of the kit were mixed in a ratio of 50:1. The reaction mixture (0.03 ml) was mixed with the freshly prepared BCA solution at 37°C for 50 min to allow color formation from the redox reaction of the released reducing sugars and chelated copper ions. The samples were analyzed using UV-Vis spectroscopy at 560 nm. The concentration of reducing sugars was quantified using a calibration plot obtained with a glucose standard.

4.4.3. Biomass pretreatment

Switchgrass, *Panicum virgatum*, samples were subjected to either alkali or acid pretreatment. Acid pretreatment of 200 g of switchgrass was done using 3 L of 1% sulfuric acid (w/w) solution in an autoclave reactor (5L Hastelloy Kiloclave, Büchi AG; Switzerland) at 140^{o}C with continuous stirring at 62 rpm for 20 min. Soak in aqueous ammonia pretreatment was conducted using 10% (w/v) aqueous ammonia at 1:6 solid-liquid ratio in a 1-L screw-capped Pryex bottle at 60^{o}C for 24 h. The pretreated samples were washed with distilled water until the pH reached approximately 6.5 or 7.5 for acid and alkali pretreated samples, respectively. The solid pretreated biomass samples were drained using four layers of cheese cloth and stored at -20^{o}C until needed.

4.4.4. Biomass hydrolysis

Hydrolysis of alkaline- and acid-pretreated switchgrass was tested using free enzymes (FE) and PECs in 50-ml Erlenmeyer flasks with a working volume of 25 ml. The hydrolysis mixture contained FE or PECs (12 FPU equivalent per gram of cellulose), 0.04% sodium azide (to prevent microbial contamination), and biomass sample (as per experimental design) in

sodium citrate buffer. The hydrolysis conditions were varied with temperatures of 45 – 65ºC, and pH of 4 – 5.5, and biomass loading of 1 – 3% (w/v) glucan equivalent according to the experimental design. All hydrolysis experiments were conducted at 130 rpm. Xylanase (Cellic HTec - Novozymes; Denmark) (30 XU per flask) was added to alkaline-pretreated switchgrass in order to ensure xylan hydrolysis. Samples (2 ml) were collected after 12, 24, 48 and 72 h, centrifuged at 13,000 rpm for 5 min, and filtered through a 0.2-µm nylon filter (Pall Corporation; West Chester, PA, USA). All filtered samples were stored at -20°C for glucose analysis. Similar steps were followed for glucose inhibition study with the addition of 45 and 90 mg/ml glucose concentrations.

4.4.5. Membrane enzyme recovery

Hydrolysis with PECs was conducted using in duplicate 1-L flasks, each containing 250 mL total working volume. Hydrolysate was separated from residual solids using vacuum filtration in a 3-L Buchner funnel through a Whatman filter paper and washed with 100 mL of sodium citrate buffer at pH 4.5. The PECs in the hydrolysate were recovered using tangential field filtration (TFF Centramate^{TM} 500 S, Pall Life Sciences; East Hillis, NY, USA) with a 50-kDa molecular weight cutoff membrane (Omega Centramate™, Pall Corporation; Hauppauge, NY, USA). The TFF operation pressure was less than 0.3 MPa. A fresh 500-ml volume of citrate buffer (pH 4.5) was introduced to the retentate during ultrafiltration. The glucose and protein contents of retentate and permeate were measured. The retentate was used to perform another round of hydrolysis.

4.4.6. Glucose analysis

The amount of glucose released during hydrolysis of pretreated biomass was determined using High Performance Liquid Chromatography (HPLC Waters Corporation; Milford, MA,

USA). The parameters that were used during HPLC analysis were 20-µL injection volume, 18-mΩ nanopure water mobile phase, 50°C column temperature, 85°C detector temperature, and 0.6 ml/min flow rate. A Bio-Rad Aminex HPX-87P column (Bio-Rad Laboratories; Hercules, CA, USA) and refractive index (RI) detector (model 2414, Waters Corporation) were used for separation and quantification. The amount of sugar released at each hydrolysis sampling time was compared to the initial amount in the pretreated biomass to calculate the conversion percentage.

4.4.7. Protein analysis

Protein content of hydrolysate and retentate were analyzed using Bradford method with protein dye (Bio-Rad). Bovine serum albumin at concentration range of 0.1 – 1.4 mg/ml was used to construct a standard curve. After addition of 5 ml of Bradford reagent to 0.1 ml of sample and a 15-min incubation period at room temperature, the absorption was measured at 595 nm. The enzyme recovery was calculated using Equation 4.1.

$$\text{Enzyme recovery (\%)} = \frac{C_1 \times V_1}{C_0 \times V_0} \times 100 \qquad \text{(Equation 4.1)}$$

Where C_0 and C_1 are the initial hydrolysate and retentate protein concentrations, respectively, and V_0 and V_1 are of hydrolysate and retentate volume, respectively.

4.5. Results and Discussion

4.5.1. Characteristics of polymer ligands and polymer enzyme conjugates

^{1}H NMR spectrum (Figure 19) shows chemical structure and confirms copolymer composition of poly(GMA-*co*-PEGMA) where the experimental molar ratio of GMA to PEGMA in copolymer is determined to be 0.34 to 0.66, which is close to the calculated ratio of 0.3 to 0.7. The copolymer was used as a scaffold in the conjugation reaction with the cellulase enzyme mixture to generate the PECs. The conjugation of enzymes with the poly(GMA-*co*-PEGMA)

described by reaction between epoxy functional groups of the copolymer with amino groups of the lysine residuals present on the exterior of the enzymes' molecules. The analysis of PEC protein before and after dialysis shows that 84% of initial protein (enzyme) amount used in reaction were conjugated to the polymer ligand. The biocatalytic activity of purified PECs was estimated based on the results of reducing sugar where CMC (2% solution) was used as a substrate for both free and conjugated enzymes. The amounts of reducing sugar were 721±10 and 546±12 µg/ml, respectively, for PECs and free enzymes.

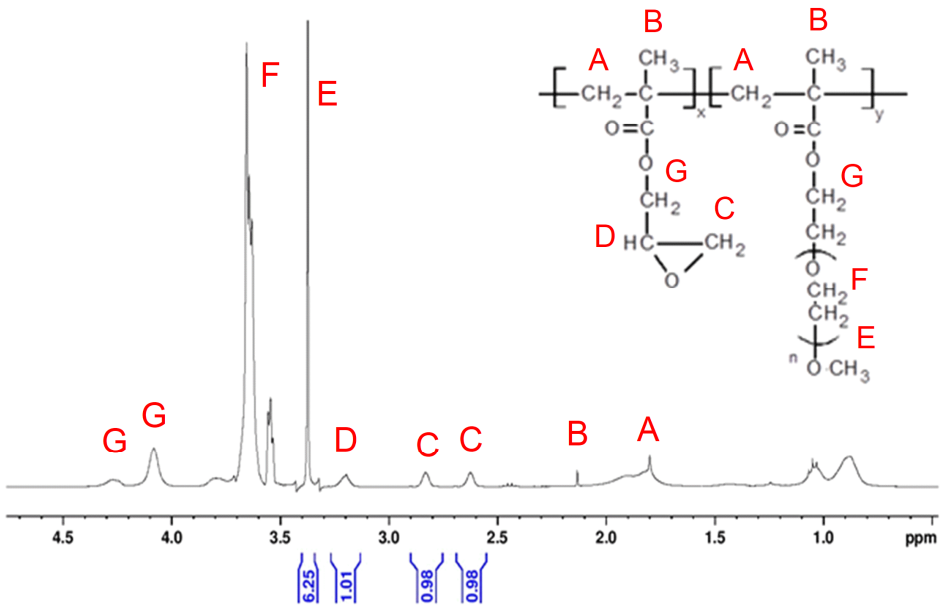

Figure 19. ^{1}H NMR spectrum of poly(GMA-co-PEGMA)

4.5.2. Hydrolysis of acid and alkaline pretreated biomass

Alkali-pretreated biomass typically retains most or all of its hemicellulose while some of its lignin has been removed. Conversely, acid-pretreated biomass retains all or most of its lignin but little hemicellulose. Since these pretreatments modify biomass in different ways, testing PECs with alkali- and acid-pretreated biomass allows us to understand if PEC effectiveness is affected by biomass composition or structure.

Figure 20 shows the glucan conversion using PECs and FE during hydrolysis of alkali- and acid-pretreated biomass. Cellulose conversion for acid pretreated biomass was approximately 100% while only 46% of cellulose was converted with the alkaline-pretreated sample. Although the efficacy of FE with alkali-pretreated biomass was relatively low, the results were similar for PECs. There was no significant difference between glucan conversion using PECs and FE with either pretreatment method.

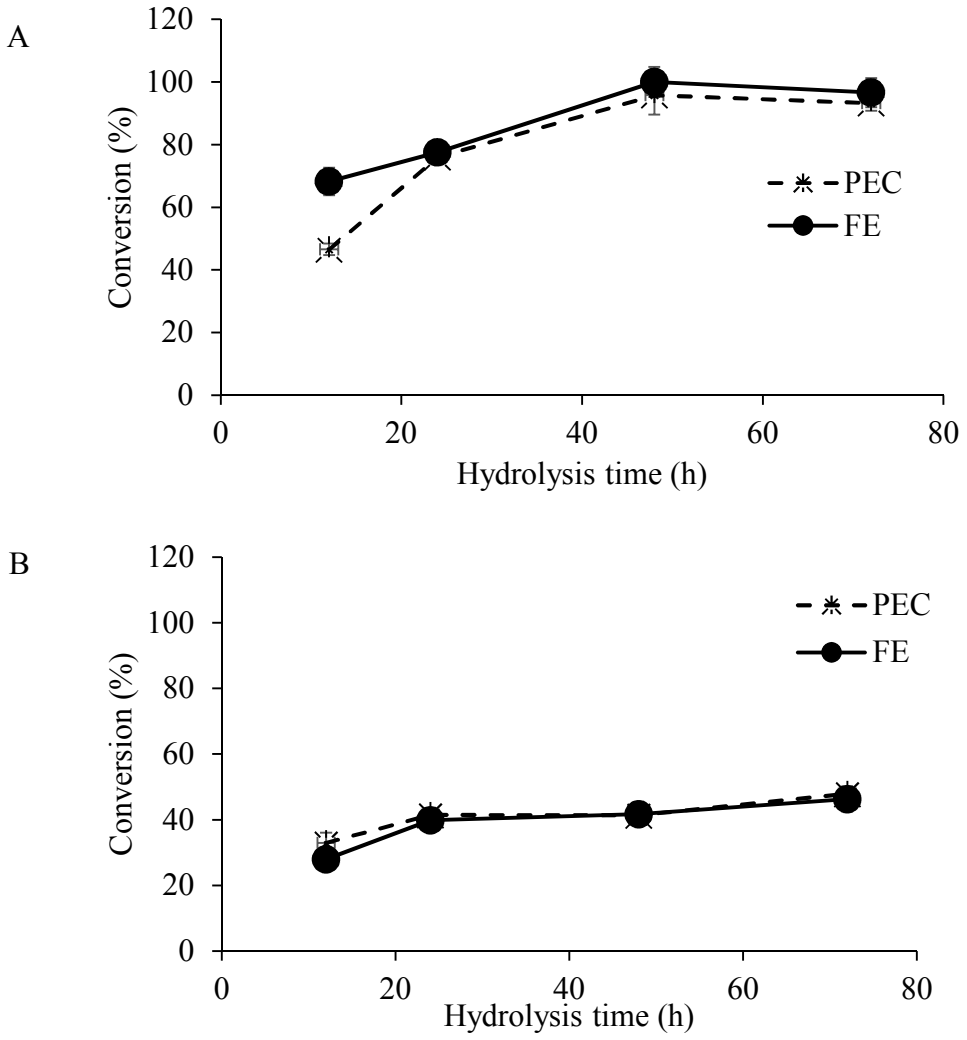

Figure 20. Effect of polymer-enzyme conjugation conversion of glucan to glucose during enzymatic biomass hydrolysis at a 1% glucan loading with polymer enzyme conjugates (PECs) and free enzymes (FE). A: acid pretreatment and B: alkaline pretreatment

The similar efficacy between PECs and FE is unusual for immobilized enzymes. One study of polymer-immobilized cellulase reported that immobilization reduced enzyme effectiveness due to movement restriction or steric hindrance (Nonaka, Kobayashi, & Funaoka, 2014). In another study involving cellulase enzyme immobilization on a polymer-brush system, it was reported that polymer flexibility ensures that immobilized enzymes are unrestricted from interacting with substrate (Kohut, Pryor, Voronov, & Minko, 2017). Flexible polymers spread and align easily on the substrate thereby providing an intrinsic contact between the immobilized enzymes and the substrate (Kohut et al., 2017). Similarly, we use flexible polymer that may contribute to the observed effectiveness of PECs similar to that of FE.

4.5.3. Effect of temperature on the efficacy of immobilized enzymes

The conformation of macromolecules is dependent on temperature. Changes in macromolecular conformation can also affect the proximity of immobilized enzymes to each other. Polymer conformation changes during hydrolysis have been shown to affect the activity of polymer-immobilized enzymes (Mao et al., 2006). To determine if conformational changes occur with macromolecules in PECs and if this may impact the enzymes effectiveness, we conducted hydrolysis at different temperature using PECs and FE. Glucan conversion during 48-h enzymatic hydrolysis using PEC and FE is shown in Figure 21. Conversion using PECs and FE follows similar patterns with temperature change. Increasing temperature from 45 to 55^{o}C has little impact while further temperature increase causes a similarly rapid decrease in conversion rates for both PECs and FE.

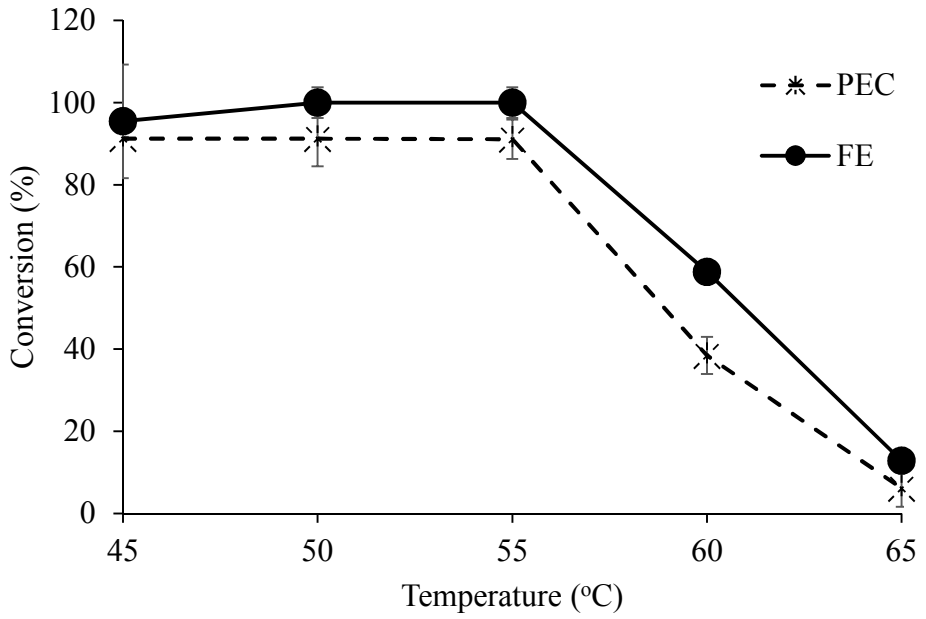

Figure 21. Effect temperature on 48 h conversion of glucan to glucose using acid-pretreated biomass at a 1% glucan loading with polymer enzyme conjugates (PECs) and free enzymes (FE)

4.5.4. Effect of pH on the efficacy of immobilized enzyme

The pH could alter polymer configuration and thereby change interaction of attached enzymes with the substrate (Yanxia Wang, Zhang, Han, Cheng, & Li, 2012; Zhang, Xu, Li, & Yuan, 2010; Zhou, 2010). Effects of pH and temperature can be pronounced when the immobilization process ionizes amino acid side chains resulting in enzyme conformation changes (Zdarta, Pinelo, Jesionowski, & Meyer, 2018). In order to determine if the attachment to the polymer affects enzyme differently as pH changes, the efficacy of PECs and FE was investigated during biomass hydrolysis at different pH values. As shown in Figure 22, glucan conversion using both FE and PECs increases gradually as pH increases from 4 to 4.5. Both FE and PECs effectiveness are stable between pH range of 4.5 to 5.0 and then reduce as pH increases further. This result shows that the cellulase attachment to polymer in PECs does not alter how the enzyme responds to changes in pH. Other studies have also shown that cellulase

immobilized on soluble polymers or microspheres does not show a different response to changes in pH (Mao et al., 2006; Wongkhalaung, Kashiwagi, Magae, Ohta, & Sasaki, 1985).

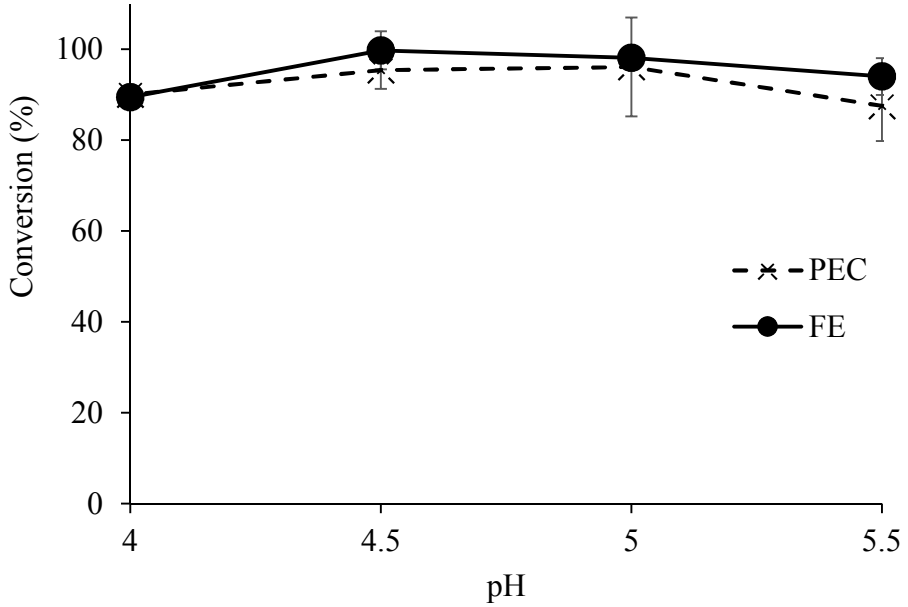

Figure 22. Effect of pH on hydrolysis of acid-pretreated biomass with polymer enzyme conjugates (PECs) and free enzymes (FE)

4.5.5. Effect of substrate loading on the efficacy of immobilized enzyme

Enzyme-substrate ratio is an important parameter affecting enzyme activity during biomass hydrolysis. Increasing substrate loading results in higher glucose concentrations that can eventually inhibit hydrolysis via enzyme product inhibition. Glucose concentration increases at high substrate loadings could also alter macromolecular conformation (Akira Matsumoto, Syuhei Ikeda, Atsushi Harada, & Kataoka*, 2003). Therefore, the effect of different substrate loadings on the efficacy of PECs and FE was studied during hydrolysis using acid-pretreated biomass (Figure 23). At 1.5% glucan (w/v) loading, FE and PECs hydrolyzed 97 and 100% of available glucan, respectively. Increasing substrate loading reduces the fraction of glucan conversion for both treatments, but increases solution glucose concentrations. This result agrees with previous

studies showing that high substrate loading negatively affects cellulose hydrolysis using both free and immobilized enzymes (Shen, Zhong, Saddler, & Liu, 2011; W. Wang, Kang, Wei, Arora, & Lee, 2011; Yang, Zhang, Yong, & Yu, 2011).

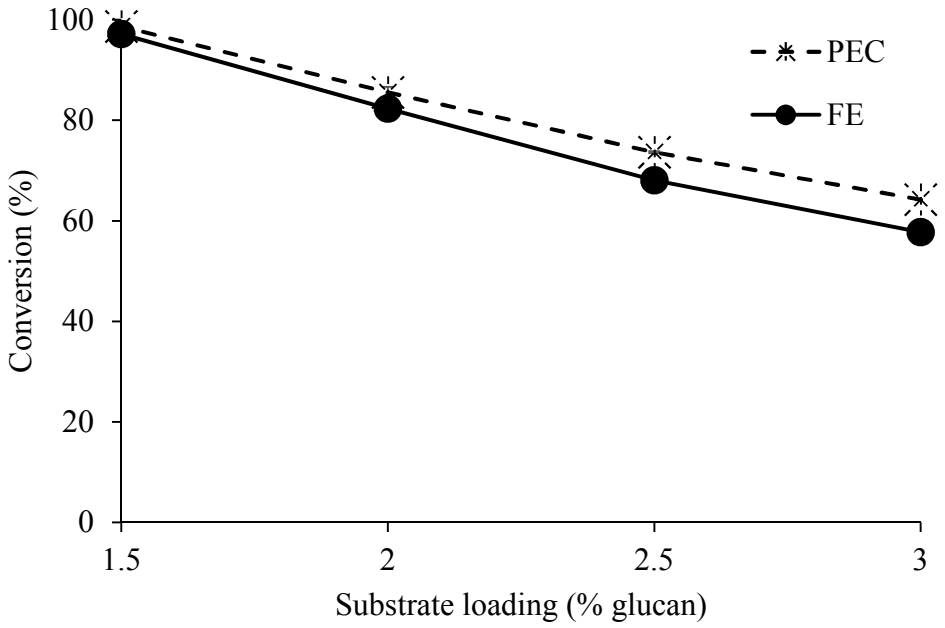

Figure 23. Effect of higher substrate loading (1.5 – 3% glucan equivalent) on hydrolysis of acid-pretreated biomass with polymer enzyme conjugates (PECs) and free enzymes (FE) for 48 h at 4.5 pH and 50°C

The properties of poly(GMA-*co*-PEGMA) used as immobilization ligand might contribute to PEC efficacy. The effect of polymer ligand on cellulases activity has been associated with the polymer chemical and physical properties and enzymes loading on the polymer (Winarni et al., 2013). Amphiphilic polymers can alter biomass surface activity and prevent non-productive cellulase binding (Li, Li, Fan, & Yan, 2012; Xu et al., 2008). Since amphiphilic polymers have both hydrophilic and hydrophobic fragments , the hydrophobic part could selectively bind to lignin and prevent nonproductive lignin-cellulase interaction (Cheng, Zhu, Kang, & Neoh, 2005; Zhu et al., 2005). Previous studies have added amphiphilic polymers to improve biomass hydrolysis (Sipos et al., 2010; Tu & Saddler, 2010). High cellulase activities

have been reported with the addition of surfactants Tween 80, polyethylene glycol (PEG), and lignin-based polyoxyethylene ether during biomass hydrolysis (Sipos et al., 2010; Tu & Saddler, 2010). It is important to note that these studies did not involve enzyme attachment on polymer, unlike our study. Enzyme activities are not significantly affected when attached on flexible polymers as earlier stated. Therefore, the copolymer used in this study might have contributed towards to PECs effectiveness compare to FE by either modifying biomass surface and improving substrate alignment.

4.5.6. Glucose inhibition of polymer enzyme conjugate

PEC efficacy was only slightly higher than that of FE at higher substrate loading which glucose concentration was high. It is unknown if PEC can resist the effect of known hydrolysis inhibitors like glucose. Hence, I investigated the inhibitory effect of glucose on PEC efficacy by adding different concentrations of glucose (45 and 90 mg/ml) during hydrolysis of alkaline pretreated biomass.

The results (Figure 24) show that glucose inhibits FE and PECs differently. Generally, glucose inhibition of FE is greater than that of PEC. Glucose exhibited dose-dependent inhibition of FE. Although glucose inhibition was evident with PECs at 24 h, hydrolysis levels after 72 h were not different than treatments with FE or PECs without glucose addition. PEC was able to overcome the initial inhibitory effect even when supplemented with 90 mg/ml of glucose. PEC resistance to glucose inhibition suggests that earlier observed increases in conversion at higher substrate loadings may be due to PEC resistance to glucose inhibition. The mechanism of PEC inhibition resistance is not clear. The copolymer used for PEC assembly may be glucose responsive. Glucose responsive polymers assume different conformation with change in glucose concentration. Therefore, the high glucose concentration during hydrolysis at high substrate

loading could compete with aqueous in the solution and trigger change in copolymer conformation to a coil. A coil conformation could have made the attached enzymes to rearrange in to a form that is resistant to glucose inhibition.

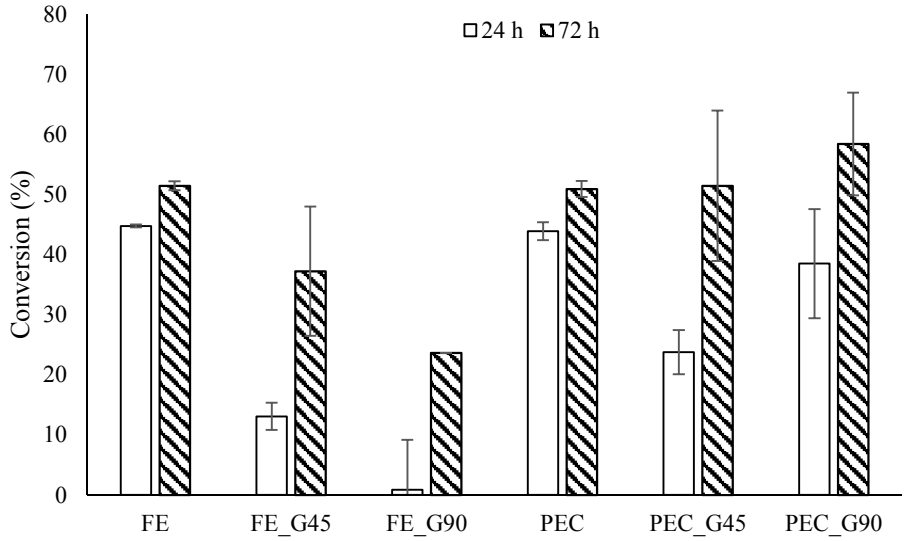

Figure 24. Biomass conversion upon hydrolysis of alkaline-pretreated biomass with added glucose at different concentrations: G45 and G90, respectively, represent 45 and 90 ml/ml glucose concentration

4.5.7. Membrane recovery of polymer enzyme conjugate

Since enzymes are estimated at about 30 – 50% of cellulosic ethanol production cost, enzyme recycling has been identified as a means to improve economic efficiency. One of the aims of enzyme immobilization is to facilitate enzyme recovery and reuse. Immobilization of enzymes on relatively long macromolecules produces a larger construct than individual free enzymes. These larger biocatalysts could be more easily recovered with technology such as tangential flow filtration (TFF). The recovered PECs were successfully separated after 48 h biomass hydrolysis using 50-kDa molecular weight cutoff membrane in TFF. The recovered PEC efficacy was estimated by measuring conversion of glucan when contacted with acid pretreated biomass (Figure 25). The result shows that the conversion of glucan to sugar by recovered PECs is 30% after 48 h hydrolysis time. Glucan conversion using recovered PECs

increase between 12 and 24 h, but further increase in hydrolysis time does not improve biomass conversion. Extended exposure could potentially cause enzyme deterioration and protein modification thus inactivating enzymes (Ishihara et al., 1991).

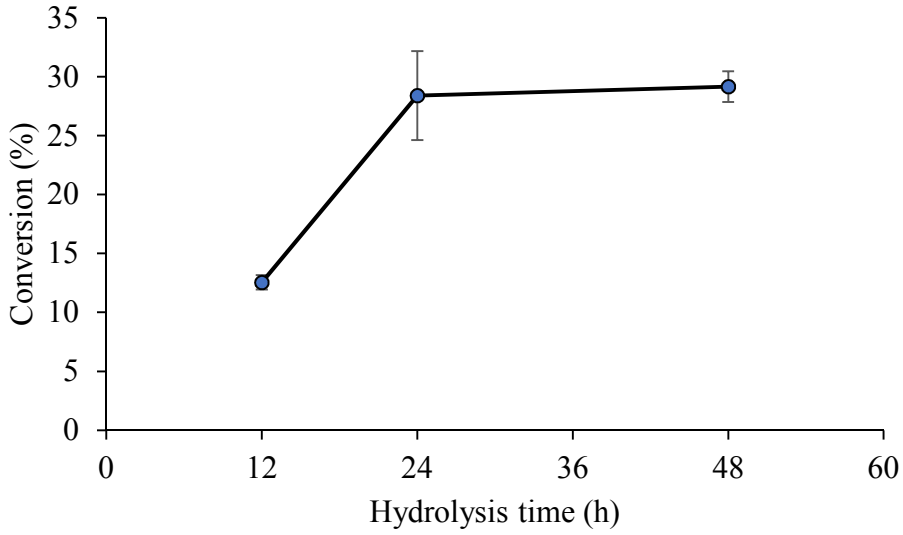

Figure 25. The conversion of glucan to glucose using membrane recovered PECs with acid pretreated biomass at 1% glucan loading, 50°C and 4.8 pH

The amount of enzyme recovered was determined by comparing the total protein in the retentate and permeate. We determined that about 60% of PECs were recovered from the hydrolysis solution with a 50-kDa membrane (Figure 26). Previous work showed that a 50-kDa membrane was unable to recover free cellulase enzymes from solution (Knutsen & Davis, 2004). Immobilization of enzymes makes enzyme recovery possible with a relatively large-pore membrane. Although the portion of PECs that is recovered is less than the 84% of that was immobilized, some PECs could remain adsorbed on biomass and were not recovered. Others have reported that reduction in membrane-recoverable enzymes is due to irreversible enzyme adsorption on biomass (Ishihara, Uemura, Hayashi, & Shimizu, 1991).

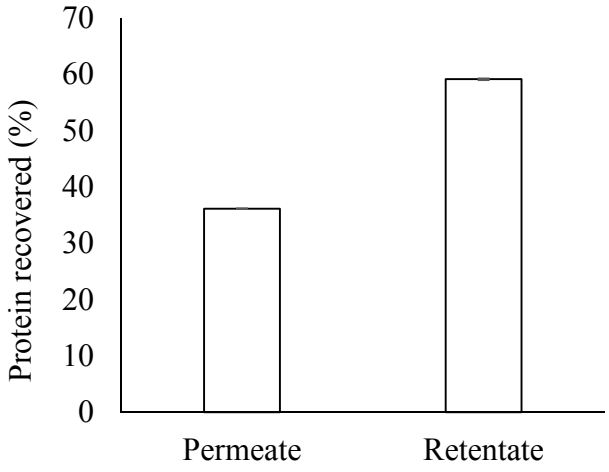

Figure 26. Protein recovered in permeate and retentate during membrane recovery of PEC after first hydrolysis

4.5.8. PEC reuse with enzyme supplementation

Since recovered PECs achieved lower conversion, we added FE as supplement to increase conversion of glucan. Figure 27 shows that although increasing enzyme supplementation increases the glucan conversion in the first 24 h, there is no benefit to increasing beyond 40% of the original FE loading. This result suggests that recovery and reuse of PECs enables reducing enzyme dosage by about 60% in a subsequent batch. This result is higher than 30% reduction in enzyme supplementation reported with enzymes recovered from biomass residue (Weiss, Börjesson, Pedersen, & Meyer, 2013).

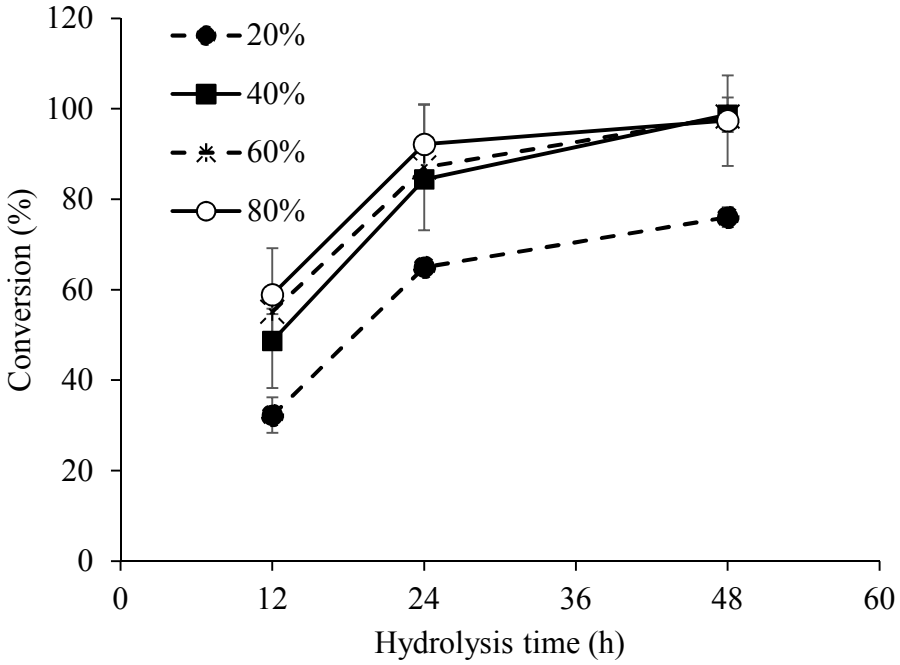

Figure 27. Effect of free enzyme supplementation levels (20, 40, 60 and 80% of initial enzyme loading) on biomass hydrolysis using membrane-recovered PECs

4.6. Conclusion

PEC efficacy during biomass hydrolysis and subsequent recovery and reuse is studied. This study shows that immobilization of cellulase on poly(GMA-co-PEGMA) does not affect glucan conversion under baseline conditions or with changes to pH and temperature. PECs demonstrate potential to moderately increase conversion at high substrate loadings. PECs can be partially recovered using membrane ultrafiltration with 50-kDa molecular weight cutoff weight from hydrolysis solution. Reuse of PECs reduces the amount of enzyme needed in a subsequent hydrolysis reaction by 60%. Future study will investigate continuous hydrolysis of biomass using PECs in a membrane reactor.

4.7. References

Akira Matsumoto, Syuhei Ikeda, Atsushi Harada, and, & Kataoka*, K. (2003, August 19). Glucose-Responsive Polymer Bearing a Novel Phenylborate Derivative as a Glucose-

Sensing Moiety Operating at Physiological pH Conditions [Research-article]. https://doi.org/10.1021/bm034139o

Budinova, G. A. L. G., Mori, Y., Tanaka, T., & Kamiya, N. (2018). Casein-based scaffold for artificial cellulosome design. *Process Biochemistry*, *66*, 140–145. https://doi.org/10.1016/j.procbio.2017.12.013

Cassales, A., de Souza-Cruz, P. B., Rech, R., & Záchia Ayub, M. A. (2011). Optimization of soybean hull acid hydrolysis and its characterization as a potential substrate for bioprocessing. *Biomass and Bioenergy*, *35*(11), 4675–4683. https://doi.org/10.1016/j.biombioe.2011.09.021

Cellulosic Ethanol: Environmentally Friendly, But Costly. (n.d.). Retrieved January 16, 2021, from http://large.stanford.edu/courses/2014/ph240/zarubin1/

Cheng, Z., Zhu, X., Kang, E. T., & Neoh, K. G. (2005). Brush-type amphiphilic diblock copolymers from "living"/controlled radical polymerizations and their aggregation behavior. *Langmuir*, *21*(16), 7180–7185.

Dutta, S., & Wu, K. C.-W. (2014). Enzymatic breakdown of biomass: Enzyme active sites, immobilization, and biofuel production. *Green Chemistry*, *16*(11), 4615–4626.

Gross, R. A., & Kalra, B. (2002). Biodegradable polymers for the environment. *Science*, *297*(5582), 803–807.

Harrison, R. G., Todd, P., Rudge, S. R., & Petrides, D. P. (2015). *Bioseparations science and engineering*. Oxford University Press, USA.

Ishihara, M., Uemura, S., Hayashi, N., & Shimizu, K. (1991). Semicontinuous enzymatic hydrolysis of lignocelluloses. *Biotechnology and Bioengineering*, *37*(10), 948–954.

Jiang, J., Zhao, J., He, C., Cui, B., Xiong, J., Jiang, H., … Xiang, G. (2017). Recyclable magnetic carboxymethyl chitosan/calcium alginate – cellulase bioconjugates for corn stalk hydrolysis. *Carbohydrate Polymers*, *166*, 358–364. https://doi.org/10.1016/j.carbpol.2017.03.003

Knutsen, J. S., & Davis, R. H. (2004). Cellulase retention and sugar removal by membrane ultrafiltration during lignocellulosic biomass hydrolysis. *Proceedings of the Twenty-Fifth Symposium on Biotechnology for Fuels and Chemicals Held May 4–7, 2003, in Breckenridge, CO*, 585–599. Springer.

Kohut, A., Pryor, S. W., Voronov, A., & Minko, S. (2017). Enzymogel Nanoparticles Chemistry for Highly Efficient Phase Boundary Biocatalysis. In *Biocatalysis and Nanotechnology* (pp. 369–399). Jenny Stanford Publishing.

Lee, C. C., Kibblewhite, R. E., Paavola, C. D., Orts, W. J., & Wagschal, K. (2017). Production of D-Xylonic Acid from Hemicellulose Using Artificial Enzyme Complexes. *Journal of Microbiology and Biotechnology*, *27*(1), 77–83. https://doi.org/10.4014/jmb.1606.06041

Lee, D., Owens, V. N., Boe, A., & Jeranyama, P. (2007). Composition of herbaceous biomass feedstocks. North Central Sun Grant Center, South Dakota State University. *Brookings, USA*.

Li, J., Li, S., Fan, C., & Yan, Z. (2012). The mechanism of poly (ethylene glycol) 4000 effect on enzymatic hydrolysis of lignocellulose. *Colloids and Surfaces B: Biointerfaces*, *89*, 203–210.

Lu, L., Zhang, L., Yuan, L., Zhu, T., Chen, W., Wang, G., & Wang, Q. (2019). Artificial Cellulosome Complex from the Self□Assembly of Ni□NTA□Functionalized Polymeric

Micelles and Cellulases. *ChemBioChem*, *20*(11), 1394–1399. https://doi.org/10.1002/cbic.201900061

Mao, X., Guo, G., Huang, J., Du, Z., Huang, Z., Ma, L., … Gu, L. (2006). A novel method to prepare chitosan powder and its application in cellulase immobilization. *Journal of Chemical Technology & Biotechnology: International Research in Process, Environmental & Clean Technology*, *81*(2), 189–195.

Mori, Y., Ozasa, S., Kitaoka, M., Noda, S., Tanaka, T., Ichinose, H., & Kamiya, N. (2013). Aligning an endoglucanase Cel5A from Thermobifida fusca on a DNA scaffold: Potent design of an artificial cellulosome. *Chemical Communications*, *49*(62), 6971–6973.

Nguyenhuynh, T., Nithyanandam, R., Hwa Chong, C., & Krishnaiah, D. (2017). A review on using membrane reactors in enzymatic hydrolysis of cellulose. *J. Eng. Sci. Technol*, *12*(4), 1129–1152.

Nonaka, H., Kobayashi, A., & Funaoka, M. (2014). Enzymatic Hydrolysis of Carboxymethylcellulose and Filter Paper by Immobilized Cellulases on Lignophenols. *Journal of Wood Chemistry and Technology*, *34*(3), 169–177. https://doi.org/10.1080/02773813.2013.851246

Osborne, S. (n.d.). *Assessing the Economic Efects of Commercialization of Cellulosic Ethanol*. 20.

Padella, M., O'Connell, A., & Prussi, M. (2019). What is still limiting the deployment of cellulosic ethanol? Analysis of the current status of the sector. *Applied Sciences*, *9*(21), 4523.

Saltik, M. B., Özkan, L., Jacobs, M., & van der Padt, A. (2016). Optimal Start-Up and Operation Policy for an Ultrafiltration Membrane Unit in Whey Separation**The work presented

here is generated by the Institute for Sustainable Process Technology (ISPT) project IMPROVISE. In Z. Kravanja & M. Bogataj (Eds.), *Computer Aided Chemical Engineering* (pp. 1599–1604). Elsevier. https://doi.org/10.1016/B978-0-444-63428-3.50271-X

Shen, F., Zhong, Y., Saddler, J. N., & Liu, R. (2011). Relatively high-substrate consistency hydrolysis of steam-pretreated sweet sorghum bagasse at relatively low cellulase loading. *Applied Biochemistry and Biotechnology*, *165*(3–4), 1024–1036.

Sipos, B., Dienes, D., Schleicher, Á., Perazzini, R., Crestini, C., Siika-Aho, M., & Réczey, K. (2010). Hydrolysis efficiency and enzyme adsorption on steam-pretreated spruce in the presence of poly (ethylene glycol). *Enzyme and Microbial Technology*, *47*(3), 84–90.

Stickel, J. J., Adhikari, B., Sievers, D. A., & Pellegrino, J. (2018). Continuous enzymatic hydrolysis of lignocellulosic biomass in a membrane-reactor system. *Journal of Chemical Technology & Biotechnology*, *93*(8), 2181–2190.

Sun, Q., & Chen, W. (2016). HaloTag mediated artificial cellulosome assembly on a rolling circle amplification DNA template for efficient cellulose hydrolysis. *Chemical Communications*, *52*(40), 6701–6704.

Torabi, S., Satari, B., & Hassan-Beygi, S. R. (2020). Process optimization for dilute acid and enzymatic hydrolysis of waste wheat bread and its effect on aflatoxin fate and ethanol production. *Biomass Conversion and Biorefinery*, 1–9.

Tu, M., & Saddler, J. N. (2010). Potential enzyme cost reduction with the addition of surfactant during the hydrolysis of pretreated softwood. *Applied Biochemistry and Biotechnology*, *161*(1–8), 274–287.

Wang, F.-Y., Li, H.-Y., Liu, H.-M., & Liu, Y.-L. (2015). Fractional Isolation and Structural Characterization of Hemicelluloses from Soybean Hull. *BioResources*, *10*(3), 5256–5266. https://doi.org/10.15376/biores.10.3.5256-5266

Wang, W., Kang, L., Wei, H., Arora, R., & Lee, Y. Y. (2011). Study on the decreased sugar yield in enzymatic hydrolysis of cellulosic substrate at high solid loading. *Applied Biochemistry and Biotechnology*, *164*(7), 1139–1149.

Wang, Yanxia, Zhang, X., Han, Y., Cheng, C., & Li, C. (2012). PH- and glucose-sensitive glycopolymer nanoparticles based on phenylboronic acid for triggered release of insulin. *Carbohydrate Polymers*, *89*(1), 124–131. https://doi.org/10.1016/j.carbpol.2012.02.060

Wang, Ying, Leng, L., Islam, M. K., Liu, F., Lin, C. S. K., & Leu, S.-Y. (2019). Substrate-Related Factors Affecting Cellulosome-Induced Hydrolysis for Lignocellulose Valorization. *International Journal of Molecular Sciences*, *20*(13), 3354.

Weiss, N., Börjesson, J., Pedersen, L. S., & Meyer, A. S. (2013). Enzymatic lignocellulose hydrolysis: Improved cellulase productivity by insoluble solids recycling. *Biotechnology for Biofuels*, *6*(1), 5. https://doi.org/10.1186/1754-6834-6-5

Winarni, I., Oikawa, C., Yamada, T., Igarashi, K., Koda, K., & Uraki, Y. (2013). Improvement of enzymatic saccharification of unbleached cedar pulp with amphipathic lignin derivatives. *BioResources*, *8*(2), 2195–2208.

Wongkhalaung, C., Kashiwagi, Y., Magae, Y., Ohta, T., & Sasaki, T. (1985). Cellulase immobilized on a soluble polymer. *Applied Microbiology and Biotechnology*, *21*(1–2), 37–41.

Xiong, G. Y., Chen, X., Zhang, X. X., Miao, Y., Zou, Y., Wang, D. Y., & Xu, W. M. (2020). Process optimization and the relationship between the reaction degree and the antioxidant

activity of Maillard reaction products of chicken liver protein hydrolysates. *Poultry Science*, *99*(7), 3733–3741.

Xu, F., Ding, H., Osborn, D., Tejirian, A., Brown, K., Albano, W., … Langston, J. (2008). Partition of enzymes between the solvent and insoluble substrate during the hydrolysis of lignocellulose by cellulases. *Journal of Molecular Catalysis B: Enzymatic*, *51*(1–2), 42–48.

Yadavalli, N. S., Borodinov, N., Choudhury, C. K., Quiñones-Ruiz, T., Laradji, A. M., Tu, S., … Minko, S. (2017). Thermal Stabilization of Enzymes with Molecular Brushes. *ACS Catalysis*, *7*(12), 8675–8684.

Yang, J., Zhang, X., Yong, Q., & Yu, S. (2011). Three-stage enzymatic hydrolysis of steam-exploded corn stover at high substrate concentration. *Bioresource Technology*, *102*(7), 4905–4908.

Zdarta, J., Pinelo, M., Jesionowski, T., & Meyer, A. S. (2018). Upgrading of biomass monosaccharides by immobilized glucose dehydrogenase and xylose dehydrogenase. *ChemCatChem*, *10*(22), 5164–5173.

Zhang, Y., Xu, J.-L., Li, D., & Yuan, Z.-H. (2010). Preparation and properties of an immobilized cellulase on the reversibly soluble matrix Eudragit L-100. *Biocatalysis and Biotransformation*, *28*(5–6), 313–319. https://doi.org/10.3109/10242422.2010.516391

Zhou, J. (2010). Immobilization of Cellulase on a Reversibly Soluble−Insoluble Support: Properties and Application. *Journal of Agricultural and Food Chemistry*, *58*(11), 6741–6746. https://doi.org/10.1021/jf100759c

Zhu, J., Tang, A., Law, L. P., Feng, M., Ho, K. M., Lee, D. K., … Li, P. (2005). Amphiphilic core- shell nanoparticles with poly (ethylenimine) shells as potential gene delivery carriers. *Bioconjugate Chemistry*, *16*(1), 139–146.

5. SCALABLE AND SUSTAINABLE SYNTHESIS OF SUPERPARAMAGNETIC IRON OXIDE NANOPARTICLES USING NEW TUBULAR ELECTROCHEMICAL SYSTEM[2]

5.1. Abstract

A new tubular electrochemical system (TES) was developed to overcome scalability and sustainability challenges during synthesis of superparamagnetic iron oxide (Fe_3O_4) nanoparticles **(**SPIONs). The SPION yield and productivity were 8.3 mg $mole^{-1}$ Fe and 163 μg $mole^{-1}$ Fe min^{-1}, respectively. The TES functions efficiently with electrolyte reuse and supplementation without any reduction in productivity. Gradual electrolyte supplementation (0.5 mL min^{-1}) resulted in 75% higher yield than the non-supplemented system. TEM and XRD analyses confirmed the presence of Fe_3O_4. TES enables the use of a new reaction parameter – flow rate – for controlling SPION properties. Increasing electrolyte flow rate caused a decrease in SPION average size and size-distribution. TES offers advantages of scalability and sustainability for large scale production of Fe_3O_4 nanoparticles.

5.2. Keywords

Magnetite, Nanoparticle electrosynthesis, Nanoparticles, Iron oxides, Tubular reactor

5.3. Introduction

Nanoparticles have novel functionalities making them useful in numerous applications including biomedical, agriculture, food and electronics. Among nanoparticles, superparamagnetic iron-oxide nanoparticles (SPIONs) have received most attention because they are non-toxic to human health. SPIONs have been used in biomedical applications for site-

[2] This paper is published in Journal of Applied Electrochemistry. Cited as: Hammed, A., Voronov, A. & Pryor, S. Scalable and sustainable synthesis of superparamagnetic iron oxide nanoparticles using new tubular electrochemical system. Journal of Applied Electrochemistry **51,** 1093–1100 (2021). https://doi.org/10.1007/s10800-021-01560-2. Ademola Hammed had primary responsibility of conducting, collecting, and analyzing laboratory data under direct supervision of Dr. Scott W. Pryor. and Dr. Voronov helped in proofreading.

directed application of active-medicinal compounds (Ramimoghadam, Bagheri, & Hamid, 2014). Recently, SPIONs have been used in the development of cellulolytic magnetic nanobiocatalysts (CM-NBCs) to achieve enzyme recovery and reuse in bioprocessing (Kohut, Pryor, Voronov, & Minko, 2017; Kudina et al., 2014; Samaratunga et al., 2015b, 2015a). Continuous improvement of SPION synthesis is important for achieving CM-NBC application in bioprocess industrial.

Synthesis of SPIONs is the first step for SPION-based applications. Size control, and scalability are among the main challenges of SPION synthesis (Robertson et al., 2016). Production of SPIONs with a narrow size-distribution is desired to understand their physical properties (Robertson et al., 2016). Research has shown that production methods affect SPION properties such as morphology, and size distribution (Cabrera, Gutierrez, Menendez, Morales, & Herrasti, 2008; Veriansyah, Kim, Min, & Kim, 2010; Xu & Teja, 2008). Conventional chemical precipitation methods are simple but difficult to control, and the resulting nanoparticles have broad size ranges and irregular morphology (Park et al., 2008). Although, thermal methods produce monodispersed nanoparticles, they require high temperatures (100 – 300^{o}C) and toxic expensive reagents, and do not allow control of nanoparticle morphology (Park et al., 2008). Other approaches for SPION synthesis involve the use of supercritical fluids (Pascu, Marre, Aymonier, & Roig, 2013; Veriansyah et al., 2010), and hydrothermal fluids (Xu & Teja, 2008) which are costly and industrially unfeasible.

Cathodic and anodic electrochemical synthesis are promising methods for producing size-controlled SPIONs on a large scale (Ramimoghadam et al., 2014). However, anodic methods are more complicated because they require high voltage and chemical surfactants. Cathodic electrochemical methods could possibly overcome the drawbacks of anodic electrochemical methods, but the synthesized nanoparticles often contain impurities (Aghazadeh, Karimzadeh,

Ganjali, & Mohebi Morad, 2017). Most cathodic electrochemical studies have been performed with batch reactions which suffer from poor mixing and reduced productivity (Ali et al., 2016; Fajaroh, Setyawan, Nur, & Lenggoro, 2013; Park et al., 2008; Ramimoghadam et al., 2014; Salazar-Alvarez, Muhammed, & Zagorodni, 2006). Also, the electrode surface in batch processes becomes covered with deposited SPIONs reducing electrode electrical conductivity and reactivity, and thus experimental reproducibility (Ali et al., 2016). Improvement efforts should focus on achieving sustainability and scalability, while reducing processing time, energy use and capital costs (Cheng, Li, & Liu, 2012; Karthikeyan, Selvam, & Wong, 2016).

Among several approaches to improve SPION synthesis is by passing the reactant through a reaction zone. SPIONs were produced in a flow injection system (FIS) system that involves chemical method with flowing reactant (Salazar-Alvarez et al., 2006). FIS can be used to control SPION morphology, improve product reproducibility, and eliminate contamination (Salazar-Alvarez et al., 2006). FIS frees the material surface from chemically and/or physically bound substances that alter material surface properties. FIS also ensures continuous separation of product from the reaction zone preventing further reaction of products responsible for irregular growth rates, secondary nucleation, and particle ripening (Ali et al., 2016). Immediate separation of growing SPIONs can improve particle size control by eliminating the Oswald ripening mechanism where large particles grow at the expense of small ones (Marques et al., 2008). However, being a chemical method, FIS still has scalability challenges.

We have developed a new tubular electrochemical system (TES) that frees electrode surfaces from bound substances, thereby increasing SPION yield and productivity. The TES has a magnetic base that allows for separation of SPIONs as they are formed. We have investigated the effect of electrolyte concentration, flow rate, and current density on SPION size and

morphology, and investigated electrolyte supplementation strategies to increase SPION yield and productivity.

5.4. Methods

5.4.1. SPION synthesis

SPION preparation of was conducted using the TES (Figure 28). TES was comprised of two sections, a tubular electrochemical reactor and a magnetic separator connected. The electrolyte solution used for SPION synthesis was 1 L aqueous solution of $Fe(NO_3)_3$ and $FeCl_2$ in a molar ratio of 2:1. A peristaltic pump was used to pump the electrolytes around. The electrodes (carbon/aluminium rod anode, copper pipe cathode) were connected to a DC power supply (Extech Instrument). Current density, reaction time and total Fe concentration for all SPION synthesis were 18 mA cm^{-2}, 30 min and 0.015 M, respectively, except otherwise stated. A strong neodymium magnet was positioned within the separating vessel for recovery of synthesized magnetic nanoparticles. Distilled water was pumped through the tubular reactor to wash any trapped particles after each run. SPIONs were collected and washed three times with ethanol and oven dried overnight at 70^{o}C. For the electrolyte supplementation, the steps were similar with addition of electrolytes (10 ml containing 0.015M total iron) in three modes: a one-time batch supplementation strategy (1-bSS) involved addition all the 10 ml at ones; a four-time supplementation strategy (4-bSS) involved the addition of 2.5 ml four times at 5 min interval; and a continuous strategy involved the continuous flow of the electrolytes at 0.5mL min^{-1}. The supplementation was started after 30 min of the first SPION synthesis run and allowed to run for additional 30 min. SPION yield and productivity were estimated as follows:

$$\text{Yield} = \frac{SPION\,dry\,mass}{mole\,of\,Fe} \qquad \text{(Equation 5.1)}$$

$$\text{Productivity} = \frac{SPION\ yield}{reaction\ time} \qquad \text{(Equation 5.2)}$$

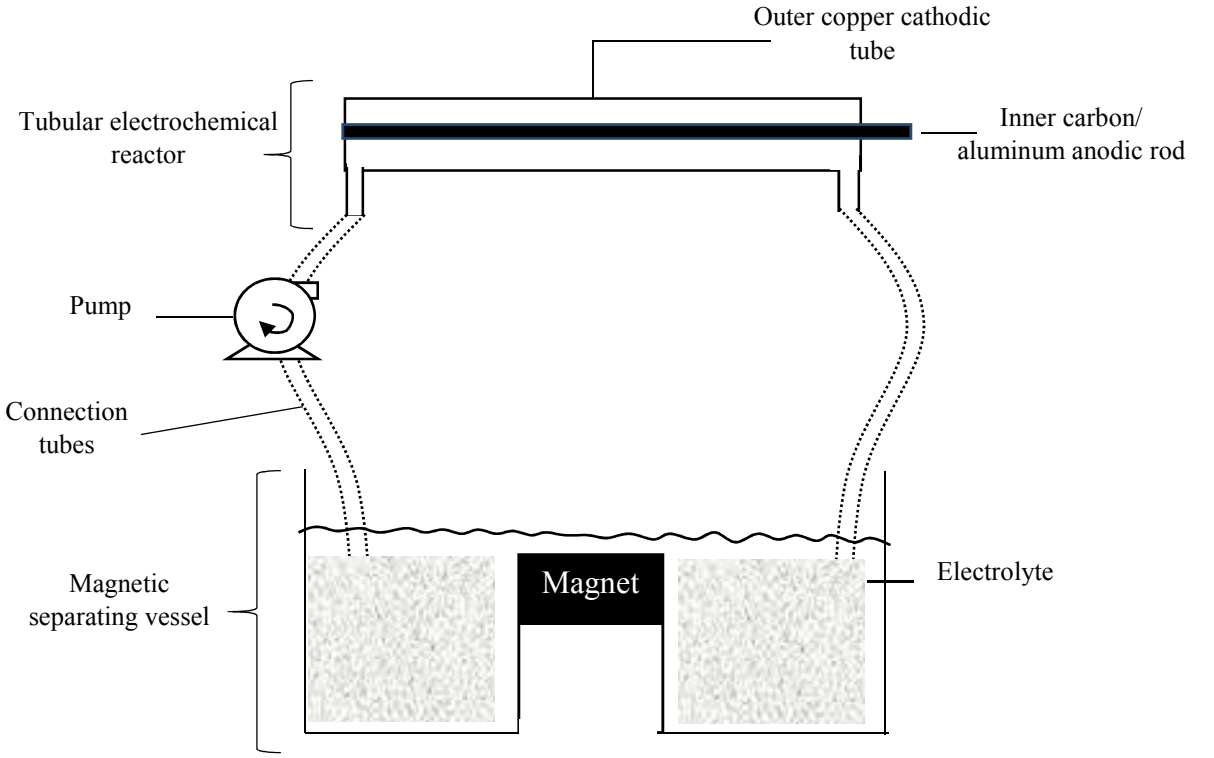

Figure 28. Setup of tubular electrochemical synthesis of SPIONs

5.4.2. SPION morphology determination

SPION samples were ground using an agate mortar and pestle, and ethanol was added to the ground sample. The mixture was transferred to a test tube and placed into an ultrasonic bath for 2 – 3 min. A drop of the suspended sample was then placed on a 300-mesh carbon-coated copper transmission electron microscope grid (Electron Microscopy Sciences; Hatfield, PA) and the excess liquid was wicked off with filter paper. After the grids dried, particle images were acquired using a JEOL JEM-2100 LaB_6 transmission electron microscope (JEOL USA; Peabody, MA) running at 200 kV. Image J program was used to determine the particle size distribution from the images.

5.4.3. Determination of iron content

The concentration of Fe(II) and total iron of the electrolyte during SPION electrosynthesis was determined using UV–Vis spectrophotometry based on the reaction of Fe(II) and 1,10-phenanthroline (Xue et al., 2020). About 1 mL of 0.1 mg mL^{-1} 1, 10-phenanthroline was added to 40 µL of electrolyte solution and the absorbance of the solution was determined at 510 nm. For total iron concentration, 0.2 mL of 10% ascorbic acid was added to the electrolyte solution. A range of 0 – 4 µg mL^{-1} ammonium iron (II) sulfate hexahydrate was used for a standard curve. The concentration of Fe(III) was calculated as the difference between the concentrations of the total iron and Fe(II).

5.4.4. XRD crystallography

Nanoparticle crystallinity was determined using an Rigaku MiniFlex II X-ray diffractometer (The Woodlands, Texas) equipped with 8 position autosampler and D/teX Ultra silicon strip detector. SPION samples were placed in a zero-background sample holder (indent size: 24 mm dia × 0.1 mm deep). The spectra of X-ray diffractometer were subjected to phase identification. Rietveld method was used for quantitative analysis and crystallinity analysis. SmartLab Studio II software package from Rigaku, Crystallography Open Database, and NIST SRM 660e LaB_6 were used for instrument profile correction (Winburn et al.,2000).

5.5. Result and Discussion

5.5.1. Effect of reaction conditions on SPION morphology and size distribution

In electrochemical system, current flow (electron movement) that converts Fe ions to SPIONs occurs between the electrode surface to the electrolyte. The combination of the current flow and the electrode surface area – also known as current density – affect Fe ions to SPIONs conversion. In order to understand the effect of reaction conditions, SPION synthesis was carried

out under different current densities (7, 10, and 18 mA cm^{-2}), electrolyte concentrations (0.05, 0.025, and 0.015 M) and flow rates (3, 6, and 9 mL s^{-1}). According to TEM micrographs in Figures 29, 30, and 31, SPIONs are aggregates of individual spheres with varying diameter, similar to what has been shown in previous work (Karimzadeh et al., 2016). SPION size distribution is affected by flow rate, current density, and electrolyte concentration according to the histogram plots in Figures 29, 30, and 31, respectively. Increasing flow rate (Figure 29) or current density (Figure 30) decreases SPION size; however, increasing electrolyte concentration (Figure 31) increases SPION size.

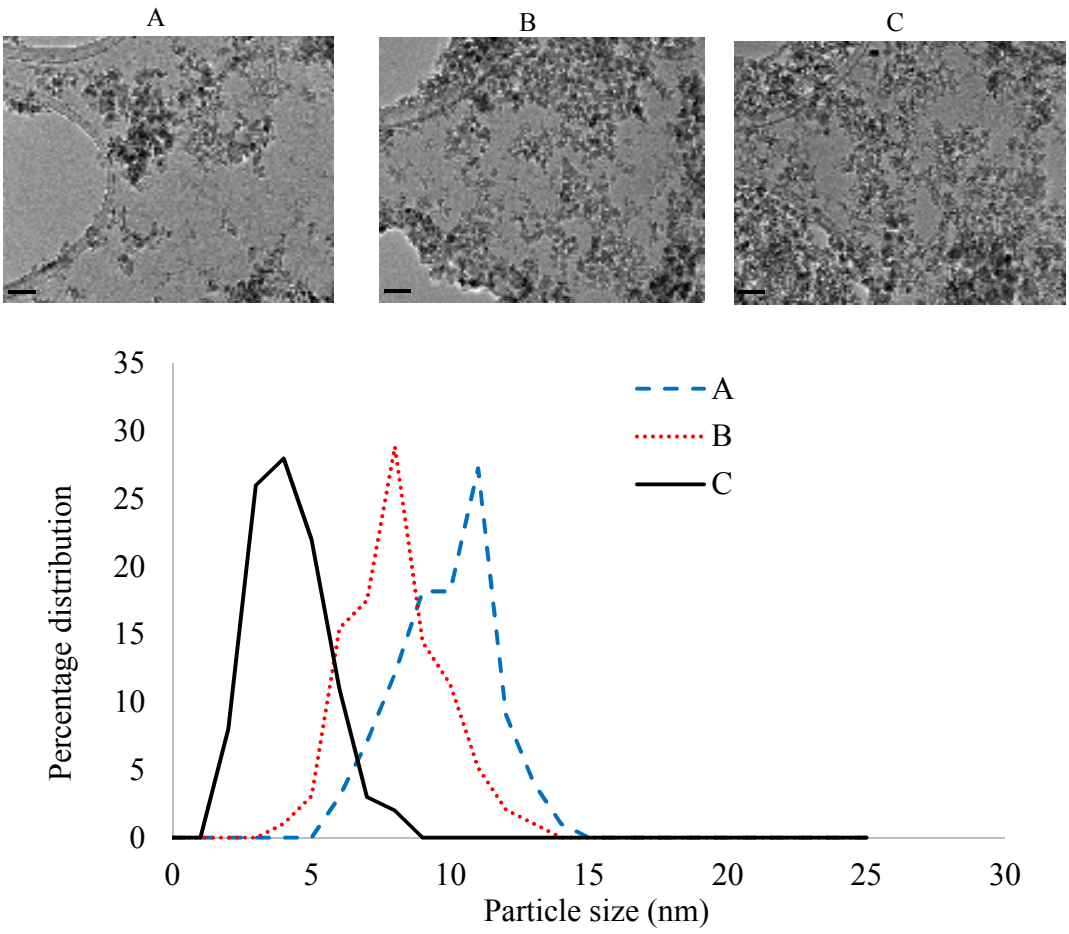

Figure 29. TEM micrographs and size distributions of SPIONs produced from 0.015 M electrolytes, 18 mA/cm^2 current density at different flow rates (A) 3 mL s^{-1}, (B) 6 mL s^{-1}, and (C) 9 mL s^{-1}. Scale bars are 100 nm

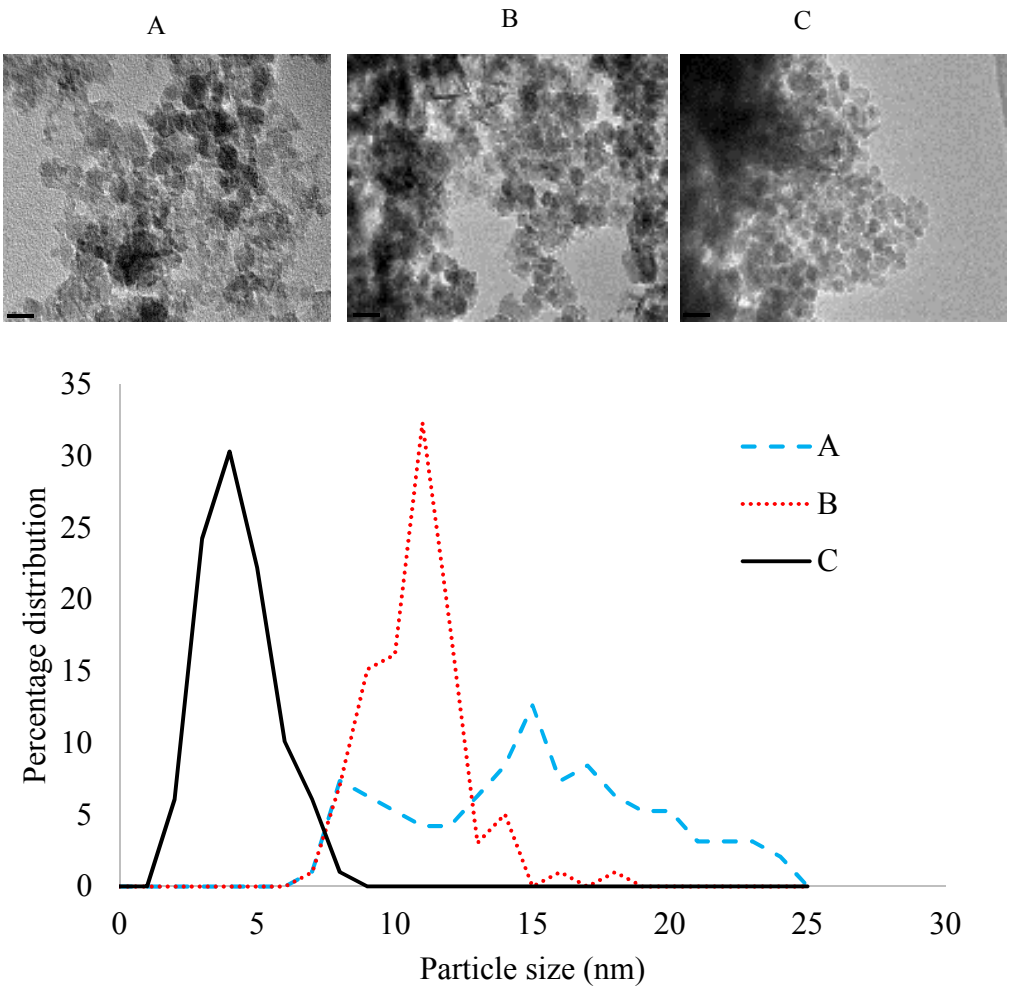

Figure 30. TEM micrographs and size distributions of SPIONs produced from 0.015 M electrolytes, 9 mL s^{-1} flow rate at different current densities (A) 7 mA cm^{-2}, (B) 10 mA cm^{-2}, and (C) 18 mA cm^{-2}. Scale bars are 50 nm

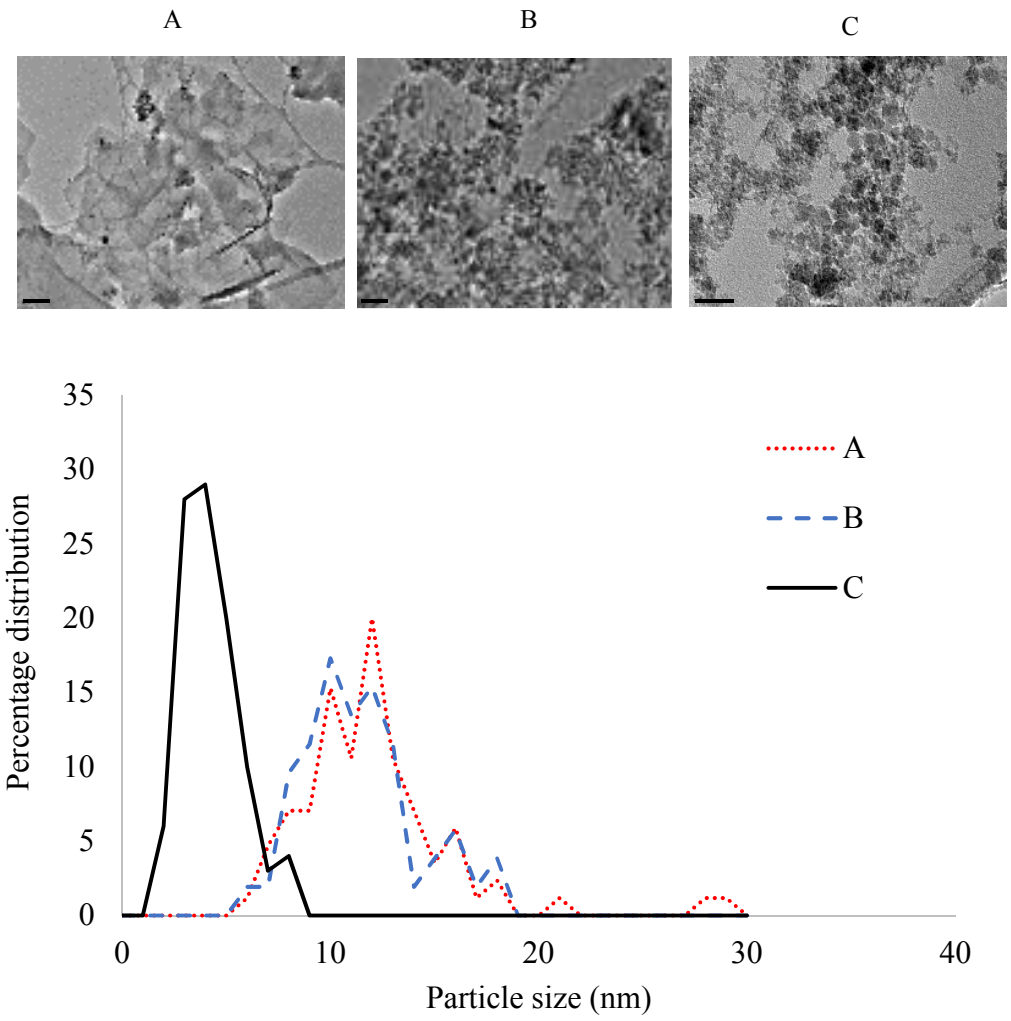

Figure 31. TEM micrographs and size distributions of SPIONs produced using 18 mA cm^{-2} current density, 9 mL s^{-1} flow rate at different electrolyte concentrations (A) 0.05 M, (B) 0.025 M, and (C) 0.015 M. Scale bars are 50 nm

SPION average size increased from 4 nm to 11 nm as flowrate decreased from 9 mL s^{-1} to 3 mL s^{-1}. At high flow rates, the particle diffusion in the tubular reactor increases. The increase in particle diffusion between electrodes during SPION electrosynthesis has been shown to decrease SPION mean size (Marques et al., 2008) . High flow plus instant magnetic separation decreases SPION exposure to the reaction site thereby reducing nanoparticle ripening or growth. In contrast to our observation, previous research on chemical synthesis of SPION in a flow injection system reported that increasing flow rate did not affect SPION mean size (Salazar-

Alvarez et al., 2006). The disagreement could be due to difference in synthesis method. I used an electrochemical method while other study used chemical method. The main difference between these methods is the process of creating a high pH zone required for SPION formation. A high pH zone is created with an electric current in electrochemical method while that is achieved by addition of alkali in the chemical method. Since electric current is the rate of change of charge, it is time dependent and can be affected by any factor that affects time. Increasing the electrolyte flow rate reduces the residence time of electrolyte in the TES reaction zone. Hence, the electrolyte flow rate in TES could reduce reaction time in the high pH zone which consequently affect SPION size growth.

The effect of current density is one of the most reported parameters in SPION electrosynthesis. As reported elsewhere, the results in Figure 30 show that increasing current density decreases SPION size (Cabrera et al., 2008). The lowest current density of 7 mA/cm^2 did not only increase mean SPION size but also broadened size distribution. The mean SPION size can be controlled by adjusting current density, in agreement with previous work (Ramimoghadam et al., 2014). In addition, we observed higher yield of SPIONs with increasing current density. Therefore, 18 mA cm^{-2} was used in subsequent experiments.

Chemical parameters have been reported to have more impact on SPION morphology than hydrodynamic parameters (Salazar-Alvarez et al., 2006). We found drastic change in the SPION size distribution with changes in electrolyte concentration. Increases in concentration caused an increase in SPION size and broadened the size distribution (Figure 31). Higher concentrations create more nucleation sites for nanoparticle growth (Karimzadeh et al., 2016). TEM analysis revealed some transparent flake-like particles in SPIONs produced with 0.05 M electrolyte. SPIONs produced under high electrolyte concentration have also been reported to

have some contaminants including non-crystalline amorphous substances (Cabrera et al., 2008; Ibrahim, Serrano, Noe, Garcia, & Verelst, 2009). The lowest electrolyte concentration (0.015 M), which produced SPIONs with a low mean size and narrow size distribution, is therefore preferred and was used in subsequent experiments. To understand the observed flake-like particles in the TEM images, we investigated SPION composition using XRD.

5.5.2. Crystallography of SPIONs

The crystal characteristics and composition of SPIONs were determined using XRD-crystallography. Figure 32 shows the raw X-ray diffraction (XRD) spectra of SPION samples produced under different reaction conditions. The spectra phase identification revealed the presence of magnetite (Fe_3O_4), goethite (FeOOH), and graphite, which confirms that the nanoparticles are magnetite. It has been reported that magnetite electrosynthesis involves the production of FeOOH as an intermediate product (Aghazadeh, 2018). Equation 5.3 shows the possible reaction pathway of SPION synthesis in TES.

$$3\gamma\text{-FeOOH} + \tfrac{1}{2}\,H_2 \rightarrow Fe_3O_4 + 2H_2O \qquad \text{(Equation 5.3)}$$

The graphite in the sample is due to carbon anode corrosion. In line with literature (Melnig & Ursu, 2011), electrochemical reaction corrodes the carbon anode due to surface oxidation at voltages greater than 1.7–1.9 V. The voltage in this study ranged between 3 – 5 V. The highest graphite content of SPIONs were produced with the highest electrolyte concentration, which suggests the possibility that the flakes observed in TEM were graphite. In order to reduce the presence of graphite, the carbon anode electrode was replaced with an aluminium electrode in subsequent experiments.

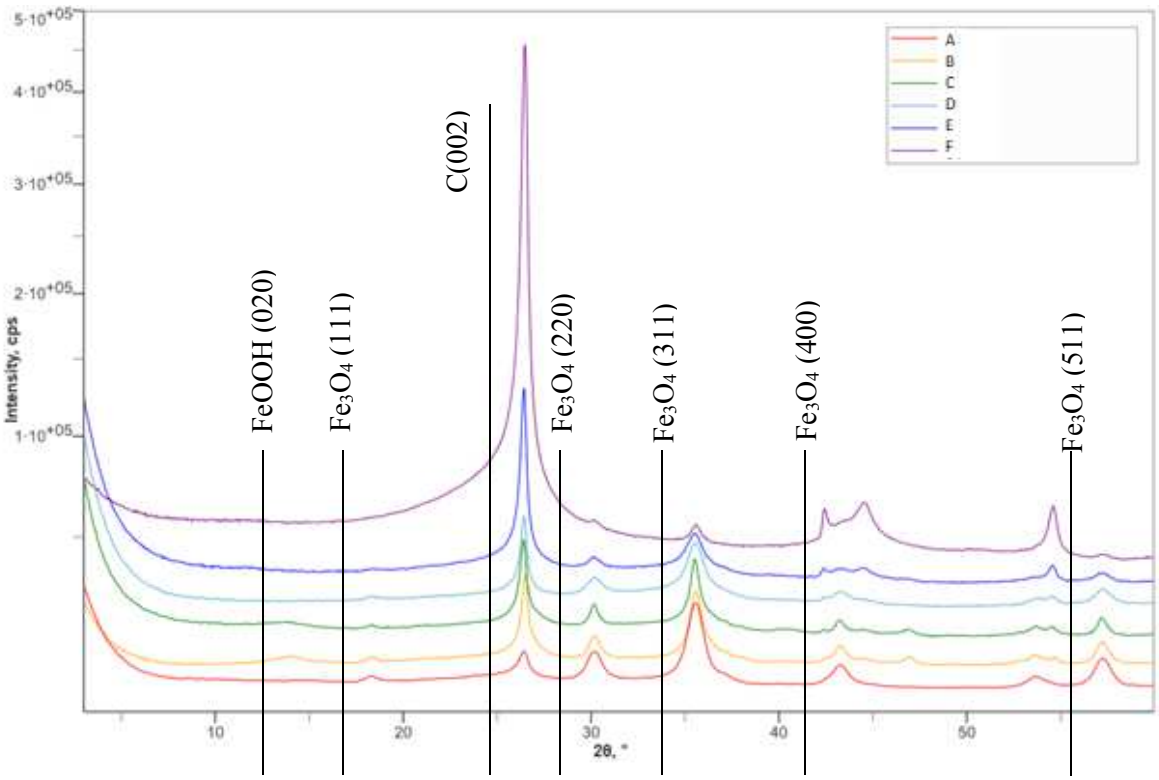

Figure 32. XRD-Crystallography analysis of SPIONs A: 0.015 M, 18 mA cm^{-2}, 9 mL s^{-1}, B: 0.015 M, 18 mA cm^{-2}, 3 mL s^{-1}, C: 0.015 M, 10 mA cm^{-2}, 9 mL s^{-1}, D: 0.015 M, 7 mA cm^{-2}, 9 mL s^{-1}, E: 0.025 M, mA cm^{-2}, 9 mL s^{-1}, and F: 0.05 M, 18 mA cm^{-2}, 9 mL s^{-1}

5.5.3. Change in iron ion concentration

Since one goal was to reuse the electrolyte, the first approach was to determine how the reactant concentration changes with time. SPION electrosynthesis involves complex reactions that cause variation in electrolyte concentration. We determined the change in Fe(III), Fe(II) and total iron concentrations during the first 30 min of SPION electrosynthesis (Figure 33). Fe(III), Fe(II) and total iron concentrations decreased sharply in the first 5 minutes and then stabilized. Similar reductions in reactant concentration in batch electrochemical processes have been reported, but for a longer stabilization time (Ibrahim et al., 2009). The difference from this result might be attributable to the difference in reaction conditions. Compared to the reaction conditions in Ibrahim et al. (2009), lower initial reactant concentrations and aqueous reaction medium were used in this study.

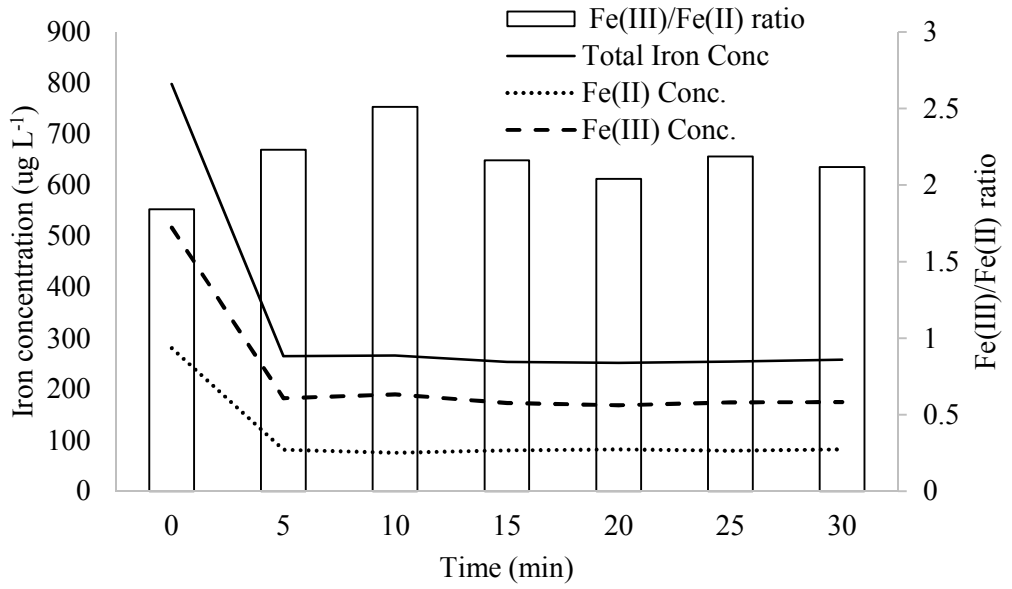

Figure 33. Change in iron ion concentration during SPION electrochemical synthesis

The characteristics and yield of electrochemical reaction depends on the electrolyte concentration and the ratio of Fe(II) and Fe(III). The Fe(III) to Fe(II) ratio increased from 2 to 2.5 in the first 10 min and then stabilized at approximate 2.1. An increase in Fe(III):Fe(II) suggests that there was an internal conversion of Fe(II) to Fe(III). The reduction in iron ratio from 10 – 20 min corresponds to the time when SPIONs started forming. It is understood that initial conversion of Fe(II) to Fe(III) is required for SPION formation. This is in line with the SPION production mechanism in Figure 18. The concentration of all the ion species stabilized by the end of 30 min marking the end of the reaction. Previous research has shown that 30 min is enough for electrochemical reaction during SPION synthesis (Aghazadeh, 2018).

The SPION synthesis mechanism involves reversible reactions that require reactants to be available in the system (Ramimoghadam et al., 2014). Electrochemical reactions require electrolyte containing free moving ions for current flow; therefore, the residue ions maintained the electrochemical process. The minimum amount of reactant in the reaction medium are

approximately 200, 100, and 300 μg L^{-1} for Fe(III), Fe(II) and total iron, respectively. The amount of used reactant is valuable to know the amount required for supplementation.

5.5.4. Effect of electrolyte supplementation strategy on SPION yield and productivity

Product yield and productivity are important to industry, especially for a new process design. Figure 34 shows SPION yield and productivity of TES. The yield ranges from 4.7 to 8.3 mg $mole^{-1}$ Fe while the productivity ranges from 107 to 163 μg $mole^{-1}$ Fe min^{-1}. There are limited reports on SPION yield and productivity in electrochemical systems and the available reports were not based on the amount of starting materials and the reaction time. For instance, 80% SPION yield was reported in electrochemical system after 1800 s reaction time using sacrificial electrode (Cabrera et al., 2008). In another report, electrochemical synthesis of 0.7 g SPION requires 20 h and 0.3 $mAcm^{-2}$ current density (Setyawan & Widiyastuti, 2019). It was not clear the amount of substrate that was utilized and how the yield was estimated in both reports.

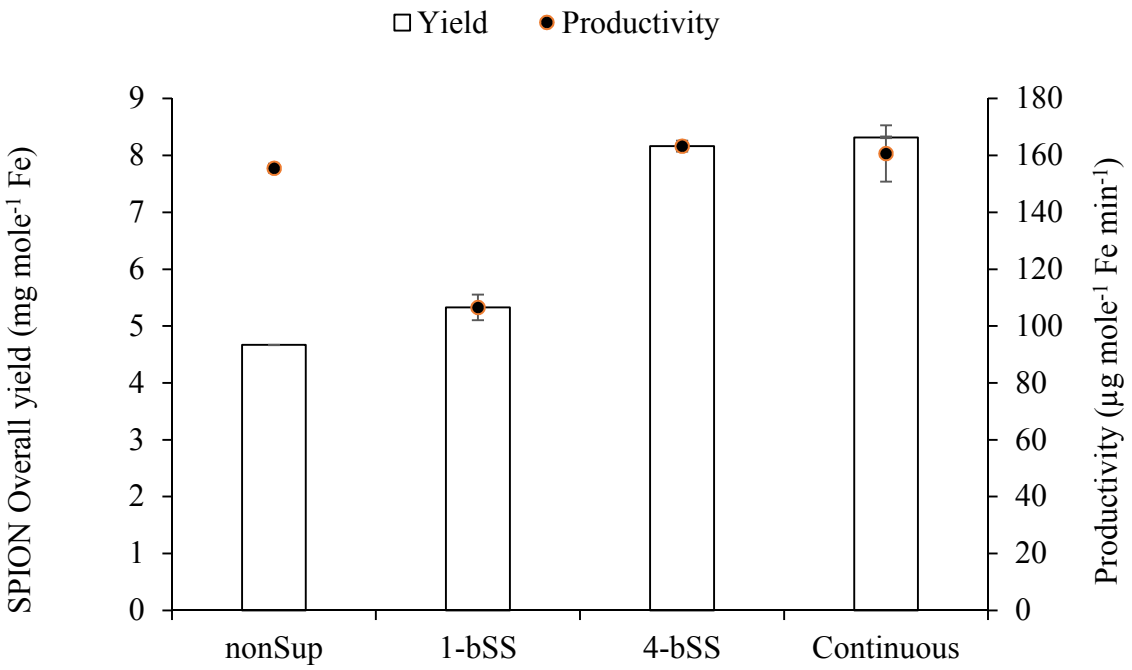

Figure 34. SPION overall yield and productivity at different supplementation strategies, nonSup: no supplementation with 0.015 M, 1-bSS: one-time batch supplementation strategy, 4-bSS: four-time supplementation strategy with 0.00375 M Fe, and Continuous: an addition of 10 mL of 0.015 M at 0.5 mL min^{-1} flowrate

Overcoming scalability and sustainability challenges is essential for large scale application of SPION electrosynthesis. Many studies on SPION electrosynthesis use repeated batch process that require electrolyte replacement. One disadvantage of repeated batch processes is release of effluent that could overwhelm wastewater treatment plants. In order to reduce TES effluent and increase SPION yield and productivity, we investigated the possibility of electrolyte reuse combined with electrolyte replenishment. Therefore, the electrolyte was supplemented with 0.015 M Fe and run for an additional 20 min. This supplementation strategy is referred to as one-time batch supplementation strategy (1-bSS). Although, 1-bSS SPION yield was 14% higher than non-supplemented control sample, productivity dropped by ~32%. As expected, we observed an increase (~3A) in current with supplementation due to increase in electrolyte concentration with the addition of electrolyte in 1-bSS feeding strategy. The sudden change in

concentration and current causing unintended shift in the processing conditions. SPION electrosynthesis is complex and consists of a sequence of unit steps that are sensitive to change in reactant concentration and reaction conditions (Ramimoghadam et al., 2014). The reduction in productivity might be due to the change in processing conditions which could delay product formation.

Low productivity has been identified as a common processing system bottleneck including in electrochemical systems (Anasontzis et al., 2011). Since the reduction in productivity seems uneconomical, we therefore conducted two gradual supplementation strategies to reduce current fluctuation and increase productivity. The two strategies that were employed are four-time batch supplementation strategy (4-bSS) consisting of four additions of 2.5 ml of 0.015 M Fe at 5 min intervals; and a continuous strategy with an addition of 10 mL of 0.015 M Fe at flowrate of 0.5 mL min^{-1}. The overall yield increased by 75 and 78%, respectively, for these strategies without significant reduction in productivity. The continuous reactant supplementation strategy eliminated the current fluctuation observed with the batch supplementation strategies (1-bSS and 4-bSS).

5.6. Conclusion

Spherical SPIONs were synthesized in a tubular electrochemical system with few challenges. Contrary to increasing the electrolyte concentration, increasing the current density and flowrate reduced reduce SPION size distribution. By controlling the current density and flow rate, 2 - 10 nm diameter SPIONs can be synthesized in an aqueous solution with the TES. Gradual supplementation strategies of electrolyte are preferred to batch supplementation because they increase SPION yield without a decrease in productivity. TES allows for electrolyte reuse

and therefore reduces process effluent. SPION aggregation problems can be overcome by surface functionalization in future work.

5.7. References

Aghazadeh, M. (2018). One-step cathodic electrosynthesis of surface capped Fe3O4 ultra-fine nanoparticles from ethanol medium without using coating agent. *Materials Letters*, *211*, 225–229. https://doi.org/10.1016/j.matlet.2017.09.086

Aghazadeh, M., Karimzadeh, I., Ganjali, M. R., & Mohebi Morad, M. (2017). A novel preparation method for surface coated superparamagnetic Fe3O4 nanoparticles with vitamin C and sucrose. *Materials Letters*, *196*, 392–395. https://doi.org/10.1016/j.matlet.2017.03.064

Ali, A., Zafar, H., Zia, M., ul Haq, I., Phull, A. R., Ali, J. S., & Hussain, A. (2016). Synthesis, characterization, applications, and challenges of iron oxide nanoparticles. *Nanotechnology, Science and Applications*, *9*, 49–67. https://doi.org/10.2147/NSA.S99986

Anasontzis, G. E., Zerva, A., Stathopoulou, P. M., Haralampidis, K., Diallinas, G., Karagouni, A. D., & Hatzinikolaou, D. G. (2011). Homologous overexpression of xylanase in Fusarium oxysporum increases ethanol productivity during consolidated bioprocessing (CBP) of lignocellulosics. *Journal of Biotechnology*, *152*(1–2), 16–23.

Cabrera, L., Gutierrez, S., Menendez, N., Morales, M. P., & Herrasti, P. (2008). Magnetite nanoparticles: Electrochemical synthesis and characterization. *Electrochimica Acta*, *53*(8), 3436–3441. https://doi.org/10.1016/j.electacta.2007.12.006

Cheng, X.-Y., Li, Q., & Liu, C.-Z. (2012). Coproduction of hydrogen and methane via anaerobic fermentation of cornstalk waste in continuous stirred tank reactor integrated with up-flow

anaerobic sludge bed. *Bioresource Technology*, *114*, 327–333. https://doi.org/10.1016/j.biortech.2012.03.038

Fajaroh, F., Setyawan, H., Nur, A., & Lenggoro, I. W. (2013). Thermal stability of silica-coated magnetite nanoparticles prepared by an electrochemical method. *Advanced Powder Technology*, *24*(2), 507–511. https://doi.org/10.1016/j.apt.2012.09.008

Ibrahim, M., Serrano, K. G., Noe, L., Garcia, C., & Verelst, M. (2009). Electro-precipitation of magnetite nanoparticles: An electrochemical study. *Electrochimica Acta*, *55*(1), 155–158. https://doi.org/10.1016/j.electacta.2009.08.026

Karimzadeh, I., Aghazadeh, M., Ganjali, M. R., Norouzi, P., Shirvani-Arani, S., Doroudi, T., … Gharailou, D. (2016). A novel method for preparation of bare and poly(vinylpyrrolidone) coated superparamagnetic iron oxide nanoparticles for biomedical applications. *Materials Letters*, *179*, 5–8. https://doi.org/10.1016/j.matlet.2016.05.048

Karthikeyan, O. P., Selvam, A., & Wong, J. W. C. (2016). Hydrolysis–acidogenesis of food waste in solid–liquid-separating continuous stirred tank reactor (SLS-CSTR) for volatile organic acid production. *Bioresource Technology*, *200*, 366–373. https://doi.org/10.1016/j.biortech.2015.10.017

Kohut, A., Pryor, S. W., Voronov, A., & Minko, S. (2017). Enzymogel Nanoparticles Chemistry for Highly Efficient Phase Boundary Biocatalysis. In *Biocatalysis and Nanotechnology* (pp. 369–399). Jenny Stanford Publishing.

Kudina, O., Zakharchenko, A., Trotsenko, O., Tokarev, A., Ionov, L., Stoychev, G., … Minko, S. (2014). Highly efficient phase boundary biocatalysis with enzymogel nanoparticles. *Angewandte Chemie International Edition*, *53*(2), 483–487.

Marques, R. F. C., Garcia, C., Lecante, P., Ribeiro, S. J. L., Noé, L., Silva, N. J. O., … Verelst, M. (2008). Electro-precipitation of Fe3O4 nanoparticles in ethanol. *Journal of Magnetism and Magnetic Materials*, *320*(19), 2311–2315. https://doi.org/10.1016/j.jmmm.2008.04.165

Melnig, V., & Ursu, L. (2011). Poly(amidehydroxyurethane) template magnetite nanoparticles electrosynthesis: I. Electrochemical aspects and identification. *Journal of Nanoparticle Research*, *13*(6), 2509–2523. https://doi.org/10.1007/s11051-010-0144-7

Park, H., Ayala, P., Deshusses, M. A., Mulchandani, A., Choi, H., & Myung, N. V. (2008). Electrodeposition of maghemite (γ-Fe2O3) nanoparticles. *Chemical Engineering Journal*, *139*(1), 208–212. https://doi.org/10.1016/j.cej.2007.10.025

Pascu, O., Marre, S., Aymonier, C., & Roig, A. (2013). Ultrafast and continuous synthesis of crystalline ferrite nanoparticles in supercritical ethanol. *Nanoscale*, *5*(5), 2126–2132. https://doi.org/10.1039/C3NR33501A

Ramimoghadam, D., Bagheri, S., & Hamid, S. B. A. (2014). Progress in electrochemical synthesis of magnetic iron oxide nanoparticles. *Journal of Magnetism and Magnetic Materials*, *368*, 207–229. https://doi.org/10.1016/j.jmmm.2014.05.015

Robertson, J. D., Rizzello, L., Avila-Olias, M., Gaitzsch, J., Contini, C., Magoń, M. S., … Battaglia, G. (2016). Purification of Nanoparticles by Size and Shape. *Scientific Reports*, *6*, 27494. https://doi.org/10.1038/srep27494

Salazar-Alvarez, G., Muhammed, M., & Zagorodni, A. A. (2006). Novel flow injection synthesis of iron oxide nanoparticles with narrow size distribution. *Chemical Engineering Science*, *61*(14), 4625–4633. https://doi.org/10.1016/j.ces.2006.02.032

Samaratunga, A., Kudina, O., Nahar, N., Zakharchenko, A., Minko, S., Voronov, A., & Pryor, S. W. (2015a). Impact of enzyme loading on the efficacy and recovery of cellulolytic enzymes immobilized on enzymogel nanoparticles. *Applied Biochemistry and Biotechnology*, *175*(6), 2872–2882.

Samaratunga, A., Kudina, O., Nahar, N., Zakharchenko, A., Minko, S., Voronov, A., & Pryor, S. W. (2015b). Modeling the effect of pH and temperature for cellulases immobilized on enzymogel nanoparticles. *Applied Biochemistry and Biotechnology*, *176*(4), 1114–1130.

Setyawan, H., & Widiyastuti, W. (2019). Progress in the preparation of magnetite nanoparticles through the electrochemical method. *KONA Powder and Particle Journal*, 2019011.

Veriansyah, B., Kim, J.-D., Min, B. K., & Kim, J. (2010). Continuous synthesis of magnetite nanoparticles in supercritical methanol. *Materials Letters*, *64*(20), 2197–2200. https://doi.org/10.1016/j.matlet.2010.07.018

Winburn, R. S., Lerach, S. L., Jarabek, B. R., Wisdom, M. A., Grier, D. G., & McCarthy, G. J. (2000). Quantitative XRD analysis of coal combustion by-products by the Rietveld method. Testing with standard mixtures. *Adv. X-ray Anal*, *42*, 387-396.

Xu, C., & Teja, A. S. (2008). Continuous hydrothermal synthesis of iron oxide and PVA-protected iron oxide nanoparticles. *The Journal of Supercritical Fluids*, *44*(1), 85–91. https://doi.org/10.1016/j.supflu.2007.09.033

Xue, D.-S., Chen, G.-J., Su, B.-X., Liu, Y.-H., Zhang, D.-P., Guo, Q., … Sun, J.-F. (2020). On-line spectrophotometric determination of ferrous and total iron in monominerals by flow injection combined with a Schlenk line-based digestion apparatus to exclude oxygen. *Microchemical Journal*, *155*, 104743.

6. TUBULAR ELECTROSYNTHESIS OF SILICA COATED MAGNETITE AND EVALUATION OF MAGNETIC NANOBIOCATALYST EFFICACY DURING BIOMASS HYDROLYSIS

6.1. Abstract

Magnetic nanobiocatalysts (MNBCs) are a promising immobilization approach to ease enzyme recovery during bioprocessing. However, industrial adoption of MNBCs is unfeasible because MNBC-synthesis involves complex and potentially expensive processing steps including synthesis of silica-coated superparamagnetic iron oxide nanoparticles (Si-SPIONs). We developed a single-step process for Si-SPION synthesis using a tubular electrochemical system (TES), and investigated the effect of concentration of the Na_2SiO_3 coating agent on Si-SPION properties. The Si-SPIONs were used as a support for attachment of polymer-cellulase conjugate to make MNBCs. The spherical Si-SPIONs were 8 – 12 nm in diameter including a 2-nm silica coating. Na_2SiO_3 concentration in the reactor did not affect Si-SPION morphology, but increasing Na_2SiO_3 concentration reduced SPION productivity in the reactor. Protective properties of the SPION silica coatings were demonstrated by showing that they prevented dissolution of SPIONs in an acid solution for 48 h. Enzyme attachment was quantified as protein adsorption on Si-SPIONs which reached 55 μg/mg Si-SPION. The MNBCs were recovered and reused four times. The use of TES for Si-SPION synthesis is promising to reduce MNBC production complexity.

6.2. Keywords

Nanobiocatalyst, biomass hydrolysis, enzyme immobilization, silica coating, nanoparticles

6.3. Introduction

Some microbes have evolved to produce extracellular cellulosomes – immobilized cellulases – for efficient plant biomass hydrolysis. Cellulosomes are nanobiocatalysts containing linear protein scaffoldins with multiple docking sites where the cellulases are attached. Cellulosomes have been reported to enhance enzyme synergy and processivity, reduce non-productive adsorption, and improve degradation of recalcitrant crystalline cellulose. Many researchers have developed synthetic nanobiocatalysts that mimic cellulosome structure (Ansari & Husain, 2012). Although functional, these nanobiocatalysts are not easily recoverable negating one of the potential benefits of enzyme immobilization. Therefore, some studies have immobilized cellulase on magnetic nanoparticles (mostly superparamagnetic iron oxide nanoparticles – SPIONs) for the production of magnetic nanobiocatalysts (MNBCs) (Han et al., 2018; Roth, Schwaminger, Peng, & Berensmeier, 2016). Although, MNBCs could be magnetically recovered for reuse, there are still challenges to simplify the synthesis process.

SPIONs have low toxicity, and are also useful in the biomedical, food, chemical, and electronic industries (Lien & Wu, 2008). However, SPIONs are readily oxidized by oxygen under ambient conditions. The reactivity of SPIONs limits their applications for uses such as biomass hydrolysis because they corrode in aqueous media. Nanoparticles also self-aggregate reducing the available surface area needed for enzyme immobilization (Bohara, Thorat, & Pawar, 2016). Surface modifications can be done that will permanently protect iron-oxide nanoparticles from oxidation as well as prevent aggregation (Abhari, Madadlou, & Dini, 2017). Surface-modified SPIONs aggregate less and form a stable colloidal solution. SPIONs have been coated with a wide variety of organic and inorganic agents including graphene, chitosan, polyethylene glycol, polyvinyl alcohol, alginate, polyacrylic acid, dextran, chitosan, amines,

amino-silanes, citrates, metal, metal oxides, liposomes, thiols, and phosphates (Haddad et al., 2004; Sodipo & Aziz, 2016; Wang, Zhu, Yang, & Li, 2007).

Inorganic coatings are of greater interest because of their controllable chemical properties that broaden SPION applications for biolabelling, bioseparation, and catalysis (Bohara et al., 2016). Silica is a non-toxic, and biocompatible inorganic coating for SPIONs. Silica protects the SPION surface and improves adsorption of organic molecules. Silica-coated nanoparticles have been identified as useful carriers of bioactive agents for drug delivery and nanobiocatalyst applications. Silica is attractive as a SPION coating because of its low cost and well-known inertness, hydrophobicity, and non-toxicity. A silica shell eases further surface functionalization because of its silanol groups for linking other functional groups (Abbas, Abdel-Hamed, & Chen, 2017). Silica coating of SPIONs also offers the advantage of agglomeration prevention to enable the study of SPION properties since they will be well dispersed (Ahankar et al., 2018). Therefore, silica coating of SPION is necessary to develop MNBCs,

The major challenges facing silica-coated SPIONs are the process complexity and associated high cost. Researchers have used many chemical methods to produce silica-coated SPIONs (Si-SPIONs). Among the chemical methods, the sol-gel methods (Stober and microemulsion processes) are commonly used (Sodipo & Aziz, 2016). However, these approaches require multiples steps after SPION synthesis, including coating with silica followed by several washing and recovery stages (Bohara et al., 2016). Depending on the method used for SPION synthesis, the entire silica-coating process can take from 24 to 48 h to complete. The approaches also use a large amount of costly surfactant (Abbas et al., 2017).

To overcome these challenges, several studies have focused on developing a one-pot synthesis method that combines SPION synthesis and coating into a single process. One-pot

synthesis helps prevent large particle size and achieves a more narrow size distribution (Bohara et al., 2016). Haddad et al. (Haddad et al., 2004) developed a precipitation method to synthesize Si-SPIONs within 2 h, but the process requires temperatures as high as 500^{o}C. Abbas et al. (Abbas et al., 2017) developed a sonochemical process for fast synthesis of Si-SPIONs but still requires relatively high temperature (227^{o}C) and pressure (500 bar). Wang et al. (Wang et al., 2007) used an electrochemical approach to produce Si-SPIONs in an alkaline aqueous medium but the method requires an additional thermal reducing treatment that does not improve chemical stability of Si-SPIONs in acid solution (Cendrowski, Sikora, Zielinska, Horszczaruk, & Mijowska, 2017). Several studies demonstrated successful production of Si-SPIONs in an $FeSO_4$ and Na_2SiO_3 solution using one-step electrosynthesis in 30 min (Setyawan et al., 2012) (Karimzadeh et al., 2017) (Fajaroh, Setyawan, Nur, & Lenggoro, 2013). However, the electrochemical system setup used in previous studies could lead to generation of used electrolytes as effluent.

We have developed a tubular electrochemical system (TES) that could reduce electrolyte effluent, ease SPION recovery, and be operated as a continuous process. However, the alkaline conditions which are necessary for the coating process can only occur in the reaction chamber of the TES. It is not known if a TES can create adequate alkaline conditions to allow coating to occur. Therefore, we investigated the use of TES for one-pot synthesis of Si-SPIONs. The Si-SPIONs were then used to produce MNBCs and tested for biomass hydrolysis.

6.4. Methods

6.4.1. Synthesis of uncoated and silica-coated SPIONs

SPION preparation was carried out in a TES containing 1 L of electrolyte (aqueous solution of 0.01 M $Fe(NO_3)_3$ and 0.005 M $FeCl_2$), an aluminium rod anode, and a copper pipe

cathode. The electrodes were connected to a DC power supply (Extech Instrument, Model 382275; Taiwan). Synthesis was carried out for 30 min and SPIONs were continuously recovered using a strong neodymium magnet that was positioned within the separating vessel. SPIONs were collected and washed three times with ethanol and oven-dried overnight at 70°C. The same process was used for synthesis of Si-SPIONs except with the addition of Na_2SiO_3 as a coating agent into the electrolytes. Two Na_2SiO_3 concentrations (0.05 or 0.1 M) were used to determine the effect of Na_2SiO_3 concentration on Si-SPION properties and TES productivity. The SPION yield and productivity were estimated using Equations 6.1 and 6.2, respectively.

$$\text{Yield} = \frac{SPION\ dry\ mass}{mole\ of\ Fe} \qquad \text{(Equation 6.1)}$$

$$\text{Productivity} = \frac{SPION\ yield}{reaction\ time} \qquad \text{(Equation 6.2)}$$

6.4.2. Determination of SPION morphology

SPION samples were powdered with a mortar and pestle, and dispersed in ethanol by treating in an ultrasonic bath for 2 – 3 min at 40 kHz. The dispersed SPIONs were transferred to a 300-mesh carbon-coated copper transmission electron microscope grid (Electron Microscopy Sciences; Hatfield, PA, USA). Excess ethanol was removed using filter paper. The particle images were acquired using a JEOL JEM-2100 LaB_6 transmission electron microscope (JEOL USA; Peabody, MA, USA) running at 200 kV. ImageJ software was used to determine the particle size distribution from the images.

6.4.3. SPION chemical characterization

The surface chemistry of SPION was characterized using FTIR spectroscopy. The spectra of SPION functional groups was collected using Fourier transform infrared spectrometer (FTIR; Nicolet 8700 Thermo Scientific, USA). Approximately 1 mg of dried SPION sample was ground

with 30 mg of potassium bromide and pressed to form a pellet disc. The spectra were collected within a frequency range of 4000 – 400 cm^{-1}. Spectra peaks were identified using OMNIC software (Thermo Scientific).

6.4.4. Determination of SPION dissolution

A mass of 20 mg Si-SPIONs was mixed with 100 ml of 0.5 M H_2SO_4 solution. Dissolution was conducted at 50^oC under continuous stirring. Aliquots of 5 mL were taken at 24, 48 and 72 h for total iron analysis using UV–Vis spectrophotometry measurement after reaction with 1,10-phenanthroline (Xue et al., 2020).

6.4.5. Synthesis of magnetic nanobiocatalysts

Polymer enzyme conjugate (PEC) containing 2g polymer and 0.2 g cellulase in 10 ml solution was synthesized as previously described (Oksana et al., 2021). Different amounts (20, 40, 60, 80, and 100 mg) of dried Si-SPION were suspended in 0.5 ml of citrate buffer (pH 4.6, 100 mM) and mixed by two alternating cycles of 2 min stirring at 3000 rpm, and 20 min with ultrasonic mixing at 40 kHz. Then 1.5 ml of PEC solution was added and mixed under vigorous stirring for 24 h. The magnetic nanobiocatalysts (MNBCs) were magnetically separated from the solution and resuspended in 1.5 ml buffer solution at pH 4.8. The enzyme remaining in the solution was quantified using a micro-Bradford assay measuring absorbance at 590 nm. Bovine serum albumin was used as standard.

6.4.6. Biomass hydrolysis

Switchgrass (~200g) was pretreated in an autoclave reactor (5L Hastelloy Kiloclave, Büchi AG; Switzerland) containing 3 L of 1% sulfuric acid (w/w) solution at 140^oC with stirring at 62 rpm for 20 min. Hydrolysis was carried out as previously described (Samaratunga et al., 2015a) with some modification. The MNBCs were diluted with buffer solution at pH 4.8 to

create 0.08 g enzyme in 3 ml. The pretreated biomass (1% glucan loading equivalent) was weighed in a glass tube. The 3 ml MNBC was added and hydrolysis was carried out at 50°C with continuous stirring at 130 rpm for 48 h.

6.4.7. Glucose analysis

The amount of glucose released during biomass hydrolysis was determined using HPLC (Waters Corporation; Milford, MA, USA). HPLC settings included a 20-µL injection volume, mobile phase of 18-mΩ Nanopure water at a 0.6 ml min^{-1} flow rate, 50°C column temperature, and 85°C detector temperature. A Bio-Rad Aminex HPX-87P column (Bio-Rad Laboratories; Hercules, CA, USA) was used for separation. The effluent sugar content was measured using a refractive index (RI) detector (model 2414, Waters Corporation) (Samaratunga et al., 2015b). The amount of sugar release was used to estimate enzyme efficacy in terms of glucan conversion and relative glucan conversion.

6.5. Results and Discussion

6.5.1. Surface chemistry of SPION

Functional group analysis is a quick method to confirm the success of SPION Si-coating using TES. Figure 35 shows that the FTIR spectra of uncoated SPIONs are similar to those coated using 2 different treatment conditions, except in the region of 1059 - 1163 cm^{-1}. This region corresponds to siloxane (Si–O–Si) characteristic peaks confirming the success of silica coating. Similar to previous SPION studies, all samples have peaks around 584 and 442 cm^{-1} depicting Fe-O stretching vibrations that correspond to Fe_3O_4 molecules (Abbas et al., 2017; Aghazadeh, 2018; Cabrera, Gutierrez, Menendez, Morales, & Herrasti, 2008). The bands between 3600 and 3200 cm^{-1} and the peaks near 1630 cm^{-1} are due to the stretching and deformation vibrations of OH on the SPION surfaces (Aghazadeh, 2018; Cabrera et al., 2008;

Setyawan et al., 2012). The presence of peaks in the region 1059 - 1163 cm^{-1} confirms that SPIONS are being coated with silica in the single pot TES.

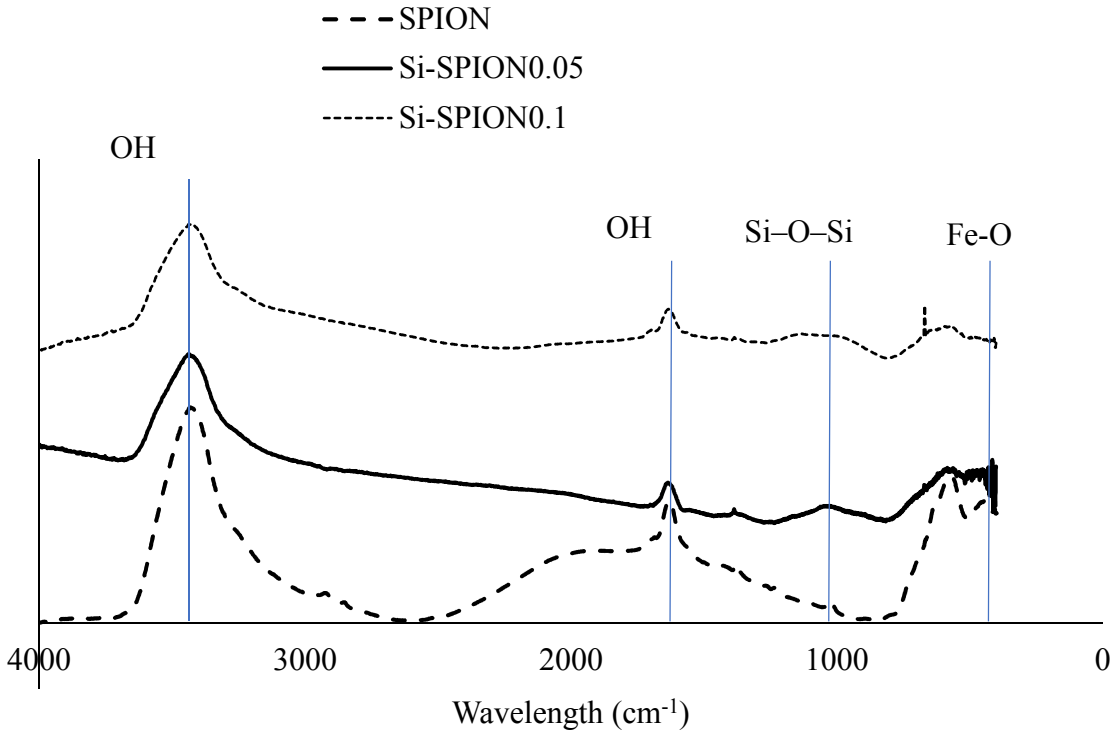

Figure 35. FTIR spectra of SPION, Si-SPION0.05 and Si-SPION0.1 synthesized with 0, 0.05 and 0.1 M concentration of Na_2SiO_3, respectively, in the TES reactor

6.5.2. Morphology

Coating SPIONs with silica can result in different morphologies which could affect available surface area for enzyme immobilization. The fact that all individual particles in Figure 36 appear to be circular indicates that both uncoated and coated SPIONs are spherical. ImageJ analysis of the images revealed that the size distribution of SPIONs and Si-SPIONs ranged between 8 and 12 nm, which is similar to the 9 -12 nm range reported previously using an electrochemical method in a batch system (Fajaroh et al., 2013). The Si-SPIONs show a silica layer unlike the uncoated SPIONs. In Figures 36b and 36c, the darker regions represent the

SPION core and the more translucent periphery is the Si coating. Silica layers with 2 nm thickness have also been reported for electrochemically synthesized SPIONs by Roth et al. [3].

It was initially expected that higher Na_2SiO_3 concentrations in the media would provide more Si for continuous growth of coating resulting in thicker layers. However, increasing concentration of Na_2SiO_3 from 0.05 to 0.1 M during synthesis did not affect coating thickness or SPION size distribution. A possible reason for the lack of Na_2SiO_3 concentration effect on coat thickness might be the TES ability to separate nanoparticles from reaction region after being synthesized. Therefore, the growth of silica coating would have stopped because the particles were not allowed to return to the reaction region. Hence, all the particles are coated similarly in the reaction region irrespective of Na_2SiO_3 concentrations used in this study. However, it is important to note that the Si-coat thickness could also be a function of residence time and there could be an interactive effect between Na_2SiO_3 concentration and residence time.

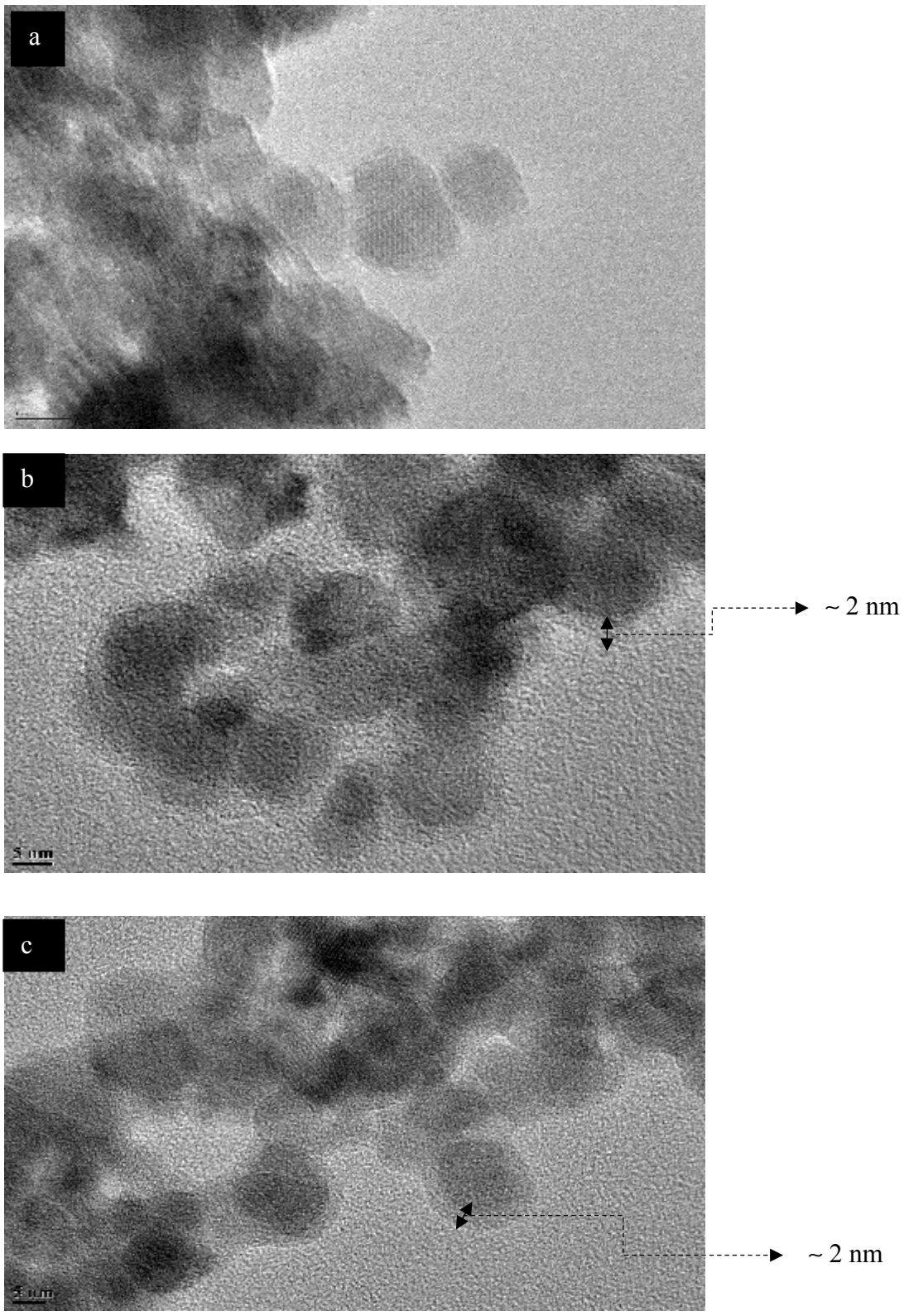

Figure 36. TEM image of uncoated and silica coated SPION, a: uncoated SPIONs, b: SPIONs coated using 0.1 M Na_2SiO_3, and c: SPIONs coated using 0.05 M Na_2SiO_3

6.5.3. Dissolution

The SPION dissolution process includes protonation, complexation, and reduction steps (Kalska-Szostko, Wykowska, Piekut, & Satuła, 2014). SPION surface OH^- functional groups are modified into hydrated oxide in water. Acting as Lewis acid, the transformed surface accepts a proton and becomes positively charged. Further adsorption of protons, especially in acidic media, enhances polarization and leads to weakening of Fe-O bonds (Kalska-Szostko et al., 2014). The acidic anions also promote Fe-O dissolution by replacing OH groups on SPION surfaces. This complexation processes result in detachment of Fe atoms into the surrounding solution.

The silica SPION coating is an interconnected network of SiO_2 six-member rings that serves as a physical barrier preventing acid diffusion (Cendrowski et al., 2017). We measured the absorbance of the acidic dissolution media at 510 nm which indicates Fe^+ released over time (24, 48, and 72 h) to investigate if TES-produced Si-SPIONs would be resistant to dissolution.

Figure 37 shows that uncoated SPIONs dissolved in acid after 72 h. Si-SPIONs released about 40% Fe compared to uncoated. Previous work has shown that SPIONs release Fe^+ in acidic solutions (Kalska-Szostko et al., 2014). Unlike uncoated SPIONs, Si-SPIONs did not dissolve by 24 or 48 h suggesting that the Si-coating protects SPIONs for at least 48 h. Others have also shown that a Si-coating delays SPION dissolution in acidic conditions at different concentrations and time (Cendrowski et al., 2017; Kalska-Szostko et al., 2014). Cendrowski et al. (Cendrowski et al., 2017) also reported that coated SPIONs were less susceptible to dissolution. However, they observed some dissolution in Si-SPIONs after 24 h when using a 100× higher acid concentration than used in our study. Increasing acid concentrations degrade the Si-coating more quickly and thereby allow SPIONs to dissolve (Cendrowski et al., 2017). The lack of dissolution

by 48 h confirmed that the silica coating completely covered the SPION surface as suggested from their morphology in Figure 36. The result also shows that the dissolution of both Si-SPION samples are equal. Therefore, Si-coating offers similar protection, irrespective of Na_2SiO_3 concentration in the TES. This observation was expected because previously results showed that the reactor silica concentration did not affect coating thickness.

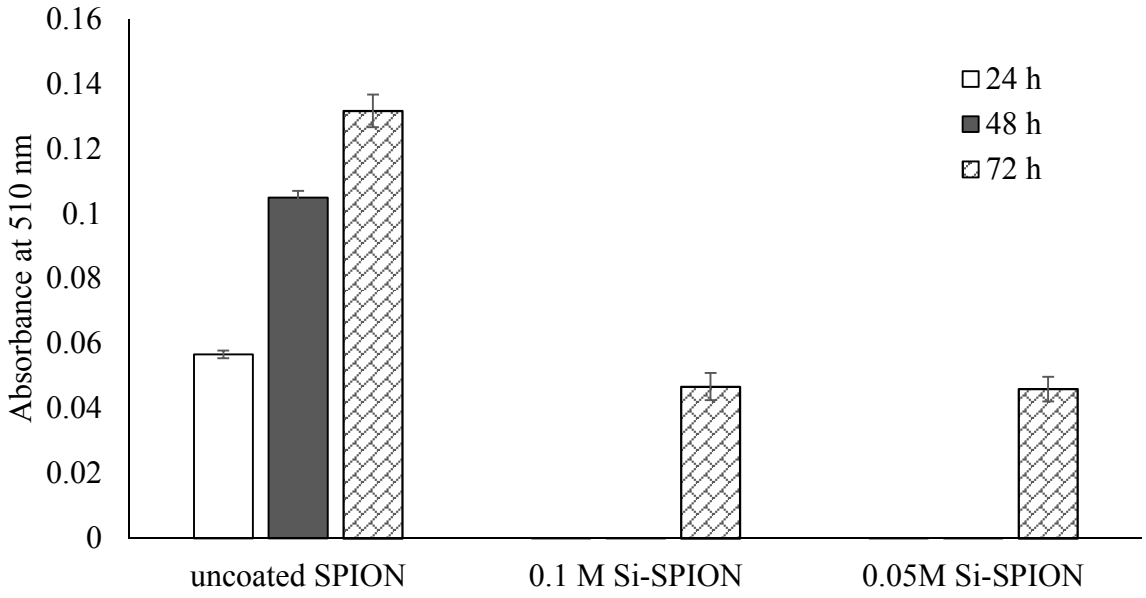

Figure 37. Absorbance of dissolved Fe^+ during dissolution of uncoated SPIONs and coated SPIONs in 0.1 M and 0.05 M Na_2SiO_3 solution, after contact with 0.5 M H_2SO_4 solution at different exposure time

6.5.4. Effect of Si concentration on SPION productivity

SPION electrosynthesis includes the formation of numerous reactive intermediate ions such as NO_2^-, Fe_2^+, Fe_3^+, OH^- and NO_3^- (Cabrera et al., 2008). These intermediates can react with Na_2SiO_3 to form products other than SPIONs. These potential alternative pathways make SPION electrosynthesis challenging in the presence of Na_2SiO_3. Most especially, Na^+ from Na_2SiO_3 ionization might change the reaction pathway away from SPION synthesis by reacting with the negatively charged intermediates. We investigated the effect of different concentrations (0.1 and 0.05 M) of Na_2SiO_3 on TES productivity. Figure 38 shows that the productivity drops with

increasing Na_2SiO_3 concentration. The decrease in productivity may be due to the presence of Na^+ from Na_2SiO_3.

Since the SPION coating with electrolyte containing 0.05 M Na_2SiO_3 caused less reduction in productivity compared to the uncoated SPIONs but still produced Si-SPIONs with a similar silica-coat thickness and dissolution protection, we used Si-SPIONs coated in electrolyte containing 0.05 M Na_2SiO_3 in our subsequent enzyme immobilization experiments.

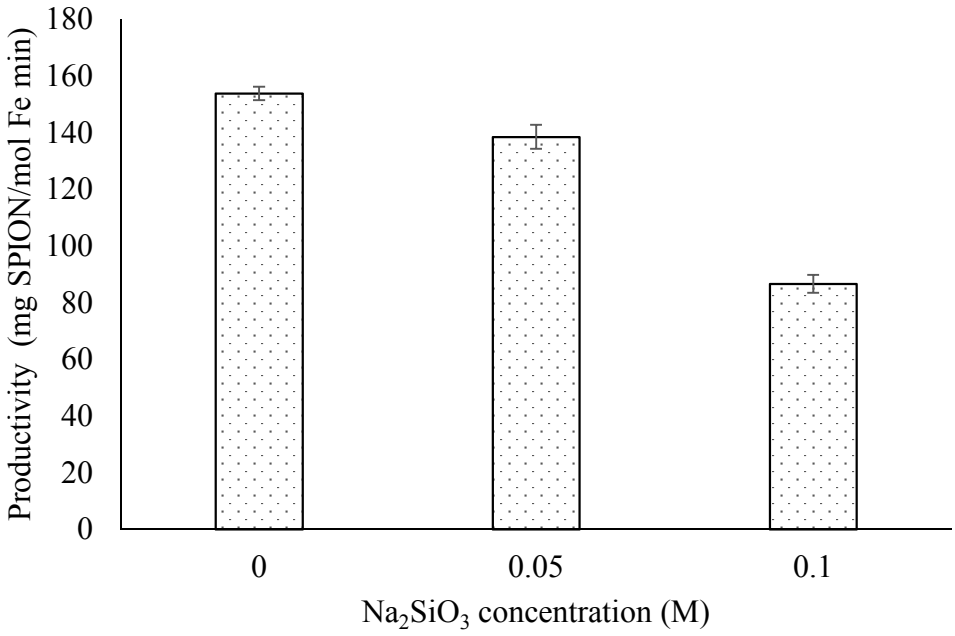

Figure 38. SPION productivity at different levels of Na_2SiO_3. Uncoated SPIONs, 0.1 M Si-SPIONs and 0.05 M Si-SPIONs, respectively, represent SPION coated using 0 M, 0.1 M and 0.05 M Na_2SiO_3

6.5.5. Si-SPION adsorption of polymer enzyme conjugate

We used Si-SPIONs to create MNBCs through adsorption of PECs to the SPION surface. The PEC adsorption capacity of Si-SPIONs was investigated by adding different masses of Si-SPION to 2 ml of PEC (2 mg protein/ml). Figure 39 shows that increasing the Si-SPION amount added to the reaction increased the mass of adsorbed PEC (measured as protein). The percentage of protein adsorbed to the Si-SPION surface increased with the increase in Si-SPIONs until the

mass of Si-SPION reached 80 mg. As expected, further mass increase to 100 mg did not show a notable increase in the adsorbed protein because >90% of the protein has been adsorbed at 80 mg SPION. Adsorption of molecules, mostly proteins, on surfaces has been reported to plateau depicting the point the surface is saturated (Hlady et al., 1999).

The protein loading (µg/mg Si-SPION) on the SPION decreased with increasing Si-SPION mass. This is expected because addition of Si-SPIONs provide more surfaces for PEC to absorbed to reducing the amount of PEC per Si-SPION. The protein loading (µg/mg Si-SPION) followed 3 slopes indicating differences in adsorption behaviors of PECs. This is in line with previous established adsorption phenomena of mixed protein samples (Meissner et al., 2015). The cellulase enzymes used in this study are a mixture of a wide variety of enzymes with different structures and chemical characteristics.

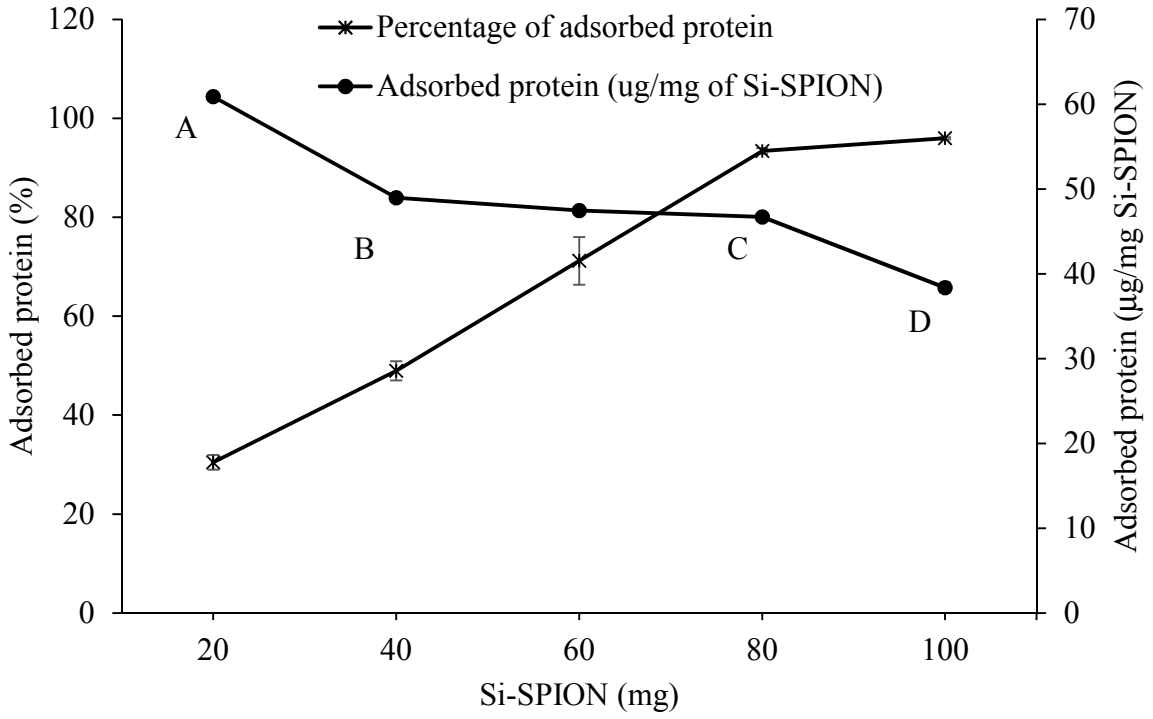

Figure 39. Adsorbed protein and protein loading for increasing amount of Si-SPION

6.5.6. Performance of magnetic nanobiocatalysts

In order to investigate how different amounts of adsorbed protein on SPIONs affects glucan conversion to glucose, MNBCs containing different protein loadings (60, 49, 46 and 38 µg/mg Si-SPION, respectively marked A, B, C and D in Figure 39) were used to hydrolyze dilute acid pretreated biomass for 48 h. MNBC efficacy for initial hydrolysis is lower than that of free enzyme (FE) for all treatments (Figure 40). Previous studies have reported that the reduction in MNBC efficacy was because of a physical limitation between enzyme and substrate (Kudina et al., 2014; Samaratunga et al., 2015a). It is therefore not unexpected that the MNBCs efficacies would be lower than that of FE.

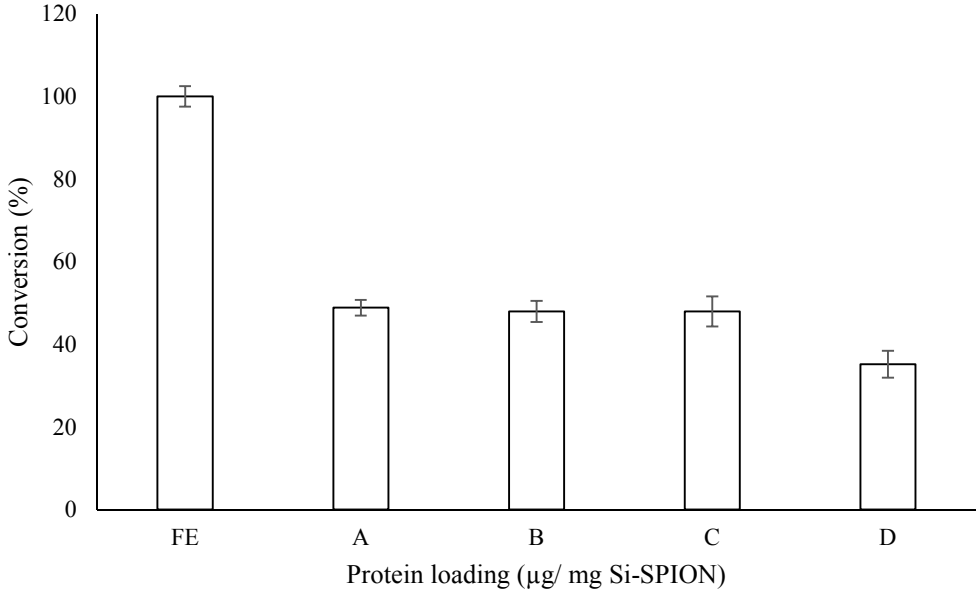

Figure 40. 48-h glucan conversion of acid pretreated biomass using magnetic nanobiocatalysts at different protein loadings A: 60 µg/mg Si-SPION, B: 49 µg/mg Si-SPION, C: 46 µg/mg Si-SPION and D: 38 µg/mg Si-SPION

Different enzyme loadings on Si-SPIONs can affect enzyme proximity and their synergy. A, B and C with high protein loading have high glucan conversion compared to D with low protein loading. This confirms the possible relationship between enzyme proximity and efficacy. Close enzyme proximity has been reported to improve enzyme efficacy in natural cellulosomes

where efficient biomass hydrolysis is achieved via synergistic actions of the immobilized cellulases (Arora, Behera, Sharma, & Kumar, 2015).

6.5.7. Reuse

One of the motivations for MNBC production is to facilitate enzyme recovery and reuse. We investigated the relative efficacy of MNBCs (treatment C, Figures 39 and 40) during 4 recovery and reuse cycles. As shown in Figure 41, the conversion of glucan to glucose drops with each successive cycle. By the fourth cycle, the performance has dropped to 55% of initial efficacy at cycle 1. A similar study that attached cellulases on polymer grafted SPION (enzymogel) also reported a reduction in glucan conversion during recovery and reuse (Kohut et al., 2017), possibly due to loss of enzyme activity after extensive exposure to hydrolysis conditions during repeated use. Extended enzyme reuse could cause protein modification which could inactivate enzymes (Ishihara, Uemura, Hayashi, & Shimizu, 1991). The previous study show that the reduction in efficacy is due to the change in polymer conformation after each cycle of hydrolysis that could prevent enzyme interactions with substrate (Grunwald, 2017).

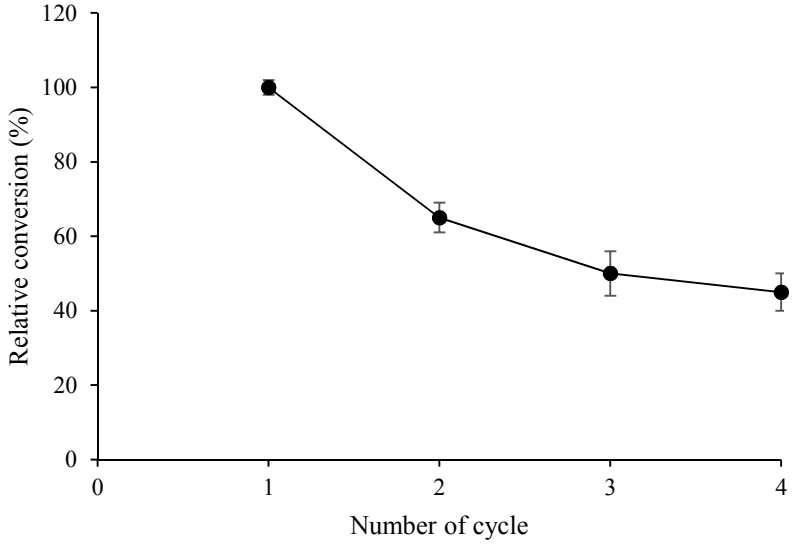

Figure 41. Relative glucan conversion of MNBCs during successive cycles of recovery and reuse. Glucan conversion at cycle 1 was used as bases of comparison. Each hydrolysis stage was 48 h biomass hydrolysis at 50°C and 130 rpm

The immediate effect of SPION dissolution is the loss of the NBC magnetic core that inevitably led to reduction in magnetic recoverability of MNBCs. Since Si-SPION dissolution occurs by 72 h (according to Figure 37), it is not unexpected that continuous exposure to hydrolysis condition during the recycling experiment could have caused continued dissolution. With more SPION dissolution, recoverability of MNBCs decreases. Therefore, the reduction in efficacy of magnetic NBC could be due to reduction in recoverability.

Although SPION aggregation can be mitigated by silica coating, the degradation of the silica coating during hydrolysis in mild acid condition did not only result in dissolution but also SPION aggregation. SPION aggregation in MNBCs can impact the accessibility of attached enzymes to substrate explaining the reduction in magnetic NBC efficacy observed in this study.

6.6. Conclusion

In this study, we have investigated the effectiveness of TES for one-pot synthesis of Si-SPIONs for MNBC application. From examining the effect of coating agent (Na_2SiO_3)

concentrations (0.05 and 0.1 M) during synthesis, we found the productivity of TES was high at lower coating agent concentrations. The Si-SPIONs were 8 – 12 nm diameter spheres with ~2 nm silica coating and were stable under acidic conditions for 48 h. The Si-SPIONs were used for PEC adsorption to make the MNBCs which were recovered and reused in 4 hydrolysis cycles. Future studies should investigate effect of lower concentration of Na_2SiO_3 and TES application for synthesis of other type of nanoparticles with different coating agents. Also, further study on SPION aggregation during hydrolysis with magnetic NBCs will help explain the reduction in magnetic NBCs efficacy.

6.7. References

Abbas, M., Abdel-Hamed, M. O., & Chen, J. (2017). Efficient one-pot sonochemical synthesis of thickness-controlled silica-coated superparamagnetic iron oxide (Fe3O4/SiO2) nanospheres. *Applied Physics A: Materials Science & Processing*, *123*, 775. https://doi.org/10.1007/s00339-017-1397-0.

Abhari, N., Madadlou, A., & Dini, A. (2017). Structure of starch aerogel as affected by crosslinking and feasibility assessment of the aerogel for an anti-fungal volatile release. *Food Chemistry*, *221*, 147–152. https://doi.org/10.1016/j.foodchem.2016.10.072.

Aghazadeh, M. (2018). One-step cathodic electrosynthesis of surface capped Fe3O4 ultra-fine nanoparticles from ethanol medium without using coating agent. *Materials Letters*, *211*, 225–229. https://doi.org/10.1016/j.matlet.2017.09.086.

Ahankar, H., Ramazani, A., Fattahi, N., Ślepokura, K., Lis, T., Asiabi, P. A., … Joo, S. W. (2018). Tetramethylguanidine-functionalized silica-coated iron oxide magnetic nanoparticles catalyzed one-pot three-component synthesis of furanone derivatives. *Journal of Chemical Sciences*, *130*(12), 166. https://doi.org/10.1007/s12039-018-1572-7

Ansari, S. A., & Husain, Q. (2012). Potential applications of enzymes immobilized on/in nano materials: A review. *Biotechnology Advances*, *30*(3), 512–523. https://doi.org/10.1016/j.biotechadv.2011.09.005.

Arora, R., Behera, S., Sharma, N. K., & Kumar, S. (2015). Bioprospecting thermostable cellulosomes for efficient biofuel production from lignocellulosic biomass. *Bioresources and Bioprocessing*, *2*(1), 1–12.

Bohara, R. A., Thorat, N. D., & Pawar, S. H. (2016). Role of functionalization: Strategies to explore potential nano-bio applications of magnetic nanoparticles. *RSC Advances*, *6*(50), 43989–44012. https://doi.org/10.1039/C6RA02129H.

Cabrera, L., Gutierrez, S., Menendez, N., Morales, M. P., & Herrasti, P. (2008). Magnetite nanoparticles: Electrochemical synthesis and characterization. *Electrochimica Acta*, *53*(8), 3436–3441. https://doi.org/10.1016/j.electacta.2007.12.006.

Cendrowski, K., Sikora, P., Zielinska, B., Horszczaruk, E., & Mijowska, E. (2017). Chemical and thermal stability of core-shelled magnetite nanoparticles and solid silica. *Applied Surface Science*, *407*, 391–397. https://doi.org/10.1016/j.apsusc.2017.02.118.

Fajaroh, F., Setyawan, H., Nur, A., & Lenggoro, I. W. (2013). Thermal stability of silica-coated magnetite nanoparticles prepared by an electrochemical method. *Advanced Powder Technology*, *24*(2), 507–511. https://doi.org/10.1016/j.apt.2012.09.008.

Grunwald, P. (2017). *Biocatalysis and Nanotechnology* (Vol. 3). Singapore: Pan Standord Publishing.

Haddad, P. S., Duarte, E. L., Baptista, M. S., Goya, G. F., Leite, C. A. P., & Itri, R. (2004). Synthesis and characterization of silica-coated magnetic nanoparticles. *Surface and Colloid Science*, 232–238. Berlin, Heidelberg: Springer. https://doi.org/10.1007/b97092

Han, J., Rong, J., Wang, Y., Liu, Q., Tang, X., Li, C., & Ni, L. (2018). Immobilization of cellulase on thermo-sensitive magnetic microspheres: Improved stability and reproducibility. *Bioprocess and Biosystems Engineering*, *41*(7), 1051–1060. https://doi.org/10.1007/s00449-018-1934-z.

Hlady, V., Buijs, J., & Jennissen, H. P. (1999). [26] Methods for studying protein adsorption. *Methods in enzymology*, *309*, 402-429.

Ishihara, M., Uemura, S., Hayashi, N., & Shimizu, K. (1991). Semicontinuous enzymatic hydrolysis of lignocelluloses. *Biotechnology and Bioengineering*, *37*(10), 948–954.

Kalska-Szostko, B., Wykowska, U., Piekut, K., & Satuła, D. (2014). Stability of Fe3O4 nanoparticles in various model solutions. *Colloids and Surfaces A: Physicochemical and Engineering Aspects*, *450*, 15–24. https://doi.org/10.1016/j.colsurfa.2014.03.002.

Karimzadeh, I., Aghazadeh, M., Ganjali, M. R., Norouzi, P., Doroudi, T., & Kolivand, P. H. (2017). Saccharide-coated superparamagnetic Fe3O4 nanoparticles (SPIONs) for biomedical applications: An efficient and scalable route for preparation and in situ surface coating through cathodic electrochemical deposition (CED). *Materials Letters*, *189*, 290–294. https://doi.org/10.1016/j.matlet.2016.12.010.

Kudina, O., Zakharchenko, A., Trotsenko, O., Tokarev, A., Ionov, L., Stoychev, G., … Minko, S. (2014). Highly Efficient Phase Boundary Biocatalysis with Enzymogel Nanoparticles. *Angewandte Chemie International Edition*, *53*(2), 483–487. https://doi.org/10.1002/anie.201306831.

Lien, Y.-H., & Wu, T.-M. (2008). Preparation and characterization of thermosensitive polymers grafted onto silica-coated iron oxide nanoparticles. *Journal of Colloid and Interface Science*, *326*(2), 517–521. https://doi.org/10.1016/j.jcis.2008.06.020.

Meissner, J., Prause, A., Bharti, B., & Findenegg, G. H. (2015). Characterization of protein adsorption onto silica nanoparticles: influence of pH and ionic strength. *Colloid and polymer science*, *293*(11), 3381-3391.

Oksana, Z., Hammed, A., Zakharchenko, A., Borodinov, N., Luzinov, I., Urbanowicz, B., Patsahan, T., Ilnytskyi, J., Minko, S., Pryor, W. S., Voronov, A.. (2021). Biomimetic Cellulosomes Assembled on Molecular Brush Scaffolds: Random Complexes vs Enzyme Mixtures. *Applied Polymer Materials*.

Roth, H.-C., Schwaminger, S. P., Peng, F., & Berensmeier, S. (2016). Immobilization of Cellulase on Magnetic Nanocarriers. *ChemistryOpen*, *5*(3), 183–187. https://doi.org/10.1002/open.201600028.

Samaratunga, A., Kudina, O., Nahar, N., Zakharchenko, A., Minko, S., Voronov, A., & Pryor, S. W. (2015a). Impact of enzyme loading on the efficacy and recovery of cellulolytic enzymes immobilized on enzymogel nanoparticles. *Applied Biochemistry and Biotechnology*, *175*(6), 2872–2882.

Samaratunga, A., Kudina, O., Nahar, N., Zakharchenko, A., Minko, S., Voronov, A., & Pryor, S. W. (2015b). Modeling the effect of pH and temperature for cellulases immobilized on enzymogel nanoparticles. *Applied Biochemistry and Biotechnology*, *176*(4), 1114–1130.

Setyawan, H., Fajaroh, F., Widiyastuti, W., Winardi, S., Lenggoro, I. W., & Mufti, N. (2012). One-step synthesis of silica-coated magnetite nanoparticles by electrooxidation of iron in sodium silicate solution. *Journal of Nanoparticle Research*, *14*(4), 807. https://doi.org/10.1007/s11051-012-0807-7.

Sodipo, B. K., & Aziz, A. A. (2016). Recent advances in synthesis and surface modification of superparamagnetic iron oxide nanoparticles with silica. *Journal of Magnetism and Magnetic Materials*, *416*, 275–291. https://doi.org/10.1016/j.jmmm.2016.05.019.

Wang, P., Zhu, Y., Yang, X., & Li, C. (2007). Electrochemical synthesis of magnetic nanoparticles within mesoporous silica microspheres. *Colloids and Surfaces A: Physicochemical and Engineering Aspects*, *294*(1), 287–291. https://doi.org/10.1016/j.colsurfa.2006.08.015.

Xue, D.-S., Chen, G.-J., Su, B.-X., Liu, Y.-H., Zhang, D.-P., Guo, Q., … Sun, J.-F. (2020). On-line spectrophotometric determination of ferrous and total iron in monominerals by flow injection combined with a Schlenk line-based digestion apparatus to exclude oxygen. *Microchemical Journal*, *155*, 104743.

7. CONCLUSIONS AND RECOMMENDATIONS

7.1. Conclusions

High enzyme cost is one of the primary challenges facing cellulosic biorefinery development. Although enzyme immobilization technologies could allow processors to reuse enzyme which has the potential of reducing overall costs, immobilization also typically reduces enzyme efficacy and requires extra recovery steps. Cellulolytic MNBCs (cellulases attached to magnetic nanoparticles) make enzymes recoverable through the use of a magnet. One approach for MNBC synthesis is by attaching enzymes to flexible polymer molecules to form polymer-enzyme conjugates (PECs) which are then attached to superparamagnetic iron-oxide nanoparticles (SPIONs). However, this approach requires multiple steps that are difficult to control and scale thereby hindering their possible industrial use. Therefore, the main objective of this research was to develop a scalable process to produce effective, recoverable and reusable cellulosic MNBCs for lignocellulosic biomass hydrolysis. To achieve the overall goal, the following studies were conducted: (i) determine how attachment of cellulases to polymer ligands affects efficacy and reusability during biomass hydrolysis, (ii) develop a scalable system for SPION synthesis and coating and determine suitable processing parameters, and (iii) produce MNBSs by attaching PECs to SPIONs and investigate efficacy, recovery and reuse.

Some microbes have evolved to produce cellulosomes containing cellulase enzyme immobilized on flexible protein scaffolds. Cellulosomes have been reported to display high efficacy for lignocellulosic biomass hydrolysis. However, the production methods of artificial cellulosomes are tedious and expensive making it uneconomical for lignocellulosic industries. PECs are artificial biomimetic cellulosomes with flexible polymer instead of protein scaffolds. The efficacy and reusability of enzymes can be changed when they are immobilized on polymer

molecules. Similarly, changes in hydrolysis conditions could affect the polymer conformation which could affect the function of the attached enzymes.

Efficacy of PECs is comparable to that of free enzymes (FEs) with both alkali and acid pretreated biomass at the range of hydrolysis time (12 – 72 h), pH (4 – 5.5), temperature (45 – 65^{o}C) and substrate loading (1 – 3 % glucan) used in this study. Increasing hydrolysis temperature from 45 to 55^{o}C has little impact while further temperature increase causes rapid decrease in PEC and FE efficacy. PEC efficacy is highest (95 % glucan conversion) at pH range 4 to 4.5. Although, increasing substrate loading reduces PEC efficacy, PEC efficacy is about 2.5% higher than that of free enzymes.

In order for PECs to be used for MNBC synthesis, they should be reusable. Knowing that attaching PECs to SPIONs to make MNBCs requires additional cost, recovery of PECs was investigated to know if PECs could be reusable without attachment to SPIONs. Therefore, PEC recovery was tested with a large-pore (50 kDa) membrane and the recovered PECs were tested for efficacy. The efficacy of recovered PECs is 30% glucan conversion. This reduction in recovered PEC efficacy is because some unattached enzymes have passed through the membrane and some substrate-adhered enzymes have not been separated. To improve conversion, supplementing recovered PECs with free enzymes can achieve the same hydrolysis conversion in a subsequent batch with 40% of the enzyme loading used in the first hydrolysis stage.

Enzyme recovery can be further simplified by attaching PECs to SPIONs to make MNBCs. However, SPION production has some complex intermediate reactions and is unscalable for industrial applications. Among the SPION production methods, electrochemical methods could be scalable but the anode surface eventually becomes covered with SPIONs reducing electrode conductivity and process productivity. Therefore, a lab-scale experimental

prototype of tubular electrochemical system (TES) was developed where electrolytes are pumped through an electrically charged reactor. The reactor has a copper tube acting as the cathode with an anode rod inserted into the tube. The surface of the anode is washed with the flowing electrolytes to remove any adhering SPIONs. The TES also has a 1-L magnetic separating vessel to separate the synthesized SPIONs. The TES produces 8.3 mg SPION/mole Fe at a productivity of 163 μg SPION/mole Fe/ min. The SPION size and size distribution depend on the processing conditions. SPION average size increased from 4 nm to 11 nm as flow rate decreased from 9 mL/s to 3 mL/s. Increasing the current density from 7 mA/cm^2 to 18 mA/cm^2 decreases SPION average size from 15 nm to 5 nm and increasing electrolytes concentration from 0.05 M to 0.015 M causes an increase in SPION size and broadened the size distribution. Also, in order to improve productivity and reduce effluent, the TES can be operated with different electrolyte feeding strategies. The use of a continuous reactant feeding strategy enables the reuse of reaction media without significantly effecting productivity or SPION size distribution. Electrolyte reuse increases scalability and lowers process effluent. Therefore, TES may reduce the processing cost while ensuring scalability of SPION production.

The adsorption of PECs on SPIONs could be a simple route to make MNBCs; however, SPION adsorption capacity is poor because SPIONs aggregate, limiting available surfaces for adsorption, and have surface functional groups that are unsuitable for PEC adsorption. Also, MNBC durability is questionable because SPIONs corrode easily in the mildly acidic conditions commonly used for LB hydrolysis. SPION aggregation, dissolution, and resistance to PEC adsorption can be prevented by coating SPIONs with silica; however, most coating methods are also costly and require multiple steps. TES simplifies coating the SPIONs with silica (Si-SPIONs) by achieving production of spherical silica-coated SPIONs (Si-SPIONs) in a one-step

process. The resulting Si-SPIONs are 8 – 12 nm in diameter including a 2-nm silica coating. The concentration of coating agent (Na_2SiO_3) in the synthesis reactor has no effect on Si-SPION shape, size distribution, or thickness of the silica coating. Decreasing coating agent (Na_2SiO_3) concentration from 0.1 M to 0.05 M increases SPION synthesis productivity. This simplified process produces Si-SPIONs that are suitable for attachment with PECs. The Si-SPIONs also have improved adsorption for PECs to produce MNBCs because the absorption capacity reached about 55 μg enzyme /mg Si-SPION representing >90% protein absorption. Also, Si-SPIONs have required longevity as they have the ability to resist corrosion under typical LB hydrolysis conditions for the 48-h required duration.

PECs are adsorbed to Si-SPIONs to make MNBCs. Although MNBCs are magnetically recoverable, MNBCs have architecture with different enzyme proximity and interaction different from that of PECs. Although MNBCs have lower efficacy than free enzymes or PECs, they can be recovered magnetically which could be a less expensive recovery method than membrane. Varying enzyme loading on SPIONs affects MNBC efficacy. MNBCs with high enzyme loadings have higher efficacy than those with lower enzyme loading possibly because of close enzymes proximity. The MNBCs can be magnetically recovered and reused at least four times for LB hydrolysis, although efficacy is reduced with subsequent recovery steps.

7.2. Recommendations

In order to improve MNBC synthesis, the following research areas have been identified and recommended for future studies.

In addition to cellulose, LB also contains hydrolysable macromolecules including lignin, proteins and hemicellulose. The current research is limited to cellulase nanobiocatalysts for cellulose hydrolysis. Future work should focus on developing multifunctional nanobiocatalysts

that will include proteases and xylanases, respectively, for protein and hemicellulose hydrolysis. The recommended study on multifunctional PECs should investigate the effect of enzyme ratio and polymer properties (molecular weight, composition, and amphiphilicity). Also, membrane recovery of PECs in this research requires further studies on the effect of polymer ligands on membrane fouling and the use of a membrane reactor following biomass hydrolysis.

Since there are additional steps (silica-coating of SPIONs and PEC adsorption to Si-SPIONs) to produce MNBCs from PECs, and MNBCs have reduced efficacy, it could be economical to use PECs directly. This research has found that membrane recovery of PECs has potential to reduce enzyme requirements during LB hydrolysis, although membrane separation is a cost addition. A technoeconomic study is needed to determine if costs saved from reuse of recovered enzyme could compensate for the total cost associated with polymer synthesis and membrane separation. Another area for exploration is the development of new recovery approaches that use glucose-sensitive or thermal-sensitive polymers for PEC synthesis. Since glucose concentrations increase during hydrolysis, polymers that self-aggregate in the presence of glucose could help to recover enzyme as hydrolysis progresses. Likewise, temperature-sensitive polymers could self-aggregate with a change in temperature to ease enzyme recovery.

The ability of membrane-recovered PECs to reduce enzyme requirements during subsequent hydrolysis has been investigated with the addition of different amount of FE to the recovered PECs. It is possible that FE and PECs could have an interactive effect and their ratios should be part of the hydrolysis conditions to be investigated. Since this research did not keep the overall concentration of enzyme constant during hydrolysis with membrane recovered PECs, the result could not explain the effect of PEC/FE ratio during hydrolysis. However, it is unclear

what is the most appropriate ratio of FE and PEC. Therefore, further work is required to investigated the effect of different ratio of PEC to FE on overall efficacy during hydrolysis.

The adsorption approach used in this study may have resulted in PECs attaching to SPIONs at multiple points leading to covering of SPION surface and reduced adsorption capacity. Future work should advance TES application for single point polymer-grafting on SPIONs. This will require designing polymers with suitable endpoint functional group(s). The attachment of polymers directly on SPIONs will create brush-like structure to attach more enzyme. Also, the attaching end of the polymer can be designed to functionalized SPION surface such that the polymers will also serve as protective coating. This approach could eventually eliminate the need for silica coating-steps and reduce MNBC synthesis cost.

This research used an aluminum anode which showed signs of surface degradation in the TES. Besides the reactivity of aluminum, the degradation could also be due to washing of gently attached protective Al_2O_3 layer by the flowing electrolytes. The materials from degraded surface contaminated the electrolytes and reduced further reuse. Presence of contaminants might also reduce system productivity because SPION synthesis has intermediates that might react with the contaminants preventing SPION formation. Future work should investigate the use of an inert electrode material such as platinum to reduce electrolyte contamination and extend reuse of electrolytes to improve reactor productivity.

The TES developed is a new electrochemical system that functions based on electrochemical, thermodynamic and hydrodynamic principles. The effect of current density, flow rate, and electrolyte concentration using a one-factor-at-a-time (OFAT) experimental design have been studied. These processing conditions might also have interactive effects, especially on TES productivity. I recommend using central composite experimental design in response surface

methodology to investigate the interactive effect of the processing conditions on TES productivity for future study. Apart from process conditions studied in this work, there are a number of design factors such as tube length, tube diameter, material conductivity, and tube series arrangement that could be modelled in future studies. This type of complex model is best developed in-silico because it will give the means to investigate a wider range for each factor. In-silico studies could also leverage improvements in computer processing performance to give visual representation of the reaction. Also, an in-silico study could be used to model TES scale-up.

Among the drawbacks of using SPIONs as an MNBC platform are their predisposition for aggregation and dissolution. Although silica coating could mitigate each of these, the occurrence of dissolution after 48 h of hydrolysis indicates the possibility that the silica coat has been partially or totally removed. With degradation of the silica coat, SPION could easily aggregate again. Extended SPION aggregation could lead to formation of MNBC cluster where the attached enzymes are partially or completely covered. However, it is unknown if SPION aggregation occurs during hydrolysis. SPION aggregation could be studied using a particle size analyzer in future research. The findings from such a study could explain the observed reduction in MNBC efficacy during hydrolysis.

SPIONs are known to have anti-microbial properties suggesting that they could affect biochemical reactions in living system. Since most biochemical reactions are enzyme-driven, SPIONs could also affect enzymatic hydrolysis of biomass. Apart of losing magnetic recoverability of NBCs, the dissolution of SPIONs releases metallic ions (Fe(II) and Fe(III)) that could also affect the efficacy of the cellulase enzymes. Metallic ions facilitate electron attraction and donations during biochemical reaction and also contribute to maintaining enzyme tertiary

and quaternary structures. There is no information on the effect of soluble iron on cellulase activities, so these could be explored in a future study.